Dissertation

submitted to the

Combined Faculties for the Natural Sciences and for Mathematics

of the Ruperto-Carola University of Heidelberg, Germany

for the degree of

Doctor of Natural Sciences

presented by

M.Sc. Vlada Kogosov

born in Swerdlowsk, Russia

Oral-examination: 12.12.2013

Novel interaction partners of cutaneous HPV types and their role in skin cancer

Referees:

Prof. Dr. Rainer Zawatzky

Prof. Dr. Frank Rösl

Eidesstattliche Erklärung

Ich erkläre hiermit, dass ich die vorliegende Dissertation selbst verfasst und mich keiner anderen als der von mir ausdrücklich bezeichneten Quellen und Hilfsmittel bedient habe. Diese Dissertation wurde in dieser oder anderer Form weder bereits als Prüfungsarbeit verwendet, noch einer anderen Fakultät als Dissertation vorgelegt. An keiner anderen Stelle ist ein Prüfungsverfahren beantragt.

Heidelberg, den 17.10.2013

Vlada Kogosov

Für meinen Großvater

Vladimir M. Schkolnik

Table of contents

Summary

Ultraviolet (UV) irradiation and UVB in particular, is the major environmental risk factor for the development of skin cancer. Furthermore, an increasing body of evidence supports a role for cutaneous human papillomaviruses (HPVs) in combination with UV irradiation in the development of cutaneous squamous cell carcinoma. Moreover, cutaneous HPV E6 proteins have been described to indirectly influence pathways controlled by p53, to inhibit UV-induced apoptosis and to prolong the life span of keratinocytes, the natural host of all HPVs.

The present study identified the LIM protein Ajuba as a novel interaction partner of the E6 protein of the beta2 HPV23, the gamma1 HPV4 and the gamma11 HPV148. These E6 proteins were shown to directly interact with Ajuba both *in vitro* and *in vivo* as well as to co-localise with Ajuba in the cytoplasm. Furthermore, the E6 proteins of HPV23 and HPV148 showed a coincidental decrease in protein expression together with their interaction partner Ajuba upon DNA damage induction and siRNA-mediated Ajuba knockdown. This knockdown also revealed that the p53 protein was involved in the regulation of Ajuba and HPV E6 protein levels. On the other hand, Ajuba co-accumulated following overexpression of the cutaneous E6 proteins, further pointing to a close interaction of both proteins *in vivo*. A trimeric complex formation between p53, Ajuba and HPV148 E6 was additionally discovered, which did not take place with HPV23 E6. Moreover, p53 was shown to co-localise and to interact directly with HPV148 E6 *in vitro* and *in vivo*, even in the absence of Ajuba. A functional luciferase reporter assay revealed a strong repression of p53 activity in the presence of HPV148 E6, demonstrating an impairment of the transactivation activity of p53. This observation could however not be reported for HPV23 E6.

In summary, the present study identified the LIM protein Ajuba as a novel interaction partner of cutaneous E6 proteins. Additionally, it demonstrated for the first time that the p53 protein not only binds to cutaneous HPV E6 proteins *in vitro*, but also interacts and co-localises with HPV148 E6 *in vivo*, subsequently repressing p53 activity. These findings suggest a novel regulatory mechanism elicited by cutaneous E6 proteins and further strengthen the hypothesis that cutaneous HPVs can act as co-factors in the development of skin cancer.

Zusammenfassung

Ultraviolette (UV) Strahlung und im Besonderem UVB, gilt als Hauptursache für die Entstehung von Hautkrebs. Darüber hinaus gibt es eine wachsende Anzahl von Studien, die zeigen, dass kutane Humane Papillomviren (HPV) zusammen mit UV-Strahlung an der Entstehung von kutanen Plattenepithelkarzinomen beteiligt sind. Zudem wurden kutanen HPV E6 Proteinen verschiedene Eigenschaften zugeschrieben wie z.B. die indirekte Einflussnahme auf Signalwege, die von p53 kontrolliert werden, die Fähigkeit UV-induzierte Apoptose zu hemmen, sowie die Lebensspanne von Keratinozyten, den natürliche Wirtszellen aller HPV Typen, zu verlängern.

Die vorliegende Studie hat einen neuen Interaktionspartner für die E6 Proteine des Beta2-HPV Typs 23, des Gamma1-HPV Typs 4 und des Gamma11-HPV Typs 148 identifiziert: das LIM Protein Ajuba. Es konnte gezeigt werden, dass die erwähnten E6 Proteine mit Ajuba direkt *in vitro* wie auch *in vivo* interagieren und mit Ajuba im Zytoplasma ko-lokalisieren. Ferner wurde gezeigt, dass DNS Schädigung sowie die siRNA-vermittelte Abschaltung von Ajuba zu einer simultanen Verringerung der Proteinexpression bei den E6 Proteinen von HPV23 und HPV148 sowie Ajuba führt. Außerdem wurde durch die RNA-Interferenzversuche deutlich, dass das p53 Protein an der Regulierung der Proteinexpression von Ajuba und den E6 Proteinen beteiligt ist. Andererseits wurde die Anreicherung von Ajuba nach Überexpression der E6 Proteine festgestellt, sodass davon auszugehen ist, dass beide Proteine in einem physiologisch engen Zusammenhang stehen. Überdies wurde die Entstehung von einem Komplex aufgedeckt, der sich aus den drei Proteinen p53, Ajuba und HPV148 E6 zusammensetzt. Dies konnte im Falle von HPV23 E6 nicht gezeigt werden. Zudem wurde eine Ko-Lokalisation von p53 und HPV148 E6 beschrieben. Es wurde zum ersten Mal gezeigt, dass beide Proteine *in vitro* und *in vivo* miteinander interagieren, auch wenn Ajuba nicht präsent ist. In funktionalen Versuchen konnte gezeigt werden, dass die Aktivität von p53 allein durch die Anwesenheit von HPV148 E6 stark unterdrückt wird. Diese neue Eigenschaft von HPV148 E6 konnte für HPV23 E6 nicht festgestellt werden.

Zusammenfassend wurde in der vorliegenden Arbeit ein neuer Interaktionspartner für kutane HPV E6 Proteine beschrieben. Zusätzlich wurde zum ersten Mal gezeigt, dass das p53 Protein nicht nur kutane E6 Proteine *in vitro* binden kann, sondern auch dass es mit ihnen *in vivo* interagiert und ko-lokalisiert, was unweigerlich zu einer Repression der p53-Aktivität führt. Diese Erkenntnisse weisen auf einen neuen Regulationsmechanismus von kutanen HPV E6 Proteinen hin und bekräftigen ferner die Hypothese, dass kutane HPV Typen als Ko-Faktoren an der Entstehung von Hautkrebserkrankungen beteiligt sind.

Section 1

Introduction

1.1 Infectious agents as a cause of cancer

For a long time cancer has represented one of the major causes of death worldwide accounting for approximately 13% of all annual deceases (around 7.6 million) [World Health Organization (WHO), 2013]. Cancer development itself is a multistep process. It is mostly caused by somatic mutations and does not arise from a single mutation, but from the accumulation of several distinct alterations [Vogelstein and Kinzler, 1993]. These can release the cells from normal growth-control mechanisms and result in unconfined cellular proliferation, enabling the cancer cells to become tumourigenic and, in an ultimate step, malignant [Hanahan and Weinberg, 2011]. The development of cancer can be caused by spontaneous mutations, but it is strongly favoured in the presence of chemical, physical, or biological carcinogens. While radiation - both ionizing and ultraviolet (UV) - is a physical carcinogen, chemical carcinogens include tobacco smoke, asbestos or toxins. Additionally, biological carcinogens such as infections with certain bacteria or viruses represent another risk factor [Dalton-Griffin and Kellam, 2009; Martin and Gutkind, 2008].

The discovery of viruses being potential infectious agents goes back to the late 19th century, when the first filtration devices that were able to remove cells and bacteria were developed. At that time the first virus, the tobacco mosaic virus (TMV), was discovered [Lecoq, 2001]. So-called "tumour viruses" have been known since the discovery of the avian leukemia virus (ALV) in 1908, but back then leukemia did not belong to a tumour-causing virus [Ellerman and Bang, 1908; Epstein, 1971]. In 1911 Peyton Rous showed that a solid tumour of the fowl could be transmitted to other previously healthy animals using a cell-free, filtered extract from chicken sarcomas [Rous, 1911]. This tumour-inducing agent was later identified as a virus, now known as the Rous sarcoma virus (RSV). This discovery for the first time clearly demonstrated that malignant tumours can be induced by viral infection. Since that time, many other tumour-inducing viruses were identified and characterised, like the Shope papillomavirus found in cottontail rabbits, later termed the cottontail rabbit papillomavirus, CRPV [Shope and Hurst, 1933]. Other examples e.g. in mice [Bittner, 1942; Gross, 1951] and non-human primates [Sweet and Hilleman, 1960] were also described. Shortly after the discoveries of tumour viruses in animals, the first oncogenic human virus, the Epstein-Barr virus (EBV), was discerned in the 1960s [Epstein *et al.*, 1964].

An estimated 18% of the worldwide cancer burden can be attributed to infections [Parkin, 2006]. To date, these infectious agents include at least six viruses and several bacteria. Infections with the hepatitis B and C viruses (HBV, HBC) are well-recognised risk factors for the development of

cirrhosis and liver cancer [Perz *et al.*, 2006]. The Epstein-Barr virus, also known as human herpesvirus 4 (HHV-4), is associated with B-cell lymphoproliferative diseases and nasopharyngeal carcinomas [Raab-Traub, 1992, 2012]. Another herpesvirus, HHV-8 or Kaposi's sarcoma-associated herpesvirus (KSHV), has been linked to Kaposi's Sarcoma and primary effusion lymphomas [Antman and Chang, 2000; Damania, 2004]. Infections with the human T-cell lymphotropic virus (HTLV-1), a human retrovirus, are associated with adult T-cell leukemia (ATL) [Matsuoka and Jeang, 2007; Poiesz *et al.*, 1980]. One bacterial example for infection-induced carcinogeneses is *Helicobacter pylori*, which is linked to the development of gastric cancers [Lax and Thomas, 2002; Pagano *et al.*, 2004]. Apart from EBV, human papillomaviruses (HPVs) are one of the best studied examples of human tumour viruses. HPVs are etiologically linked to anogenital cancers [Pagano *et al.*, 2004; zur Hausen, 2002]. Almost all cervical tumours contain HPV DNA and can thus be attributed to HPV infection [Parkin and Bray, 2006; Walboomers *et al.*, 1999]. In 2008, cervical cancer was considered the second most common cancer in women worldwide with annually 530.000 to 600.000 new cases and 275.000 deaths [de Martel *et al.*, 2012; Ferlay *et al.*, 2010]. That is why further investigations of the mechanisms of HPVs remain important: first, for a better understanding of the viruses and second, to be able to fight them in a more sophisticated way.

1.2 Papillomaviruses

Papillomaviruses (PVs) are a diverse group of small non-enveloped DNA viruses that are distributed in different animal species, primarily in vertebrates ranging from birds to humans [Antonsson and Hansson, 2002]. Examples for mammals from which papillomaviruses were isolated are cattle [Campo, 1997], reindeer [Moreno-Lopez *et al.*, 1987], domestic cats [Sundberg *et al.*, 2000] and horses [O'Banion *et al.*, 1986]. Additionally, a growing number of novel papillomaviruses is being identified in other hosts [Antonsson and McMillan, 2006; Gottschling *et al.*, 2008; Schulz *et al.*, 2009; Schulz *et al.*, 2012]. Specific PVs can induce cancerous lesions in cattle, dogs or domestic rabbits [Campo, 2002]. However, by far the largest number of papillomaviruses was found in humans, encompassing over 150 distinct types [Bernard *et al.*, 2010]. Papillomaviruses are highly epitheliotropic pathogens and can induce diverse lesions in the stratified squamous epithelia of skin and mucosa. In addition, HPVs were classified as human carcinogens [Schiffman *et al.*, 2007].

1.2.1 Human papillomaviruses

Human papillomaviruses cause diseases ranging from benign warts and other benign epithelial tumours, which may regress spontaneously [van Duin *et al.*, 2002], to malignant cancers. The viruses can be classified into different groups. One group, the genital HPVs infect mucosal keratinocytes of the (ano)genital region and can be further divided into two subgroups according to

their oncogenic potential: the “high-risk” and “low-risk” types. Low-risk HPV types like HPV6 and HPV11 can cause low-grade lesions such as genital warts (*Condylomata acuminata*) and are rarely present in malignancies [Wilczynski *et al.*, 1993]. High-risk HPV types, on the other hand, are associated with the development of cervical intraepithelial neoplasia (CIN) and are therefore recognised as the causative agent of cervical carcinoma and head and neck cancer [Bosch *et al.*, 2002; Gillison *et al.*, 2012; Schiffman *et al.*, 2007]. Several studies showed that the prevalence of HPV DNA in cervical carcinomas is higher than 99% [Bosch *et al.*, 1995; Walboomers *et al.*, 1999] with HPV16 and HPV18 being the two most abundant types that are detected in 50% and 20% of all cervical cancers, respectively. Fifteen HPV types were classified as high-risk and oncogenic by the World Health Organization (16, 18, 31, 33, 35, 39, 45, 51, 52, 56, 58, 59, 68, 73, and 82) [Muñoz *et al.*, 2003]. Apart from the well-studied genital types, the large group of cutaneous HPVs can be discerned, some of whose representatives are proposed to play a role in the development of skin cancers [Harwood and Proby, 2002; Nindl *et al.*, 2007].

1.2.2 HPV classification

As already mentioned HPVs infect keratinocytes of mucosa and skin where they can cause a variety of symptoms starting from common warts (*Verruca vulgaris*), palmar and plantar warts to cervical cancer [Doorbar, 2005]. The life cycle of HPVs is directly linked to the epithelial cell differentiation of the host, rendering them very host specific [Fehrmann and Laimins, 2003]. PVs constitute a separate taxonomic family, the *Papillomaviridae*, and are generally grouped into mucosal/genital and cutaneous types [de Villiers *et al.*, 2004]. Based on sequence homologies of their L1 nucleotide sequences HPVs have been classified into five genera: alpha-, beta-, gamma-, mu- and nu-papillomaviruses [Bernard *et al.*, 2010; Doorbar *et al.*, 2012]. This classification was further validated by using a more complex analysis including the E1, E2 and L1 amino acid sequences (Fig. 1.1) [Gottschling *et al.*, 2011]. The highlighted HPV types in figure 1.1: HPV117 (Alpha PV), HPV23 and -118 (Beta PV) HPV4, -134 and -148 (Gamma PV) were the ones used for the experiments in this thesis. Most of them have been recently isolated [Köhler *et al.*, 2010; Köhler *et al.*, 2011].

The genera have different biological properties. Genitally transmitted HPVs which infect the mucosa of the cervix belong to the alpha papillomaviruses, i.e. the alpha genus, which is the largest group within the characterised HPVs. Examples are the high-risk types HPV16 and HPV18 and the low-risk types HPV6 and HPV11. Members of the remaining four genera (beta, gamma, mu, and nu) were shown to induce cutaneous lesions in humans and are not as well characterised [de Villiers *et al.*, 2004; zur Hausen, 2002]. Nonetheless, some beta-PVs, which are innocuous for the general population, are associated with the development of skin cancer in certain individuals. These patients are mostly immunocompromised organ transplant recipients (OTR) or suffer from the rare hereditary

disease *Epidermodysplasia verruciformis* (EV), which is characterised by an increased susceptibility to specific HPV types and is linked to the development of non-melanoma skin cancer (NMSC) [Doorbar, 2005; Harwood *et al.*, 2004; Lutzner, 1978; Ramoz *et al.*, 2002].

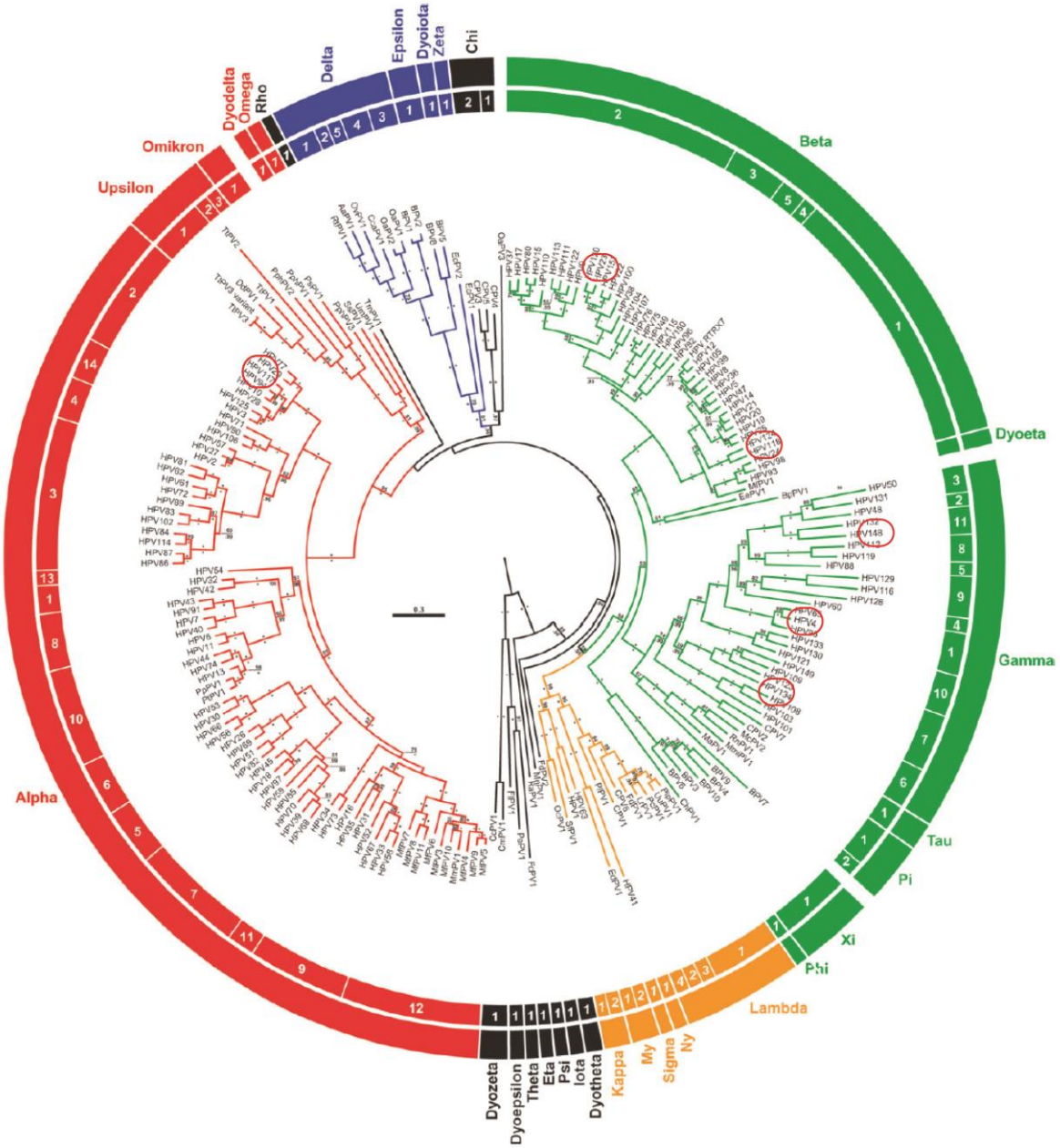

Figure 1.1: Phylogenetic tree of different papillomavirus types classified by genera.
The phylogenetic tree is based on an E1-E2-L1 amino acid sequence analysis of the indicated PV types. PV taxa are indicated in genera and species according to Bernard *et al.* [2010]. The groups are coloured in red (Alpha and Omikron PVs), green (Beta, Gamma and Xi PVs), blue (Delta and Zeta PVs), and ochre (Lambda and Mu PVs), respectively. Red circles indicate the HPV types HPV117 (Alpha PV), HPV23 and 118 (Beta PV), HPV4, 134, and 148 (Gamma PV). These HPV types were used for the experiments in this thesis. Figure adapted from Gottschling *et al.* [2011]

Furthermore, epidemiological studies have shown that infections with cutaneous HPVs of the beta genus may develop into keratotic skin lesions and even progress to squamous cell

carcinoma (SCC) in both immunocompetent and immunosuppressed individuals in combination with UV exposure, which acts as an immunosuppressive agent [Bouwes Bavinck *et al.*, 2007; de Koning *et al.*, 2007; Jackson and Storey, 2000; Murphy, 2009].

1.2.3 HPV genome organisation

Human papillomaviruses, similarly to other PVs, have a double-stranded circular genome of approximately 8kb. Cellular histones are associated with the viral DNA and form a chromatin-like structure. Most of the HPV genomes contain eight open reading frames (ORFs), whose genetic information is located on only one of the two DNA strands [Favre *et al.*, 1997] and which are transcribed as polycistronic messenger RNAs (mRNAs) [Fehrmann and Laimins, 2003]. In benign and productive infections, HPV DNA is maintained as an episome and is only rarely integrated into the host genome. High-risk HPV genomes, on the other hand, are often found integrated into the genomes of cervical cancer cells, highlighting the crucial role for viral integration into the host genome during carcinogenesis [Cullen *et al.*, 1991; Stanley, 2012].

Functionally, the HPV genome is arranged in three parts: (1) the non-coding long control region (LCR), also referred to as upstream regulatory region (URR), (2) the early region encoding the early regulatory proteins (E1, E2, E4, E5, E6, and E7), and (3) the late region coding for the major and minor capsid proteins L1 and L2, respectively (Fig. 1.2) [Favre *et al.*, 1997].

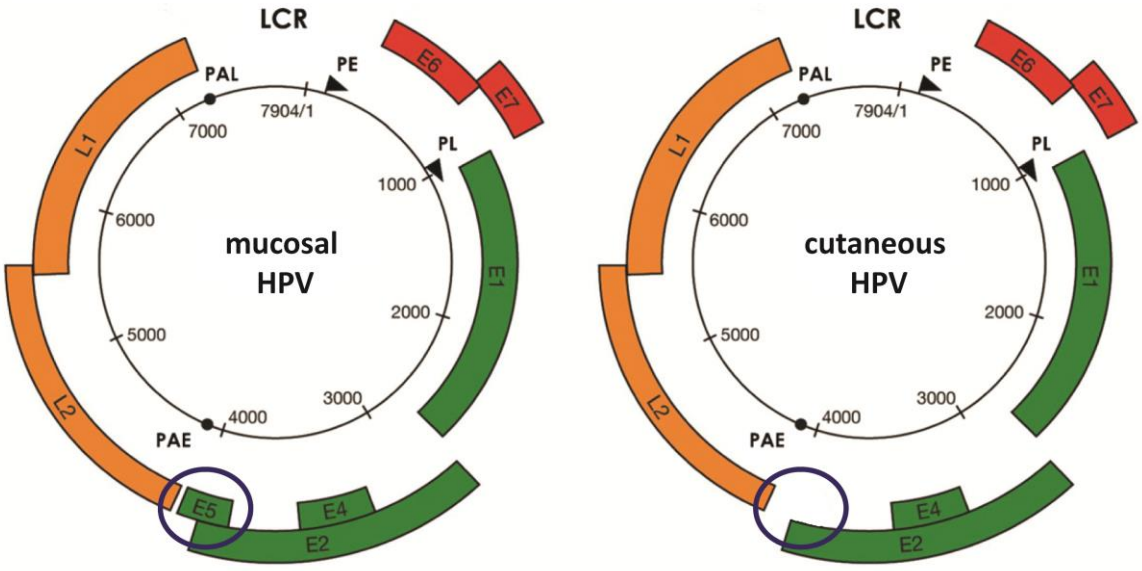

Figure 1.2: Schematic overview of the genome organisation of mucosal and cutaneous HPV types.
The genome comprises the long control region (LCR) and up to eight genes that are expressed in different stages of the viral life cycle. The early genes are shown in red and green, the late genes in ochre. The missing E5 ORF in cutaneous HPV types (right) is highlighted. Arrow heads designate the positions of the early (PE) and late (PL) promoters. PAE and PAL indicate the positions of the early and late polyadenylation sites. Figure adapted from Doorbar *et al.* [2012].

The LCR is located between the L1 and E6 ORFs. It contains the origin of replication and binding sites for different transcription factors of viral and host origin, thus being able to display regulatory functions [Doorbar, 2006]. E1 binds to the viral origin of replication and, with the help of E2, initiates DNA unwinding for the replication of the viral genome [Wilson *et al.*, 2002]. The E4 protein is expressed from spliced mRNAs encoding an E1^E4 fusion protein containing five additional amino acids from the N-terminus of E1. E4 has been suggested to be involved in the alteration of the cytoskeleton network [Doorbar *et al.*, 1991; Fehrmann and Laimins, 2003]. E5, E6 and E7 of high-risk HPVs are considered viral oncogenes whose expression induces transformation and cell immortalisation [Zheng and Baker, 2006]. The genes of the late region, L1 and L2 encode both structural proteins, which assemble into the viral capsid [Florin *et al.*, 2002].

The high-risk E5 gene encodes a membrane-associated protein with a weak transforming activity [Leptak *et al.*, 1991; Zhang *et al.*, 2002]. Upon viral DNA integration the E5 coding sequence is often deleted [Schwarz *et al.*, 1985]. While all genital HPV types encode E5, its general absence is a characteristic feature of cutaneous HPV types (Fig. 1.2) [Chan *et al.*, 1995]. The mandatory proteins to induce immortalisation and malignant transformation of cells are E6 and E7. High-risk E6 and E7 bind to and degrade the tumour suppressors p53 and members of the retinoblastoma family of proteins (pRb), respectively. The expression of the E6 and E7 oncogenes is required to maintain the transformed phenotype [Goodwin and DiMaio, 2000; Munger *et al.*, 2004; Muñoz *et al.*, 2006]. In contrast to high-risk E6 and E7 proteins, the function of their cutaneous counterparts is still not well characterised. Nevertheless, several studies showed that cutaneous HPV E6 proteins degrade the pro-apoptotic protein Bak and thus inhibit apoptosis after UVB-induced DNA damage, which is in part dependent on p53 expression [Jackson *et al.*, 2000; Simmonds and Storey, 2008; Underbrink *et al.*, 2008; Ziegler *et al.*, 1994]. The E6 and E7 proteins of the beta-PV HPV38 were shown in particular to have transforming activities by activating telomerase and inactivating pRb, which led to an extension of cell survival [Bedard *et al.*, 2008; Caldeira *et al.*, 2003].

1.3 HPV and cancer

Infections with mucosal high-risk HPVs are causally linked to the development of cervical cancer [Bosch *et al.*, 2002]. But not only genital HPV types have been associated with cancer. Certain cutaneotropic HPV types have been linked to the development of non-melanoma skin cancer, especially in patients with the rare genetic disorder *Epidermodysplasia verruciformis* [Favre *et al.*, 1997; Jablonska *et al.*, 1972] and in organ transplant recipients who undergo systemic immunosuppression [Ulrich *et al.*, 2008]. Nonetheless, the exact oncogenic potential of cutaneous HPV types remains debatable, partly because they were less studied than the genital types but also due to the large number and diversity of cutaneous types.

1.3.1 HPV and Epidermodysplasia verruciformis

The first evidence for HPV playing a role in SCC development was found in patients suffering from the rare hereditary disorder *Epidermodysplasia verruciformis* (EV) [Jablonska *et al.*, 1972]. EV is characterised by persistent disseminated wart-like skin lesions predominantly on sun-exposed sites, which result from unusually high susceptibility to infections with specific HPV types from the beta genus. In about 30% of all cases, these lesions ultimately progress to cutaneous SCC [Orth *et al.*, 1978; Orth, 2006]. Several beta-HPV types were previously isolated from these lesions and are therefore referred to as "EV HPV types". Mainly high copy numbers of episomal viral genomes of the beta1 HPV types 5 and 8 were detected in about 90% of cutaneous SCC [Majewski and Jablonska, 2006; Orth, 2006]. Individuals suffering from EV carry nonsense mutations in the two adjacent genes *EVER1* and *EVER2*. The gene products encode integral membrane proteins located in the endoplasmic reticulum. Since these proteins belong to the family of transmembrane channel-like (TMC) proteins, the gene names have however been changed from *EVER1* and *EVER2* to *TMC6* and *TMC8*, respectively [Lazarczyk *et al.*, 2008; Ramoz *et al.*, 2002]. TMC6 and TMC8 were found to interact with the zinc transporter 1 (ZnT-1) protein and were thus hypothesised to be involved in the cellular regulation of zinc homeostasis. The complex formed by these proteins can inhibit the activity of transcription factors, such as AP-1, which is a central transcription factor in the HPV life cycle. Although, HPV16 E5 was found to interact with endogenous TMC and ZnT-1 and to counteract their down-regulation, this mechanism does not apply to the EV HPV types which (lie all cutaneous types) lack the E5 ORF [Bravo and Alonso, 2004; Lazarczyk *et al.*, 2008; Lazarczyk *et al.*, 2009]. It is therefore suggested that the mutation in *TMC* in EV HPV types that renders the protein non-functional, may alleviate the host restriction and promote viral replication [Lazarczyk *et al.*, 2008].

1.3.2 HPV and Non-melanoma skin cancer

Non-melanoma skin cancer (NMSC) is the most prevalent malignancy in fair-skinned populations world-wide. It includes two main histologic types: basal cell carcinoma (BCC) and squamous cell carcinoma (SCC) with actinic keratosis (AK) as precursor lesions [Harwood *et al.*, 2000; Ko *et al.*, 1994; Nindl *et al.*, 2007; Pfister, 2003]. UV radiation is the major environmental risk factor for the development of epithelial skin cancers, which is e.g. reflected in tumour localisation at predominantly sun-exposed sites. However, UV is not the only risk factor. Other parameters contributing to skin cancer are genetic predisposition, the immune status and, in the context of HPV, viral infections [Corona *et al.*, 2001; Dubina and Goldenberg, 2009]. Still, UV irradiation, in particular UVB (ranging from 280-320nm), can lead to the induction of skin cancer through the direct formation of cyclobutane dimers and transitions in DNA. Hence, the constitutive accumulation of mutations combined with immunosuppression can progress into epithelial skin cancer [Muñoz *et al.*, 2006].

Furthermore, malfunctioning apoptosis or DNA repair mechanisms can as well result in the accumulation of genetic mutations and thus lead to epithelial skin cancer development [Rastogi *et al.*, 2010].

Additionally, UVB has three other effects on the skin which can together contribute to the formation of skin cancer. On top of the aforementioned effect of direct mutation of keratinocyte DNA, it upregulates gene expression of e.g. HPV20, -23 and -77 [Purdie *et al.*, 1999; Ruhland and de Villiers, 2001], induces tolerance to antigens and suppresses the immune system, via a process referred to as photoimmunosuppression [Ichihashi *et al.*, 2003; Schwarz, 2002]. Removal of UV-induced DNA lesions through DNA repair mechanisms was shown to result in the regression of UV-induced immunosuppression [Kripke *et al.*, 1992; Schwarz, 2005].

The tumour suppressor p53 is also known to be involved in skin carcinogenesis [Nakazawa *et al.*, 1994]. UV-induced p53 mutations are found in up to 50% of actinic keratoses, a premalignant stage of SCC [Ichihashi *et al.*, 2003; Ziegler *et al.*, 1994]. Other sources state that more than 50% of all BCC and 90% of all SCC harbour p53 mutations [Brash *et al.*, 1996]. Usually, p53, also called the "guardian of the genome", is associated with the induction of apoptosis, cell-cycle arrest or senescence following stress signals like DNA damage after UV exposure [Vousden and Lane, 2007]. Irreparable DNA damage leads to a p53-dependent induction of apoptosis pathways, thus eliminating damaged cells that could otherwise acquire a tumourigenic phenotype [Zuckerman *et al.*, 2009]. In this event the pro-apoptotic protein Bak is activated, after induction by UVB, which was also reported to happen independently of p53 [Jackson *et al.*, 2000]. Bak can multimerise in the mitochondrial membrane, release cytochrome *c* and thereby activate the pro-apoptotic caspase cascade [Underbrink *et al.*, 2008]. In contrast to genital HPVs, cutaneous HPV types were not shown to bind p53 but to indirectly influence different pathways controlled by p53. For instance, viral E6 protein binds HIPK2, prevents both HIPK2/p53 interaction and p53 phosphorylation at Ser46, resulting in the inhibition of apoptosis [Muschik *et al.*, 2011].

In addition to the UV-mediated mutation of the p53 protein, a role for cutaneous HPVs as co-factors in this multi-step process of skin carcinogenesis has been suggested in epidemiological studies [Bouwes Bavinck *et al.*, 2010; Feltkamp *et al.*, 2003; Nindl *et al.*, 2007; Pfister, 2003]. These studies uncovered an association between the presence of distinct HPV types and SCC but not BCC [Karagas *et al.*, 2006; Stockfleth *et al.*, 2004]. Yet, typically only small amounts of viral DNA are detectable in SCC and the exact mechanism of HPV-associated skin cancer development remains unclear. Cutaneous SCC represents the main type of tumour in immunosuppressed individuals e.g. organ transplant recipients (OTR), again underlining the important connection between the immune status and epithelial cancer. Organ transplant recipients have an increased risk to develop warts and NMSC, considering that up to 40% of renal transplant recipients and 90% of all OTR develop skin

cancer within 15 years after transplantation [Birkeland *et al.*, 1995; Nindl *et al.*, 2007; Nindl and Rösl, 2008]. For these patients photoimmunosuppression is a matter of particular importance [Euvrard *et al.*, 2003; Stockfleth *et al.*, 2001]. Notably, there is a 100- to 250-fold increased incidence of SCC in OTR compared to the general population underlining the important connection between the immune status and this malignancy. In contrast, the incidence of BCC is only increased by a factor of 10 [Euvrard *et al.*, 2003; Hartevelt *et al.*, 1990; Lindelof *et al.*, 2000]. DNA from cutaneous HPV types was detected in over 80% of SCC from OTR compared to 36% in immunocompetent individuals, strongly suggesting a role for cutaneous HPVs in SCC pathogenesis. Also, the percentage of HPV-positive tumours was shown to increase with the number of observed lesions [Arends *et al.*, 1997; Harwood *et al.*, 2000; Stockfleth *et al.*, 2004]. Because of constant immunosuppression, infections with usually harmless cutaneous HPVs might not be cleared in OTR and could therefore contribute to uncontrolled cell proliferation of infected cells. Unlike in the case of genital high-risk HPVs, no direct connection between specific cutaneous HPV types and SCC has been established, yet. However, several studies support a role for beta2 HPVs in the development of SCC even in immunocompetent individuals, as an overall high prevalence of HPV DNA was observed among the general population [Asgari *et al.*, 2008; Karagas *et al.*, 2006]. Contrary to high-risk genital HPV proteins that directly act as carcinogens, it is widely believed that their cutaneous analogues might act indirectly (e.g., by means of a “hit-and-run” mechanism), since not all tumour contain HPV DNA [Pfister, 2003]. Although associations have been identified in epidemiological studies, the exact role of cutaneous HPV infection in the development of SCC still remains unclear.

Because this thesis initially focused on the characterisation of the novel E6 proteins and identification of their interaction partners, the later identified interaction partner Ajuba, belonging to the LIM domain proteins, is introduced in the following chapters.

1.4 LIM domain proteins

About 25 years ago novel cysteine-rich protein motifs were described common to a group of homeodomain transcription factors. This group of proteins was named after the initials of those three homeodomain proteins in which it was first discovered: Lin11 (*Caenorhabditis elegans*), Isl-1 (rat) and Mec-3 (*C. elegans*), forming the acronym LIM [Freyd *et al.*, 1990; Karlsson *et al.*, 1990; Way and Chalfie, 1988]. The LIM domain can be found in proteins from ascidians, yeast, plants and humans and is highly conserved. The consensus sequence itself is variable between different species. Thereafter, several LIM homeodomain genes were isolated that contained two consecutive LIM domains combined with a conserved homeodomain. Additional genes were identified encoding LIM-domain proteins found in the cytoplasm as well as the nucleus. Some of the nuclear proteins mostly contain two LIM domains, and are therefore called LIM only proteins [Bach, 2000]. Individual

LIM domains consist of approximately 55 amino acids with 8 highly conserved residues (Fig. 1.3A). Initially, it was thought that the highly conserved residues might form a metal-binding structure containing iron-sulphur clusters [Li *et al.*, 1991], however other studies showed that the LIM domain binds zinc and not iron [Michelsen *et al.*, 1993]. The LIM domain arranges two zinc ions via two tetrahedral metal-coordinating centres formed by conserved cysteine, histidine, or aspartic acid residues of the consensus, thus forming a tandem zinc-finger (Fig 1.3B). This zinc coordination is necessary to stabilise the secondary and tertiary structures of the LIM domain [Kosa *et al.*, 1994; Michelsen *et al.*, 1994]. Furthermore, the two-residue linker between both zinc-finger modules seems to be indispensable for proper LIM domain function [Schmeichel and Beckerle, 1997]. In the beginnings of LIM domain research, it has been unclear whether the LIM domain was involved in protein-protein or protein-nucleic acid interactions. Although structural studies have shown that the domain has a tertiary fold indicative of a DNA-binding function, no evidence for a protein-DNA interaction has been presented to date [Perez-Alvarado *et al.*, 1994].

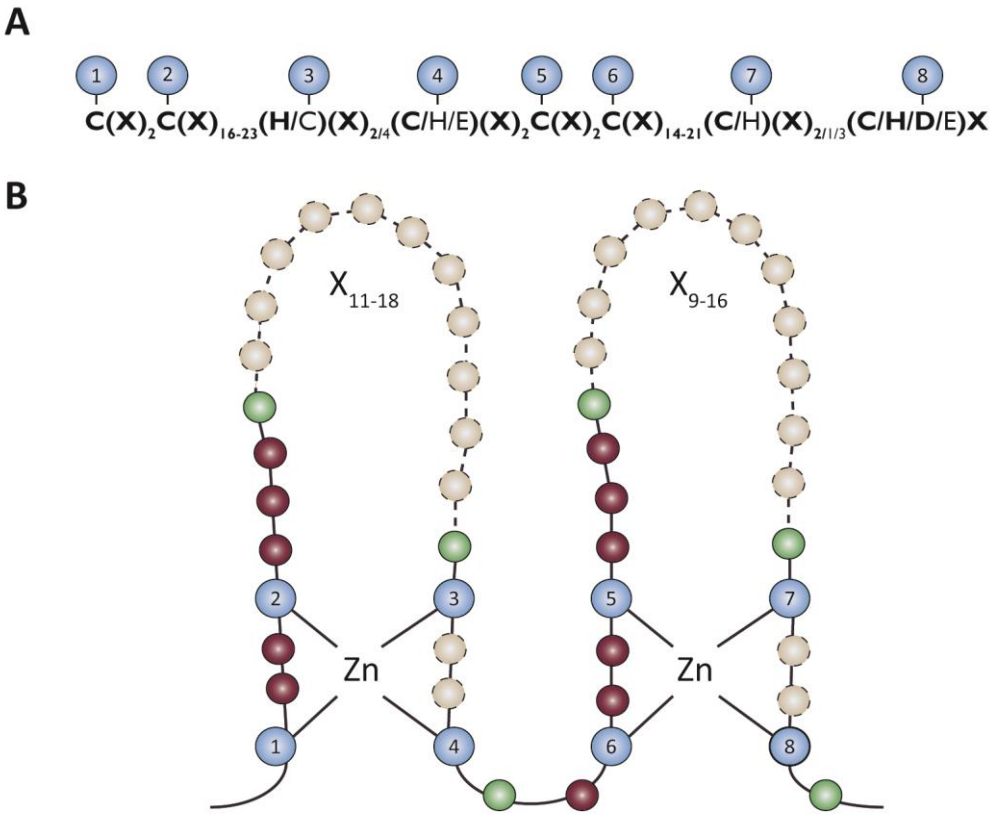

Figure 1.3: Conserved sequence topology of the LIM domain.
(A) The spacing of the eight zinc-binding residues (1-8) is based on analysis of 135 human LIM sequences. Occasionally observed patterns (seen in <10% of cases) are represented in characters that are not bold. Here, X denotes any amino acid. **(B)** Topology of the zinc coordination. Blue circles represent the zinc-binding residues. Semi-conserved aliphatic residues are shown in green. Non-conserved residues with invariant spacing are represented as bordeaux spheres. Dashed beige circles represent a variable number of residues (X) within the sequence. Figure adapted from Kadrmas and Beckerle [2004].

LIM-domain proteins are diverse and the domain itself can be found in many eukaryotic organisms. However, LIM-domain proteins have not been found in prokaryotes [Kadrmas and Beckerle, 2004]. Currently, 135 LIM-encoding sequences are found in the human genome located within 58 genes. Human LIM-domain proteins can contain up to 5 LIM domains. The proteins themselves can consist of LIM domains only or the LIM domains can be combined with other domains like catalytic domains, homeodomains or other protein-protein binding modules including SH3 or PDZ domains. LIM domains can be located N- or C-terminally, but also internally in a protein. These characteristics demonstrate the functional diversity of LIM-domain proteins [Zheng and Zhao, 2007].

LIM proteins can be located in the cytoplasm as well as the nucleus, but many LIM proteins, like the LIM homeodomain proteins, are found in the nucleus only. However, many LIM-domain proteins that were originally identified as cytoskeleton-associated proteins have been shown to shuttle between the nucleus and the cytoplasm thereby influencing gene expression [Chang *et al.*, 2003; Muller *et al.*, 2002; Petit *et al.*, 2000]. LIM domains were first classified into three groups based on sequence similarity, arrangement of the LIM domain and the overall structure [Dawid *et al.*, 1998]. Due to an increasing number of LIM-domain proteins, they were then classified into four groups. The first group contains LIM-homeodomain (LHX) proteins as well as nuclear LIM domain only (LMO) proteins, which have two repeated N-terminal LIM domains. These proteins are located in the nucleus and function as transcription factors. The second group contains LMOs which are located in the nucleus and the cytoplasm. They also contain several LIM domains located at the N- or C-terminus. Apart from the LIM domains, the third and fourth groups harbour other protein-protein interaction domains like leucine-aspartate repeats (LD) or PDZ domains. Additionally, proteins in the fourth group are catalytic, thereby differentiating them from the third group (Fig. 1.4). A similar categorisation of the four groups is: nuclear LIM proteins, LIM only proteins, actin associated LIM proteins, and catalytic LIM proteins referring to groups one to four, respectively [Kadrmas and Beckerle, 2004; Zheng and Zhao, 2007]. The protein further studied in this thesis is termed Ajuba and according to this classification belongs to the third group of LIM proteins.

The actin associated LIM-domain proteins e.g. members of the Enigma, Paxillin, and Ajuba/Zyxin protein families can shuttle between the nuclear and cytoplasmic compartments of the cell, thereby influencing gene expression [Breen *et al.*, 1998]. Since they are very heterogeneous, proteins from this group are able to interact with a variety of partners. Some of these proteins can e.g. localise at sites of focal adhesions (Paxillin, Zyxin). Their translocation into the nucleus through extracellular signals leads to transcriptional regulation of target genes but can also allow them to function as co-repressors or -activators [Wang and Gilmore, 2003].

Structural analyses demonstrated that LIM domains are protein-binding interfaces mediating protein-protein interactions [Schmeichel and Beckerle, 1994]. So far, it is not clear whether the LIM domain has a specific consensus binding sequence. It has been shown that a single LIM domain is sufficient for the binding of a specific protein partner; however, the protein sequence neighbouring the LIM domain can amplify this binding. Furthermore, single LIM domains were identified to concurrently bind several proteins and other tandem LIM domains to synergistically bind a single partner [Deane *et al.*, 2004; Sum *et al.*, 2002].

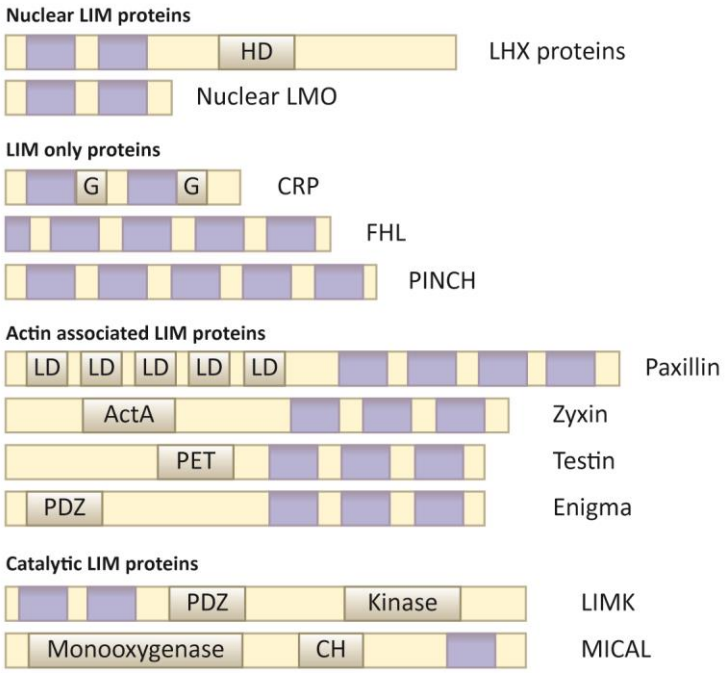

Figure 1.4: Classification and domain structure of LIM domain proteins.
LIM domain proteins are classified into four groups according to the arrangement and position of their LIM domains. These groups are: Nuclear LIM proteins, LIM only proteins, Actin associated LIM proteins, and Catalytic LIM proteins. Individual LIM domains are shown as purple boxes. All other domains are depicted as grey boxes and specified in the respective proteins. ActA, ActA repeat region; CH, calponin homology; G, glycine rich region; HD, homeodomain; PET, prickle, espinas and testin; LD, Leucine-aspartate domain; PDZ, Postsynaptic density-95, Discs large, Zona occludens-1; CRP, Cysteine-rich protein; FHL, Four-and-a-half LIM; PINCH, Particularly interesting new cysteine and histidine-rich protein; LIMK, LIM kinase; MICAL, Molecule interacting with CASL protein-1. Figure inspired by Zheng and Zhao [2007].

The LIM domain itself does not possess intrinsic catalytic activity, but LIM-domain proteins are known to induce a variety of biological processes via protein binding. Because LIM domains are protein-interaction platforms, it was suggested that they might modulate the activities of their binding partners [Schmeichel and Beckerle, 1994]. After analyses of many LIM interaction partners, four main LIM domain functions have been described: they can be adaptors, competitors, localisers, or autoinhibitors (Fig. 1.5). Whenever LIM-domain proteins contain additional protein-interaction domains they are able to function as adaptors or scaffolds and are thus capable of assembling a

multimeric protein complex. This brings the different protein partners into close proximity and can therefore have an impact on their activity (Fig. 1.5A). In addition, LIM domains can compete with each other for binding partners, thereby controlling biological activities (Fig. 1.5B) [Kadrmas and Beckerle, 2004]. Another mechanism for the control of protein activity is regulation through conformational changes (Fig. 1.5C). This autoinhibition process is common to a variety of transcription factors or members of the membrane-fusion machinery. Autoinhibition is an effective regulatory mechanism which works via inhibitory domains that negatively regulate functions of other domains through intramolecular associations [Pufall and Graves, 2002]. Lastly, LIM-domain proteins can affect subcellular protein localisation (Fig. 1.5D). They have been shown to participate in protein targeting by localising interaction partners in specific cellular compartments and by controlling their own localisation. Numerous transcription factors and kinases are regulated depending on their localisation [Cyert, 2001]. Often, combinations of the aforementioned functions can be observed in LIM-domain proteins.

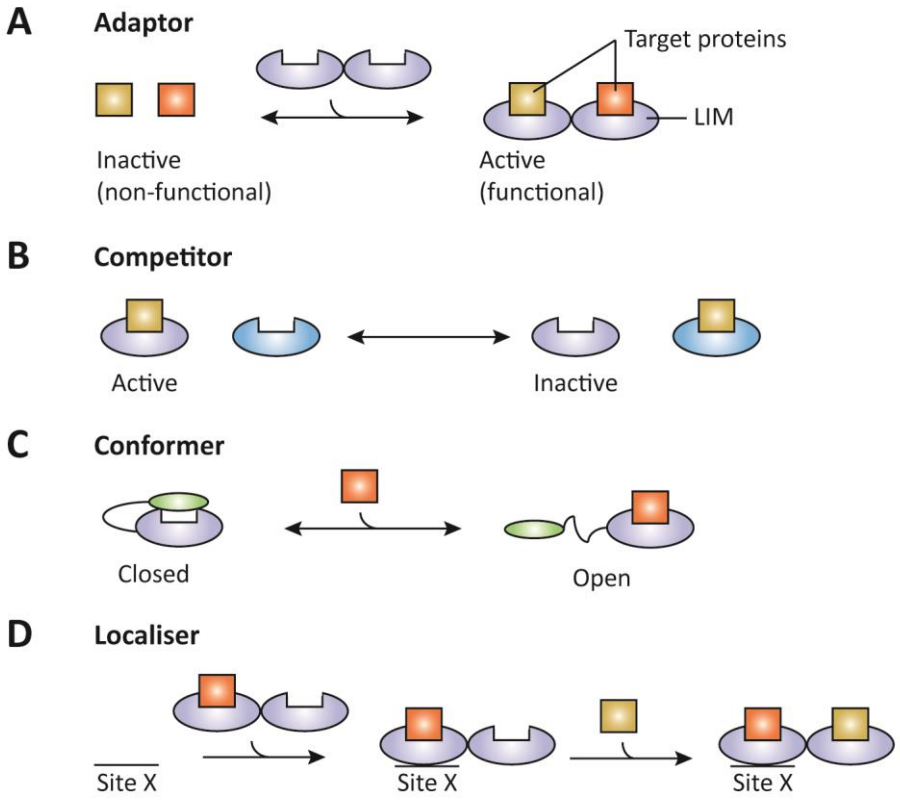

Figure 1.5: LIM domain functions.
Functions of the LIM domain elicited through binding to protein partners. **(A)** Adaptors function as molecular scaffolds assembling interaction partners thereby promoting their activity. **(B)** The affinity of target proteins for different LIM domains may result in a competition effect, thus regulating the activity of the LIM complex. **(C)** Autoinhibition of LIM domains can occur through intramolecular associations. These interactions might produce a closed conformer whose activity differs from an open, or target-protein-occupied, conformer. **(D)** LIM-domain proteins can bring themselves and/or their binding partners to a particular cellular locus. Figure adapted from Kadrmas and Beckerle [2004].

1.4.1 Ajuba/Zyxin family of LIM proteins

The Ajuba/Zyxin protein families belong to the actin associated LIM proteins and contain altogether six members in the Ajuba subfamily (Ajuba itself, LIM domain-containing protein 1 (LIMD1), and Wilms tumour 1 interacting protein (WTIP)) and the Zyxin subfamily (Zyxin, Lipoma preferred partner (LPP) and Thyroid hormone interacting protein 6 (Trip6)) (Fig. 1.6) [Crawford and Beckerle, 1991; Goyal *et al.*, 1999; Kiss *et al.*, 1999; Petit *et al.*, 1996; Wang and Gilmore, 2003; Yi and Beckerle, 1998]. All of these proteins contain three tandem-repeated homologous LIM domains at their C-terminus and a non-homologous proline-rich N-terminal PreLIM region (Fig. 1.6). Within the LIM region the six proteins share a high sequence homology [Schmeichel and Beckerle, 1997].

In fibroblasts and epithelial cells Ajuba/Zyxin family proteins are parts of cell-cell junction adhesive complexes [Marie *et al.*, 2003]. In fibroblasts they affect cell motility, whereas in epithelial cells they take part in the establishment and maintenance of cell-cell junctions [Marie *et al.*, 2003; Yi *et al.*, 2002]. Additionally, all members of the Ajuba/Zyxin family contain a nuclear export signal (NES) in their PreLIM domains, enabling shuttling to and from the nucleus (Fig. 1.6) [Nix and Beckerle, 1997]. This characteristic feature makes them excellent candidates for being involved in signal transduction, where information needs to be transported from the cell surface into the nucleus.

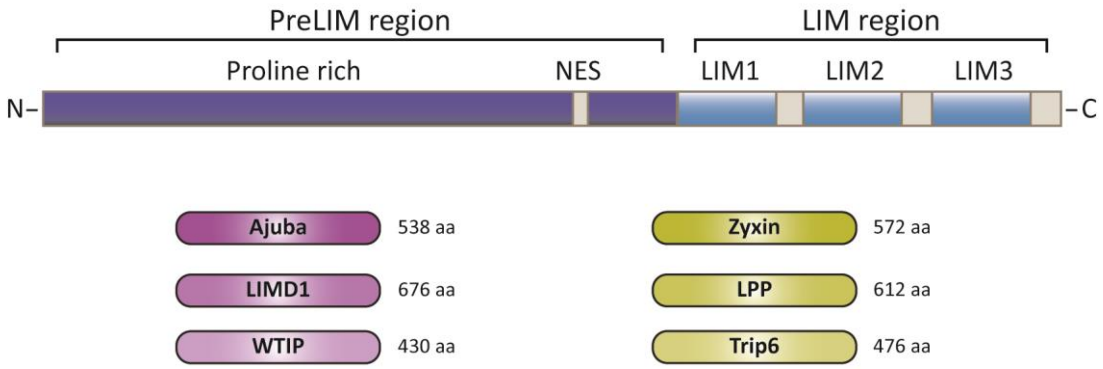

Figure 1.6: Schematic representation of the Ajuba/Zyxin family of LIM proteins.
This subgroup of LIM proteins is characterised by a non-homologous N-terminal PreLIM region including the nuclear export signal (NES) and three homologous C-terminal LIM domains. Phylogenetically, this family can be separated into two subfamilies, one being the Ajuba subfamily containing Ajuba, LIMD1 and WTIP, the other subfamily being Zyxin consisting of Zyxin, LPP, and Trip6.

Ajuba/Zyxin family members localise to sites of focal adhesion, associate with the actin cytoskeleton, and take part in cell motility [Crawford *et al.*, 1992; Petit *et al.*, 2000; Yi *et al.*, 2002]. Each subfamily also has its own special functions. Zyxin family members bind α-actinin and thus contribute to actin filament assembly. When the Zyxin-α-actinin interaction is disturbed, Zyxin is displaced from its normal subcellular localisation. This mislocalisation leads to disturbed cell migration and spreading [Drees *et al.*, 1999]. Moreover, Zyxin family members, but not the Ajuba

members, localise to cell-cell junctions in mammalian cells where they may participate together with Ena/VASP family members in the development of intercellular adhesive complexes [Renfranz *et al.*, 2003; Vasioukhin *et al.*, 2000]. Zyxin was the first protein of the family where a functional NES was detected, but the biological consequences of this nuclear translocation are still unknown. Ajuba, on the other hand, is known to affect growth control and cell differentiation upon accumulation in the nucleus. This accumulation is induced through the removal of the PreLIM domain of Ajuba, resulting in a protein with just the LIM domains and lacking the nuclear export sequence [Goyal *et al.*, 1999; Kanungo *et al.*, 2000]. Still, the exact mechanism of Ajuba recruitment to the different cellular compartments is not well understood. Both, Ajuba and Zyxin, have been implicated in cellular regulation during mitosis. Both of them interact with the LATS tumour suppressors and Ajuba additionally associates with the mitotic kinase Aurora A [Abe *et al.*, 2006; Hirota *et al.*, 2003].

A strong line of evidence proposes that the Ajuba/Zyxin family proteins do not bind DNA directly, but as they translocate into the nucleus they might have indirect effects on transcription. Both family proteins are able to bind transcription factors and other nuclear proteins. They also exhibit transactivation potential as detected in reporter assays [Petit *et al.*, 2000; Wang and Gilmore, 2003]. The Ajuba/Zyxin family of LIM proteins has also been implicated in the regulation of other signalling pathways. The PreLIM region contains consensus SH3 recognition sites and Ajuba and Zyxin have been shown to interact with SH3 domains of Grb2 (Growth factor receptor-bound protein 2) and Vav, a proto-oncoprotein, respectively [Goyal *et al.*, 1999; Hobert *et al.*, 1996]. The interaction of Ajuba with Grb2 leads to increased MAP kinase activity in fibroblasts. Upon expression of murine Ajuba in *Xenopus* oocytes, meiotic maturation takes place in a Grb2- and Ras-dependent manner. The functional significance of the interaction of Zyxin with Vav is however unclear [Goyal *et al.*, 1999]. Taken together, the Ajuba/Zyxin families play an important role in signal transduction, whereas the individual proteins might have overlapping roles. However, there is evidence that the roles of both subfamilies, Ajuba and Zyxin, diverge in the epithelial system.

1.4.2 Functions and cellular roles of the Ajuba family of LIM proteins

To further understand the role of Ajuba LIM proteins in signal transduction, interaction assays were performed and a new binding partner, the atypical protein kinase C (aPKC) scaffold protein p62, was identified. A well-known function of p62 is the regulation of NF-κB activation after interleukin-1 (IL-1) and tumour necrosis factor signalling by formation of an aPKC/p62/TRAF6 signalling complex. Hence, it was proposed that Ajuba belongs to the IL-1 signalling pathway where it modulates the IL-1-induced NF-κB activation by impacting the assembly and activity of the aPKC/p62/TRAF6 multiprotein signalling complex [Feng and Longmore, 2005].

Inside the nucleus, Ajuba LIM proteins were found to interact with the SNAG domain of Snail, a transcriptional repressor. Ajuba family members are recruited to the endogenous E-cadherin promoter, thus contributing to Snail-dependent repression of E-cadherin. This suggests that these proteins are essential regulators facilitating the communication between the surface of the cell and the nuclear response [Langer *et al.*, 2008]. Another study aiming at elucidating the function of Ajuba LIM proteins in the nucleus found that the protein arginine methyltransferase 5 (PRMT5) is recruited to Snail through the interaction with Ajuba, repressing the Snail target gene *E-cadherin*. There, PRMT5 binds to the PreLIM region and gets translocated into the nucleus in a Snail- and Ajuba-dependent manner. Therefore, PRMT5 is presented as a key component in the Snail-silencing complex through its interaction with Ajuba [Hou *et al.*, 2008].

The Ajuba subfamily of LIM proteins is expressed in organs abundant in epithelia, such as skin, lung, liver or kidney. It was shown that upon formation of cell layers, Ajuba was localised to cell-cell contacts [Goyal *et al.*, 1999; Kanungo *et al.*, 2000]. In primary human keratinocytes Ajuba was shown to co-localise with the cadherin adhesive complex at sites of cell-cell contacts, like cell-cell junctions. This localisation of Ajuba is in contrast to Zyxin localisation which is predominantly found at focal adhesion sites, again underlining that both families, the Ajuba and the Zyxin family, might have divergent functions. It was demonstrated that Ajuba is recruited to membrane cadherin adhesive complexes at adherens junctions after binding to α-catenin. In addition to α-catenin, another interaction partner of Ajuba, F-actin, was found interacting with the PreLIM region of Ajuba [Marie *et al.*, 2003]. Ajuba null mice are viable and appear healthy and fertile. However, primary skin keratinocytes isolated from these mice display abnormal cell-cell adhesion and defects in skin wound healing [Feng and Longmore, 2005]. The LIM domains target Ajuba to epithelial junctions through a regulated interaction with α-catenin [Kanungo *et al.*, 2000; Reinhard *et al.*, 1999], while the PreLIM domain of Ajuba directs its interaction with filamentous actin [Marie *et al.*, 2003]. The aforementioned data suggest that Ajuba may contribute to the bridging of cadherin adhesive complexes to the actin cytoskeleton through its interaction with α-catenin and F-actin. Therefore it may play a role in the formation or strengthening of adherens junctions [Marie *et al.*, 2003].

Although the exact mechanisms for these processes are not completely known and understood, the already obtained data give hints to the different roles of the Ajuba LIM proteins in the context of cellular processes. Based on the ability of Ajuba LIM proteins to shuttle between nucleus and cytoplasm there is a strong indication for them being involved in signal transduction between cell-cell junctions, cytoplasm and nucleus. One important complication in uncovering specific physiological roles is the possibility of functional redundancy between the Ajuba LIM family proteins Ajuba, LIMD1, and WTIP, which makes it difficult to analyse the distinct functions of the individual proteins.

1.5 Objective of the thesis

While it is proven that infections with high-risk HPV types cause cervical cancer, the role of cutaneous HPV types in the development of certain skin cancers is not fully understood. Thus, the oncogenic potential of the majority of cutaneous HPV types remains unclear, partly because of the high number of cutaneous types.

Previous studies identified several novel HPV types belonging to the genera alpha2 (HPV117), beta1 (HPV118), gamma7 (HPV134), and gamma11 (HPV148). Additionally, a yeast two-hybrid screening was performed on HPV4 E6 identifying five interaction candidates. To combine these results, the aim of this PhD thesis was to identify new interaction partners for the known and novel HPV types. Furthermore, the underlying mechanism of the successfully identified interaction of Ajuba with cutaneous HPV E6 proteins was studied, also upon UV-induced DNA damage. The major aims of this study therefore were:

(1) to verify the identified potential interaction partners for HPV4 E6 with respect to the novel HPV types;

(2) to map the protein binding region of E6 with Ajuba, once Ajuba was identified as the most promising binding partner;

(3) to analyse Ajuba's role in HPV E6 protein accumulation and DNA damage response;

(4) to examine the role of the p53 protein with HPV E6 and Ajuba.

Section 2

Results

2.1 Cutaneous HPV E6 proteins from the beta2, gamma1, and gamma11 genera interact with Ajuba

In order to identify new interaction partners for known and novel HPV types, a yeast two-hybrid screening was performed with the E6 protein of HPV4, a well-known HPV type from the gamma genus [Heilman *et al.*, 1980]. This task was processed by the South Korean company PanBioNet prior to the start of this thesis. The company identified five putative HPV4 E6 interacting candidates: Programmed cell death 6-interacting protein (PDCD6IP, Alix), an uncharacterised protein named Chromosome 9 open reading frame 102 (C9orf102), Ajuba, Leupaxin and Plectin (Fig. 2.1). The binding of these five potential interaction proteins to HPV4 E6 had to be confirmed, but first it was assessed whether it was possible to analyse all of them. Of the five above mentioned proteins, Plectin was standing out in particular because of its size. Being larger than 500 kDa, it excluded from the study, because it was considered unfeasible to deal with this protein at full length. Hence, it was decided to first work with the remaining proteins, which could be handled as full-length constructs.

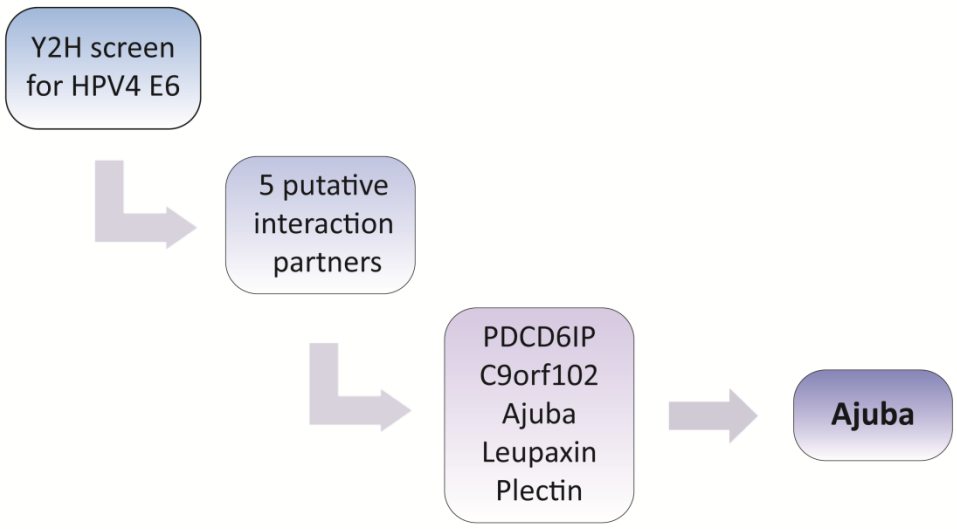

Figure 2.1: Schematic illustration of the workflow of the identification of binding partners of novel HPV types.
Prior to the project start a Yeast Two-Hybrid (Y2H) screening with HPV4 E6 was performed, identifying five putative interaction partners. These were Programmed cell death 6-interacting protein (PDCD6IP), the uncharacterised protein Chromosome 9 open reading frame 102 (C9orf102), Ajuba, Leupaxin, and Plectin. After initial experiments (see section 2.1.1) only Ajuba displayed *in vitro* and *in vivo* binding.

2.1.1 Identification of Ajuba and C9orf102 as promising candidates for interaction with HPV E6 proteins

In order to study the presence of a direct interaction of HPV E6 proteins with PDCD6IP, Leupaxin, C9orf102 or Ajuba, glutathione S-transferase (GST) pull-down experiments (see section 5.3.3) were performed (Fig. 2.2). The full-length forms of the above mentioned proteins were ^{35}S-radioactively labelled by *in vitro* translation (see section 5.3.1) and their binding to purified GST-tagged E6 fusion proteins of various HPV types was tested. Purified GST protein was used as a negative control to exclude the possibility of unspecific binding to the N-terminal GST-tag of the fusion proteins. To visualise proteins loaded on the gel and to assess the protein concentration used for the GST pull-down experiments, Coomassie staining of the SDS-PAGE gel was performed. Additionally, 10% of total ^{35}S-radioactively labelled *in vitro* translated proteins were applied to the SDS-PAGE gels as input, to estimate binding intensity. Figure 2.2A depicts the GST pull-down of PDCD6IP. There, no interactions were observed with either of the E6 proteins of the novel HPV types, belonging to the genera alpha2 (HPV117), beta1 (HPV118), gamma7 (HPV134), gamma11 (HPV148), nor with HPV4 E6 (gamma1), used as a Y2H positive control. PDCD6 (Programmed cell death protein 6) was included as an accurate positive control, which indeed was found to interact with PDCD6IP. Hence, the method itself worked under the chosen conditions, but distinct interactions with the E6 proteins could not be detected. Due to the lack of *in vitro* interaction with the novel HPV E6 proteins, PDCD6IP was excluded from further studies. Figure 2.2B shows the GST pull-down of Leupaxin (LPXN) with the E6 proteins of the novel HPV types as well as HPV4 E6 and HPV16 E6. Here, very weak interactions were observed between Leupaxin and HPV16 E6 or HPV148 E6. Both bands were however much weaker than the 10% input signal and were thus not considered as definite *in vitro* interactions. As another putative interaction partner C9orf102 was analysed (Fig. 2.2C). Here, GST-HPV4 E6 and GST-HPV148 E6, both belonging to the gamma genus, were found to strongly interact with the full-length protein of C9orf102 *in vitro*. Therefore, it was decided to test whether the *in vitro* interaction of C9orf102 with HPV148 E6 could also be verified *in vivo* (Fig. 2.3). Finally, the interaction of Ajuba with different HPV E6 proteins was assessed. Figure 2.2D depicts a strong interaction between full-length Ajuba protein and GST-HPV23 E6 as well as GST-HPV148 E6. Additionally, weak interactions with GST-HPV16 E6 and GST-HPV118 E6 were observed. On the contrary, GST-tagged E6 fusion proteins of HPV4, HPV117, and HPV134 failed to interact with Ajuba *in vitro* in this experimental setting.

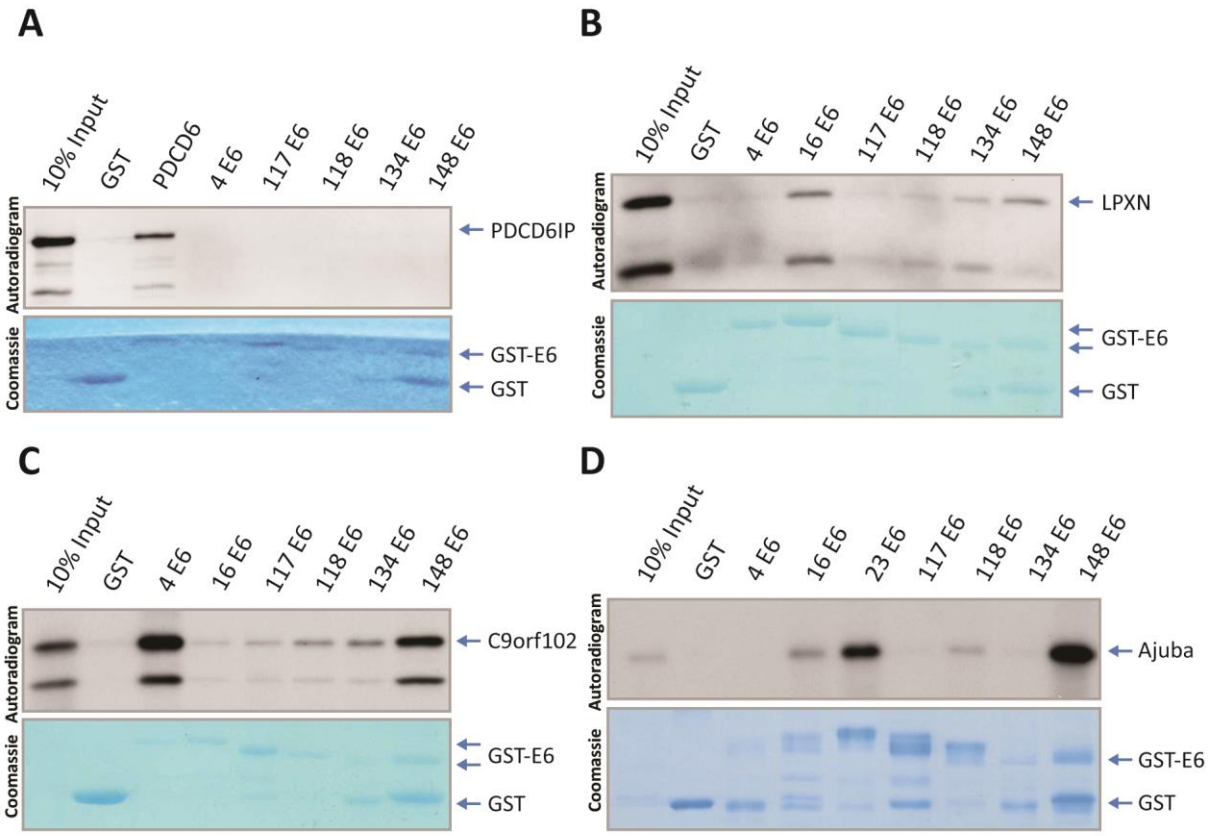

Figure 2.2: GST pull-down of novel HPV E6 proteins with the putative interaction partners of HPV4 E6.
GST-tagged E6 fusion proteins of diverse HPV types, GST or a positive control were incubated with *in vitro* translated ^{35}S-radioactively labelled **(A)** PDCD6IP, **(B)** Leupaxin (LPXN), **(C)** C9orf102 or **(D)** Ajuba. Uncoupled GST was used as a negative control. GST pull-down experiments were analysed by SDS-PAGE and Coomassie staining (lower panels). The gels were dried and exposed to X-ray films (Autoradiograms, upper panels). 10% of the respective total ^{35}S-radioactively labelled proteins were used as input.

2.1.2 C9orf102 does not interact with HPV148 E6 *in vivo*

In order to assess whether the identified protein interaction of C9orf102 with the HPV E6 proteins (Fig. 2.2C) also occurred *in vivo*, co-immunoprecipitation (Co-IP) analyses were performed using HA-tagged HPV148 E6 protein. Therefore, HEK293 cells were used because of their characteristic of being HPV-negative, easy to transfect and their ability to produce large amounts of proteins. Hence, HA-tagged HPV148 E6 and Flag-tagged C9orf102 proteins were expressed in HEK293 cells and complex formation was determined by Co-IP analyses (see section 5.4) using target protein-specific antibodies. As an input control, 30% of whole cell lysates were analysed for protein expression by Western blotting. To eliminate the possibility of unspecific protein binding, Co-IPs were additionally performed in the absence of antibody-specific target proteins. Co-IP analyses using both anti-HA and anti-Flag antibodies showed that Flag-C9orf102 and HPV148 E6-HA proteins were not able to form a complex *in vivo* (Fig. 2.3). Therefore the potential interaction partner protein C9orf102 was excluded from further experiments as it failed to interact with HPV148 E6 *in vivo*, an essential criterion, as not every *in vitro* interaction can also be verified *in vivo*.

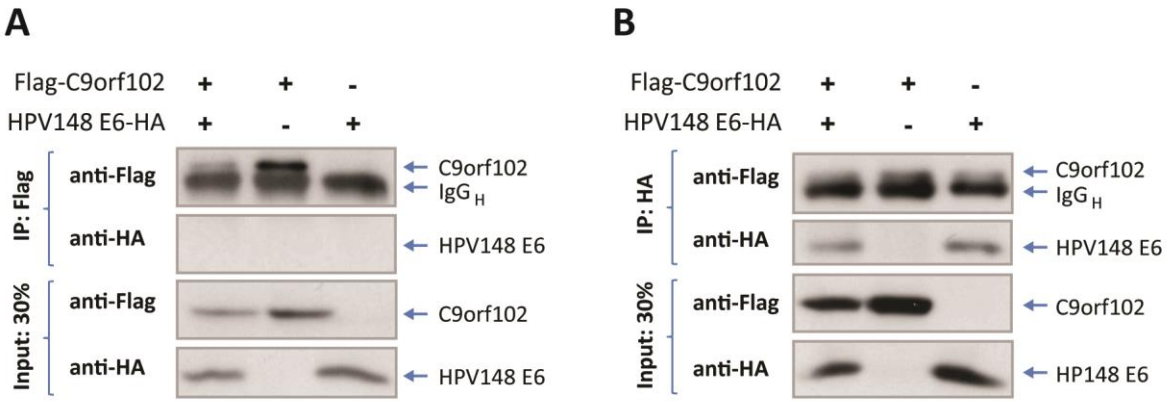

Figure 2.3: C9orf102 protein does not co-precipitate with HPV148 E6 *in vivo*.
HEK293 cells were transfected with HA-tagged HPV148 E6 and/or Flag-C9orf102 and immunoprecipitated with **(A)** Flag (IP: Flag) or **(B)** HA (IP: HA) antibodies. Complexes were analysed by Western blotting (IP, upper panel). As an input control, 30% of cell lysates were analysed for protein expression (Input: 30%, lower panel). The heavy chain of the precipitating antibody (IgG_H) is indicated.

2.1.3 Ajuba interacts with cutaneous HPV E6 proteins from the beta2, gamma1 and gamma11 genera *in vivo*

In order to evaluate whether the *in vitro* interaction of Ajuba with the HPV E6 proteins did also occur *in vivo*, Co-IP experiments were performed. Therefore, HA-tagged HPV4 E6, HPV23 E6, HPV148 E6 (Fig. 2.4A-C), HPV16 E6, HPV117 E6 proteins (Fig. 2.5A and B) and Flag-Ajuba were expressed in HEK293 cells and complex formation was investigated by Co-IP analyses. As input control, 15% of whole cell lysates were analysed for protein expression by Western blotting. To exclude unspecific protein binding, controls IPs in the absence of antibody-specific target proteins were performed. Co-IP analyses using an anti-Flag antibody revealed that Flag-Ajuba and HPV4 E6-HA, HPV23 E6-HA and HPV148 E6-HA proteins were indeed able to form a complex *in vivo* (Fig. 2.4). On the contrary, the HA-tagged HPV16 E6 protein, which was shown to weakly bind Ajuba *in vitro* (Fig. 2.2D), failed to co-precipitate with Flag-Ajuba *in vivo*. The same occurred for HPV117 E6-HA, except that for this protein it had already not been possible to show *in vitro* binding, which made it an additional negative control.

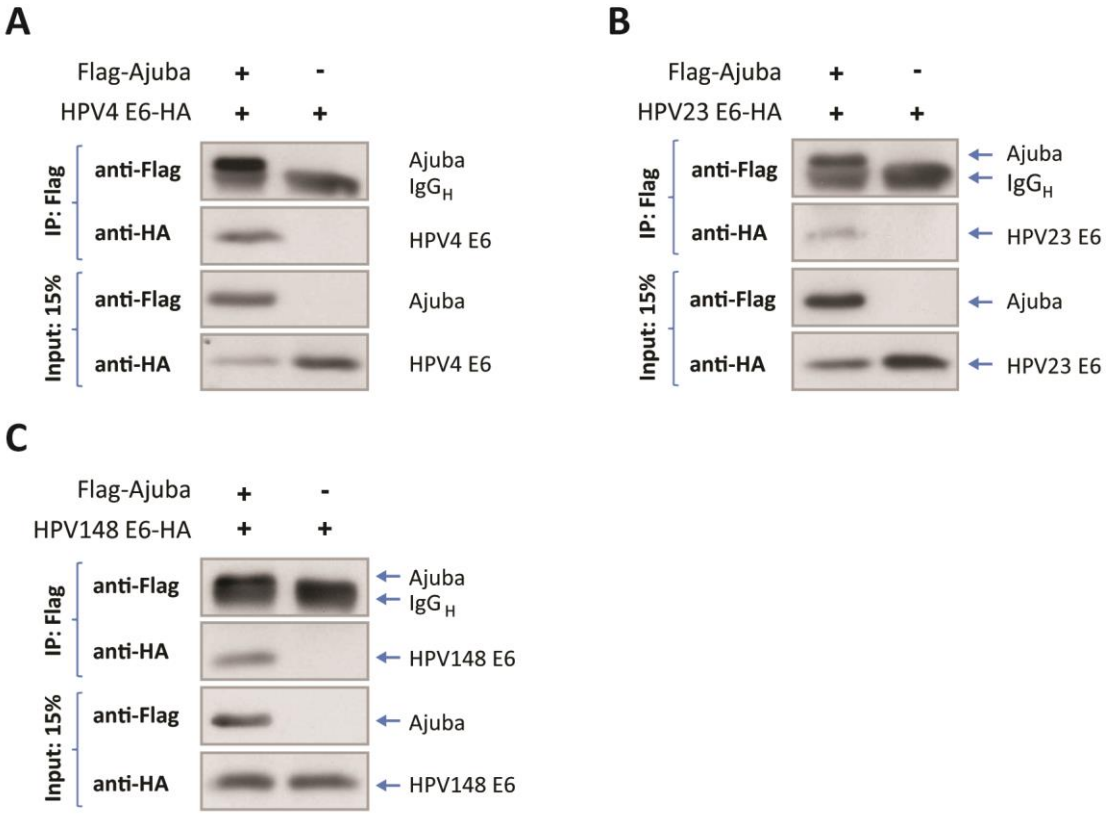

Figure 2.4: Ajuba protein co-precipitates with HPV4 E6, HPV23 E6 and HPV148 E6 *in vivo*.
HEK293 cells were transfected with HA-tagged HPV4 E6 **(A)**, HPV23 E6 **(B)** or HPV148 E6 **(C)** and/or Flag-Ajuba and immunoprecipitated with Flag antibody (IP: Flag). Complexes were analysed by Western blotting (IP, upper panels). As an input control, 15% of cell lysates were analysed for protein expression (Input: 15%, lower panels). The heavy chain of the precipitating antibody (IgG_H) is indicated.

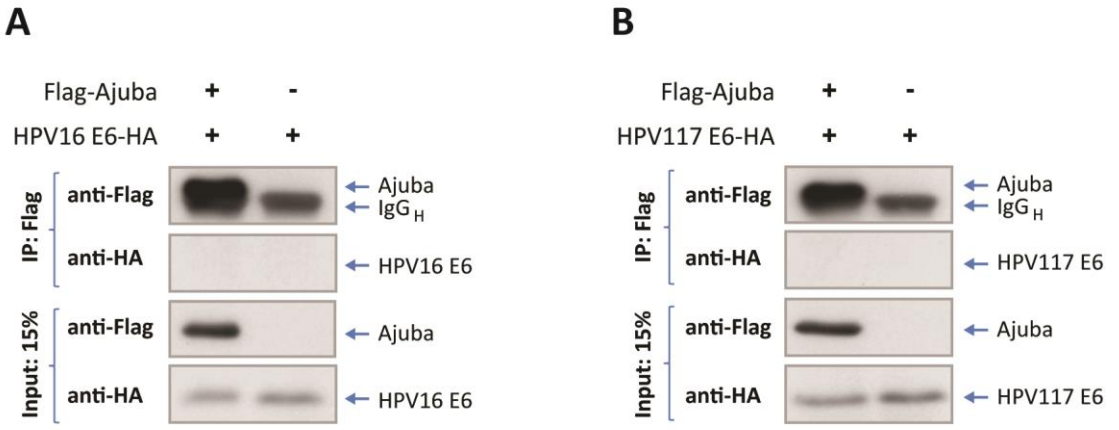

Figure 2.5: Ajuba protein does not co-precipitate with HPV16 E6 and HPV117 E6 *in vivo*.
HEK293 cells were transfected with HA-tagged HPV16 E6 **(A)** or HPV117 E6 **(B)** and/or Flag-Ajuba and immunoprecipitated with Flag antibody (Flag: IP). Complexes were analysed by Western blotting (IP, upper panels). As an input control, 15% of cell lysates were analysed for protein expression (Input: 15%, lower panels). The heavy chain of the precipitating antibody (IgG_H) is indicated.

2.1.4 Ajuba interacts with HPV4 E6, HPV23 E6, and HPV148 E6 through its PreLIM domain

In order to map the binding region required for HPV E6 protein interaction in more detail (Fig. 2.2D), two smaller deletion constructs, the PreLIM and LIM domains of Ajuba (Fig. 2.6), were employed to analyse GST-HPV E6 protein binding. Figure 2.6 shows a schematic overview of the Ajuba full-length protein and both deletion constructs which were analysed for direct interaction to GST-tagged HPV E6 proteins. The N-terminal part of Ajuba, comprising its PreLIM region, was found to strongly interact with HPV23 E6 and HPV148 E6, but also with HPV4 E6 and slightly with HPV118 E6 (Fig. 2.7A). By contrast, deletion of the N-terminus, leaving the LIM region of Ajuba, abolished the binding to the above mentioned HPV E6 proteins, but showed binding of HPV16 E6 to the LIM domain (Fig. 2.7B).

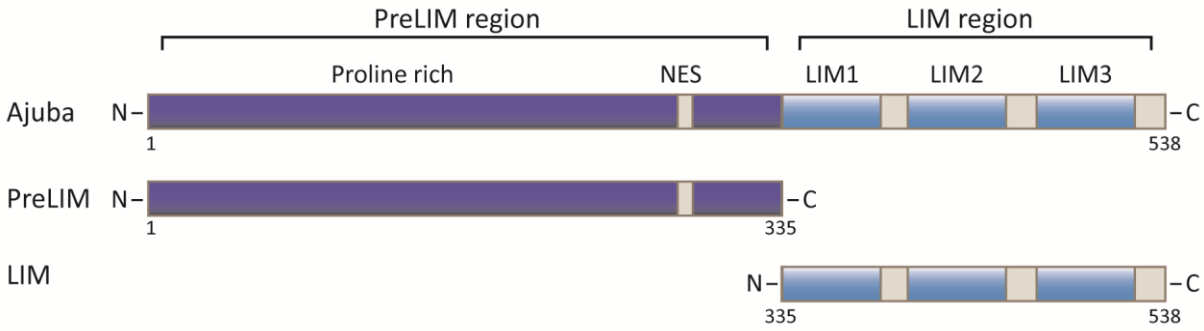

Figure 2.6: A schematic overview of the *in vitro* transcribed and translated Ajuba constructs analysed in GST pull-down experiments.
The Ajuba full-length protein can be separated into two main domains, the N-terminal PreLIM region and the C-terminal LIM region. The PreLIM region is a non-homologous domain rich in proline and contains a nuclear export signal (NES). The LIM region consists of three homologous C-terminal LIM domains.

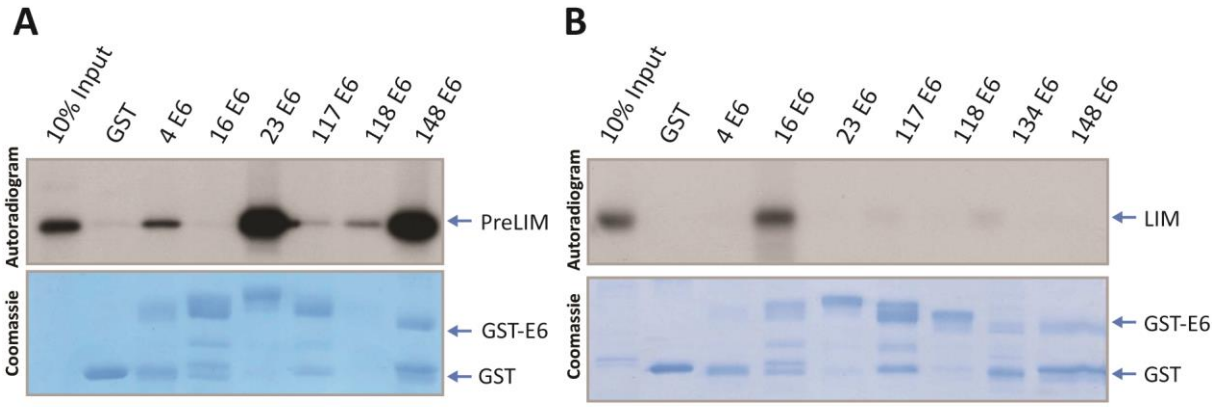

Figure 2.7: HPV4 E6, HPV23 E6 and HPV148 E6 interact with Ajuba via its PreLIM domain *in vitro*.
GST-tagged E6 fusion proteins of various HPV types or GST alone were incubated with *in vitro* translated ^{35}S-radioactively labelled **(A)** Ajuba's N-terminal PreLIM domain (PreLIM) or **(B)** Ajuba's C-terminal LIM domain (LIM). GST was used as negative control. GST pull-down experiments were analysed by SDS-PAGE and Coomassie staining (lower panels). Gels were dried and exposed to X-ray films (Autoradiograms, upper panels). 10% of total ^{35}S-radioactively labelled Ajuba was used as input.

2.2 HPV4-, HPV23-, and HPV148 E6 proteins co-localise with Ajuba in the cytoplasm

The preceding experiments depicted *in vitro* and *in vivo* interactions of cutaneous HPV E6 proteins from the beta and gamma genera with Ajuba. In order to determine whether the interaction was significant for the cellular localisation of the HPV E6 proteins and Ajuba, immunofluorescence analyses were performed (see section 5.5.7). For this and further parts of the study, U2OS cells were used due to their characteristic of undergoing apoptosis following genotoxic stress [Allan and Fried, 1999]. First, the cellular localisation of HA-tagged HPV4 E6, HPV16 E6, HPV23 E6 and HPV148 E6 proteins as well as Ajuba was investigated using immunofluorescence microscopy. Therefore, U2OS cells were transfected with expression plasmids encoding HA-tagged HPV E6 proteins or Flag-tagged Ajuba protein. 48h later, cells were fixed and stained with either anti-HA or anti-Flag antibodies. Immunofluorescence microscopy exposed a diffuse cytoplasmic localisation pattern of HA-tagged HPV4 E6 and HPV16 E6 proteins. HPV23 E6 and HPV148 E6 proteins, on the other hand, showed a strong nuclear localisation with a diffuse expression pattern in the nucleus as well as in the cytoplasm (Fig. 2.8A). When expressed alone, Flag-tagged Ajuba revealed a scattered, predominantly cytoplasmic localisation (Fig. 2.8B; Fig. 2.9, upper panel), which was consistent with previous studies [Hou *et al.*, 2008].

In order to examine the cellular localisation of Ajuba in the presence of the various HPV E6 proteins via immunofluorescence analyses, U2OS cells were transfected with expression plasmids for both Flag-Ajuba and HA-tagged HPV4 E6, HPV16 E6, HPV23 E6 and HPV148 E6 or the empty vector control pPK-CMV-E3 (Fig. 2.9).

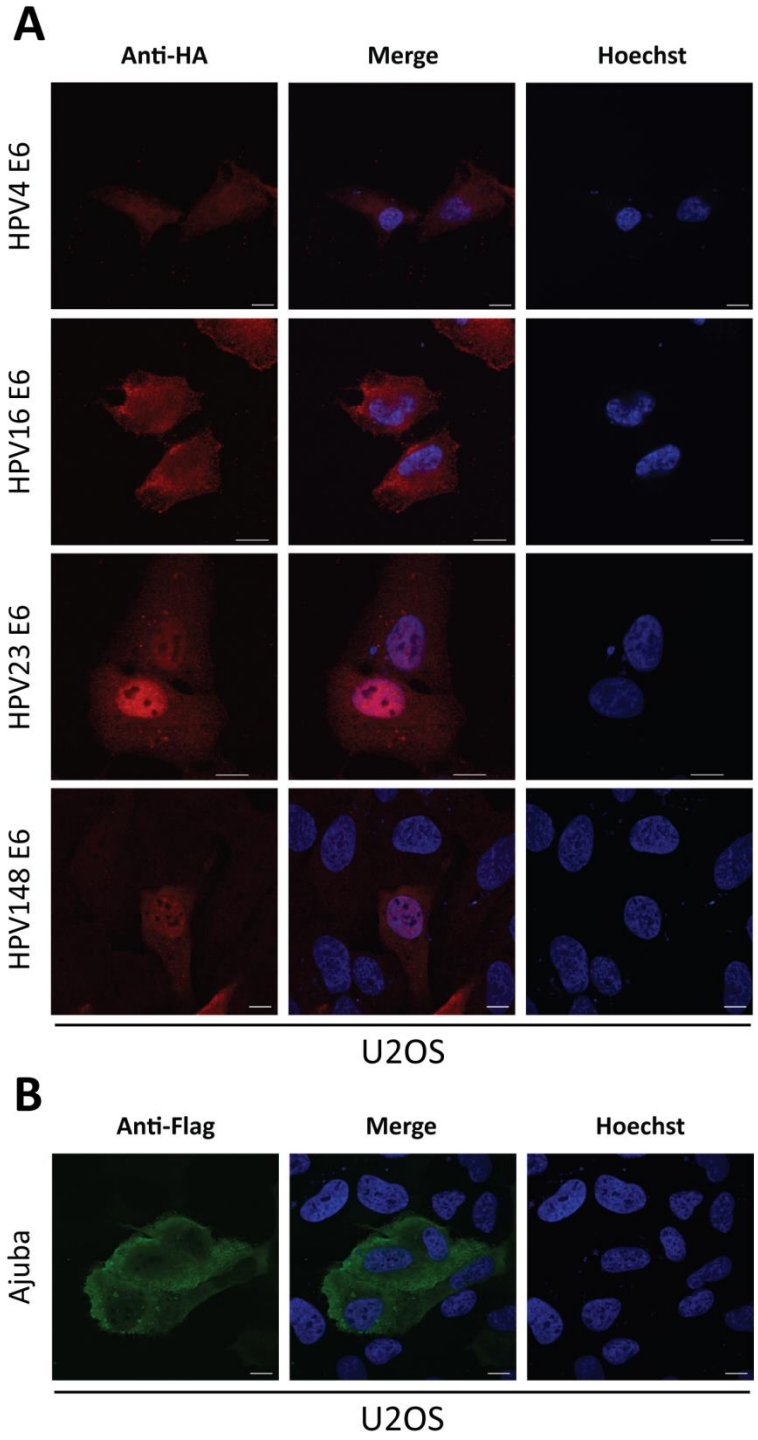

Figure 2.8: HPVE6 proteins are localised throughout the cell in a diffuse pattern.
U2OS cells were transiently transfected with **(A)** HA-tagged HPV4 E6, HPV16 E6, HPV23 E6 or HPV148 E6 or with **(B)** Flag-tagged Ajuba expression plasmids and then detected by immunofluorescence microscopy. Nuclear DNA (blue) was stained with Hoechst. The localisation of the E6 proteins is shown in red, Ajuba is represented in green. The scale bar represents 10µm.

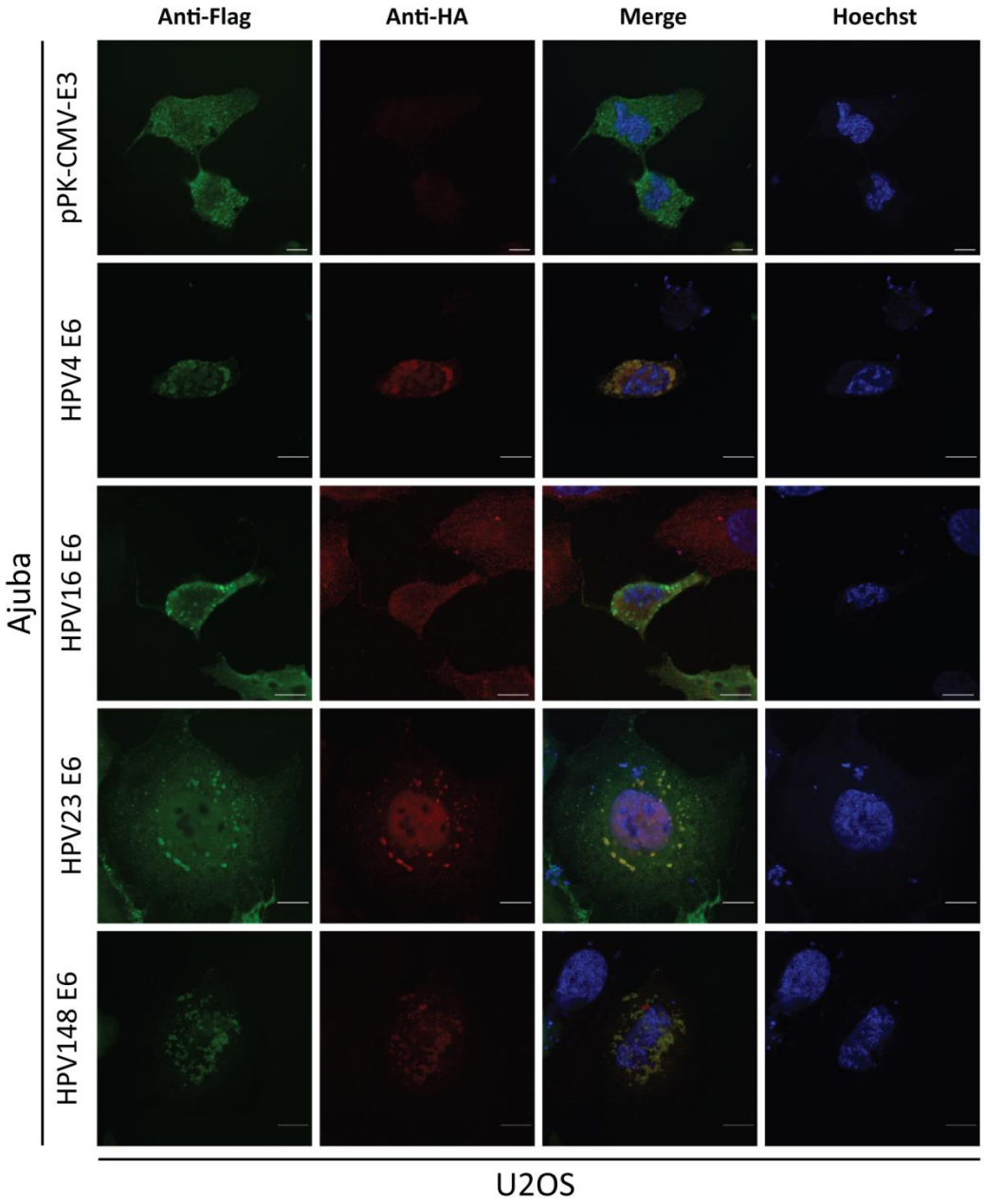

Figure 2.9: Ajuba co-localises with HPV4 E6, HPV23 E6 and HPV148 E6 in the cytoplasm.
U2OS cells were transiently transfected with the empty control vector pPK-CMV-E3, HA-tagged HPV4 E6, HPV16 E6, HPV23 E6 or HPV148 E6 in combination with Flag-Ajuba and then detected by immunofluorescence microscopy. Co-localisation of HPV E6-HA proteins (red) and Flag-Ajuba (green) is represented on merged images (yellow). Nuclear DNA (blue) was stained with Hoechst. The scale bar represents 10µm.

Upon co-expression of individual E6 proteins and Ajuba, the distribution of each protein was not significantly changed. However, co-localisation could be observed in case of Ajuba and HPV4 E6, HPV23 E6 and HPV148 E6 (Fig. 2.9) in distinct areas in the cytoplasm, confirming the interaction observed in the Co-IP experiments (Fig. 2.4). To ensure that the visualised co-localisation was dependent on the interaction of Ajuba with the above mentioned HA-tagged HPV E6 proteins, the cellular localisation of HPV16 E6, which was previously shown not to bind Ajuba *in vivo* (Fig. 2.5A),

was also analysed in the presence of Flag-tagged Ajuba. The prevalent cytoplasmic Ajuba staining did not co-localise with the diffuse HPV16 E6 staining (Fig. 2.9), demonstrating that Ajuba indeed co-localises specifically with the E6 proteins of HPV4, HPV23 and HPV148.

2.3 Ajuba's role in HPV E6 protein accumulation and DNA damage response

2.3.1 HPV23 E6 and HPV148 E6 proteins accumulate upon Ajuba overexpression

To gain insight into the general endogenous distribution of the Ajuba protein, different human epithelial cell lines were analysed for its expression by Western blotting. Interestingly, the highest expression levels were found in HPV16 E6, -E7, and -E6/E7-positive keratinocytes as well as in the metastatic HPV16-positive cervical carcinoma cell line CaSki. Medium expression levels were detected in the HPV-negative cell line C-33 A, the non-small cell lung carcinoma cell line H1299 and the osteosarcoma cell line U2OS. Background protein levels were present in the neonatal human primary keratinocytes (HPKn), the near-diploid keratinocyte cell line NIKS [Allen-Hoffmann *et al.*, 2000], the HPV16-positive carcinoma cell line SiHa and HPV18-positive HeLa cells and the malignant melanoma cell line SK-MEL-28 (Fig. 2.10).

All these cell lines were tested to determine whether Ajuba protein levels in general differ between HPV-positive and HPV-negative cell lines. As the result was not definite, it was tested whether overexpression of HPV E6 proteins or Ajuba have effects on the respective other protein.

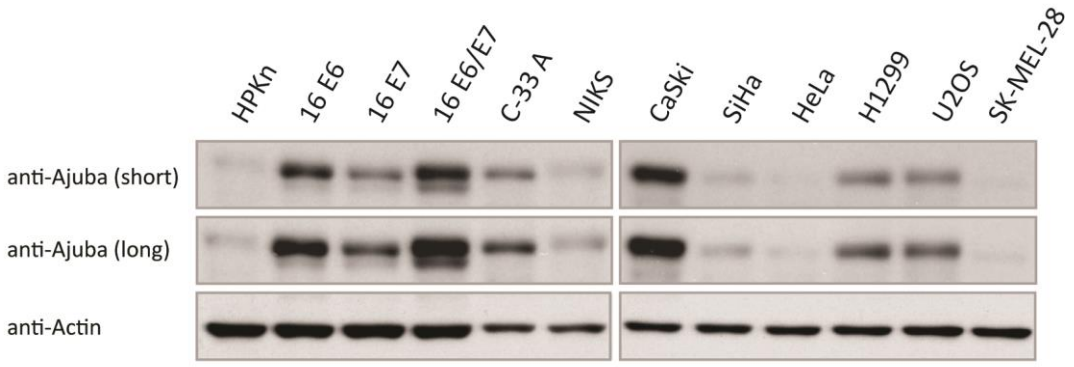

Figure 2.10: Expression of endogenous Ajuba varies in different human cell lines.
Endogenous protein levels of Ajuba were analysed by Western blotting in various cell lines. These were neonatal Human Primary Keratinocytes (HPKn), HPV16 E6, -E7, or -E6/E7 -positive primary keratinocytes, the HPV-negative cell line C-33 A, a spontaneously immortalised near-diploid keratinocyte cell line (NIKS), HPV16-positive CaSki and SiHa cells, and HPV18-positive HeLa cells, a non-small cell lung carcinoma cell line (H1299), an osteosarcoma cell line (U2OS) and the melanoma cell line (SK-MEL-28). Equal protein loading was monitored by using actin as control.

All these cell lines were tested to determine whether Ajuba protein levels in general differ between HPV-positive and HPV-negative cell lines. As the result was not definite, it was tested whether overexpression of HPV E6 proteins or Ajuba have effects on the respective other protein. Therefore, the HPV-negative p53-null cell line H1299 [Radhakrishna Pillai *et al.*, 2004] was chosen for Western blot analyses to examine this relation of Ajuba and the E6 proteins of HPV23 and HPV148, omitting a potential influence of the p53 protein. As previous study demonstrated that cutaneous HPV23 E6 accumulated upon DNA damage [Muschik *et al.*, 2011], it was decided to analyse whether this effect could also be observed in the chosen model system. Additionally, the osteosarcoma cell line U2OS was used due to its wild type p53 status, to analyse the effects of the interaction of Ajuba with HPV E6 proteins on the p53 status. Further analysis of HPV4 E6 in the context of Ajuba expression levels was adjourned and the focus was put on the novel HPV148 E6 protein and the already well characterised HPV23 E6 protein [Muschik *et al.*, 2011].

In order to evaluate whether the interaction of Ajuba with HPV23 E6 and HPV148 E6 affected E6 protein accumulation, co-transfection experiments were performed. Therefore, HA-tagged HPV23 E6 and HPV148 E6 as well as Flag-Ajuba were expressed in H1299 cells. Protein levels were assessed by Western blotting. Intriguingly, a concomitant increase in Flag-Ajuba protein levels was observed upon increasing expression of HPV23 E6-HA and HPV148 E6-HA (Fig. 2.11A and B). Moreover, Flag-Ajuba overexpression exhibited the same effect on HPV148 E6-HA protein levels (Fig. 2.11C), demonstrating that the accumulation of at least HPV148 E6 was reversible. Additionally, a GFP expression plasmid, harbouring the same promoter as the HPV E6 expression constructs, was used together with Flag-Ajuba to prove that the increase in protein levels was due to the interaction itself and not because of increased promoter availability (Fig. 2.11D).

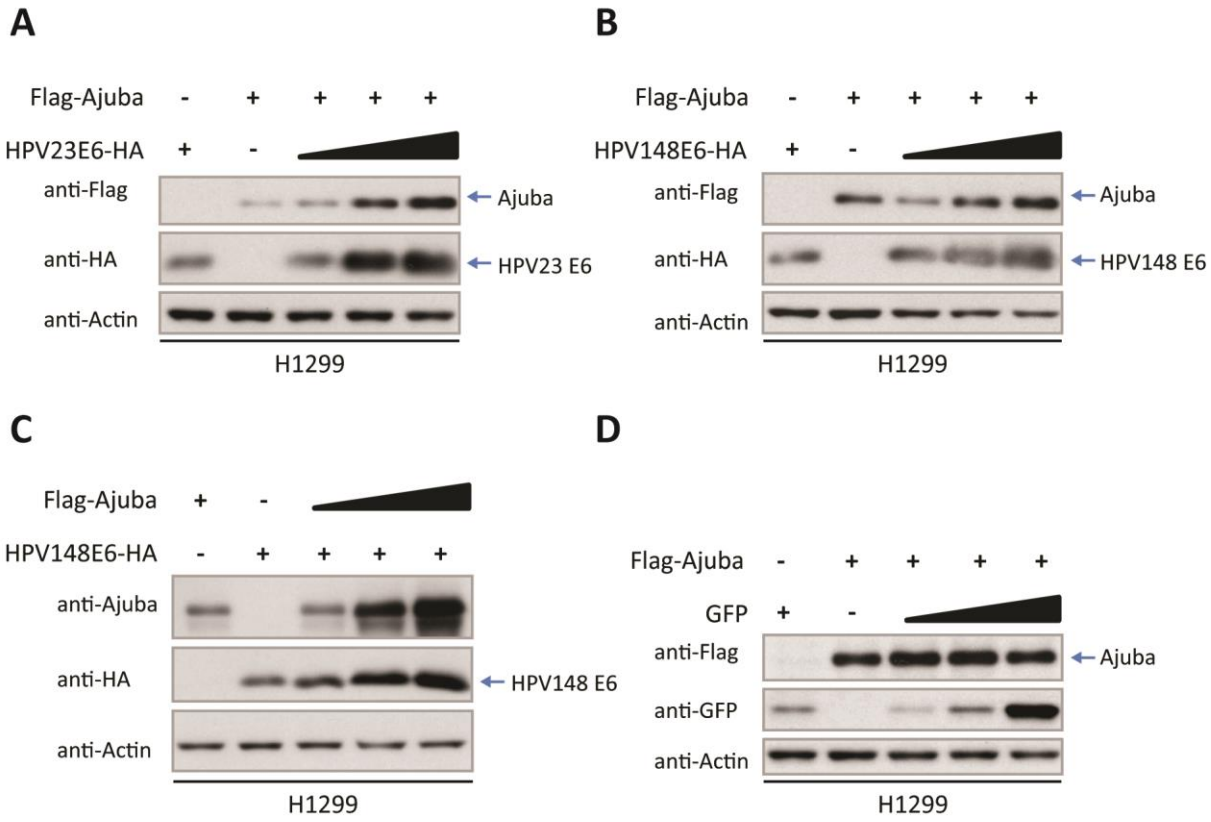

Figure 2.11: Increased expression of HPV23 E6 and HPV148 E6 leads to an accumulation of Ajuba.
H1299 cells were transiently transfected with HA-tagged HPV23 E6 **(A)**, HPV148 E6 **(B, C)**, GFP **(D)** and/or Flag-Ajuba. Protein levels were analysed by Western blotting. Actin was used to assess equal loading.

To confirm that Ajuba is essential for the accumulation of HPV23 E6 and HPV148 E6 proteins, endogenous Ajuba was down-regulated using siRNA in stably transfected H1299 and U2OS cells. Protein expression of Ajuba and the E6 proteins was determined by Western blot analyses (see section 5.2.5). Indeed, a reduction in HPV23 E6 and HPV148 E6 protein levels was observed in Ajuba knockdown cells which was more substantial in H1299 cells (Fig. 2.12A) than in U2OS cells (Fig. 2.12B), corroborating a direct role for Ajuba in HPV E6 protein accumulation. Furthermore, p53 protein levels were reduced in Ajuba knockdown cells (Fig. 2.12B), indicating a role for the p53 protein when expressed together with Ajuba and HPV E6 proteins. On the contrary, treatment with scramble control siRNA (siScr) did not affect Ajuba or HPV E6 protein levels (Fig. 2.12).

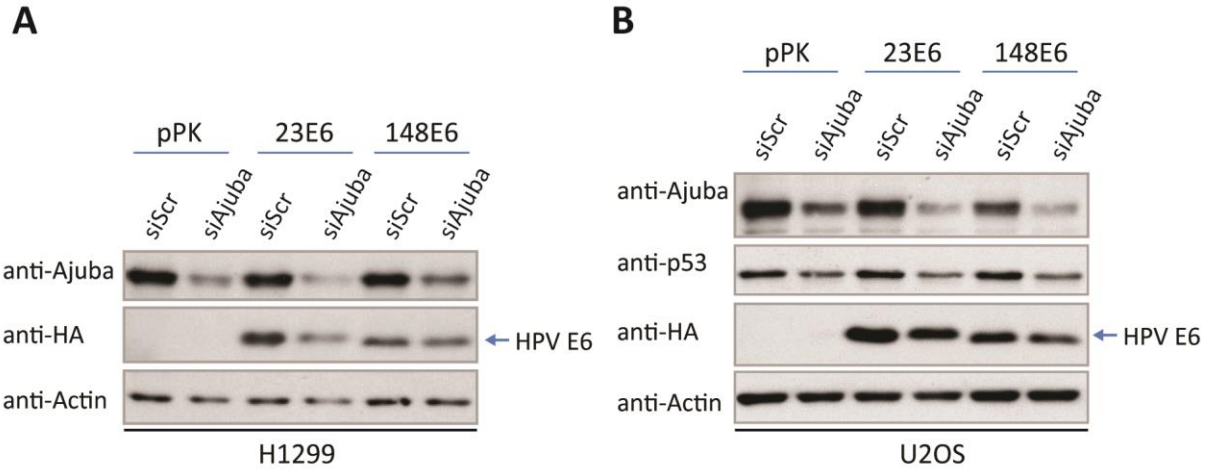

Figure 2.12: Down regulation of Ajuba by siRNA affects HPV23 E6 and HPV148 E6 protein levels.
Stably transfected **(A)** H1299 or **(B)** U2OS cells, expressing HA-tagged HPV23 E6 or HPV148 E6, were transfected with control siRNA (siScr) or with siRNA against Ajuba (siAjuba) for specific Ajuba down-regulation. Ajuba knockdown efficiency and E6 protein levels were determined by Western blotting. pPK-CMV-E3 (pPK) was used as empty vector control. Actin was used to assess equal loading.

2.3.2 HPV23 E6 and HPV148 E6 protein levels decrease upon DNA damage

Previous studies reported that LIM domain proteins might be involved in the repression of the DNA damage response at telomeres [Sheppard *et al.*, 2011]. Ajuba in particular was described to repress the ATR-mediated DNA damage response [Kalan *et al.*, 2013]. To analyse this hypothesis in the context of this study here, p53 wild type U2OS cells were used for Western blot analyses to study the effect of UVB- or chemotherapeutically induced DNA damage on HPV E6 proteins (see section 5.5.6). Therefore, U2OS cells stably expressing HA-tagged HPV23 E6 or HPV148 E6 were treated with different dosages of UVB (0, 300, or 1,000 J/m^2) or incubated with medium supplemented with Adriamycin (ADR), an agent intercalating with DNA and RNA [Momparler *et al.*, 1976] (Fig. 2.13). Remarkably, DNA damage generated by either UVB irradiation or ADR treatment resulted in the degradation of endogenous Ajuba and in a coinciding decrease in HPV E6 protein (Fig. 2.13A and B). Protein levels of p53 increased upon rising irradiation doses (Fig. 2.13A) and ADR incubation times (Fig. 2.13B). PARP protein expression and its cleavage were analysed to determine if the cells underwent apoptosis [Boulares *et al.*, 1999]. Indeed, stably transfected U2OS cells expressing the HA-tagged HPV23- and HPV148 E6 proteins showed PARP cleavage upon the longest exposure to ADR (Fig. 2.13B).

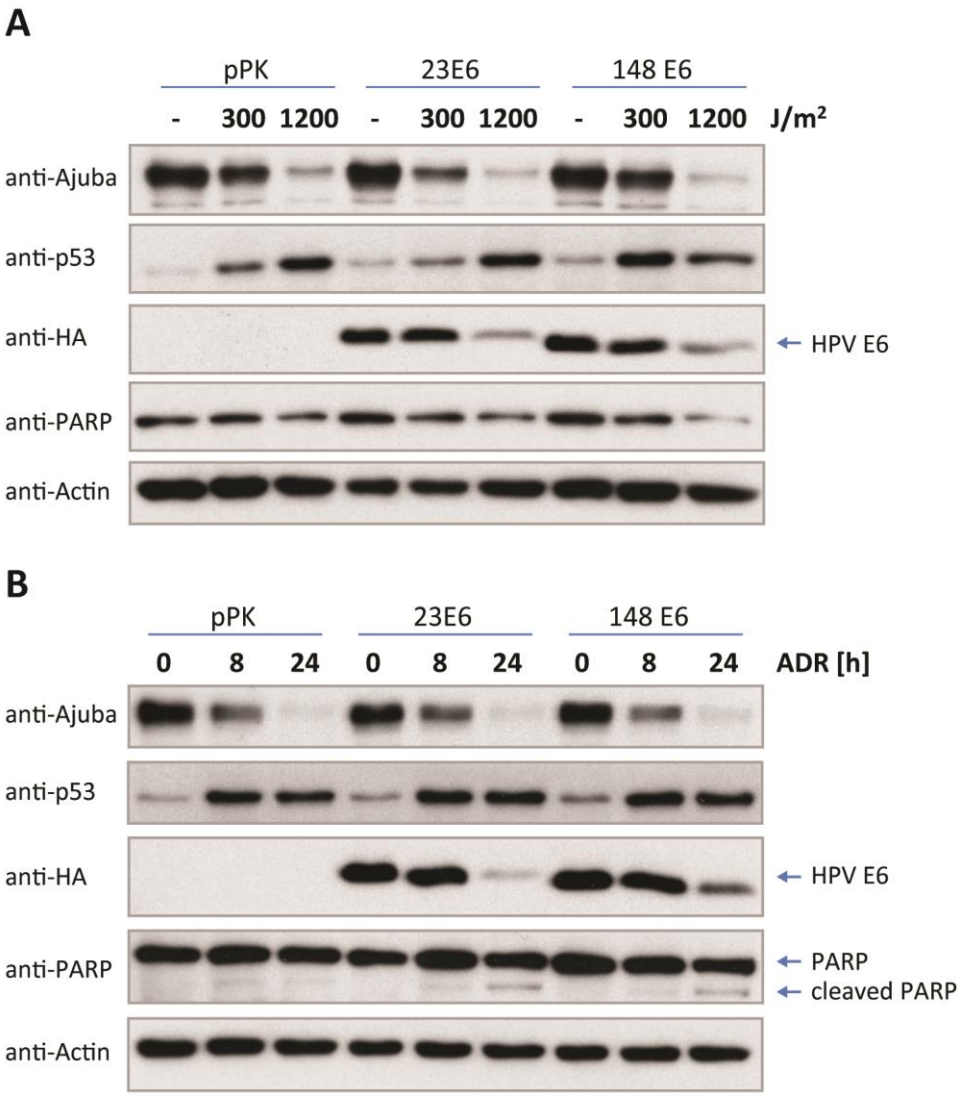

Figure 2.13: DNA damage leads to a decrease in HPV23 E6 and HPV148 E6 protein levels.
Stably transfected U2OS cells were treated with **(A)** different dosages of UVB (0, 300, 1,000 J/m^2) for 24h or **(B)** Adriamycin (1µg/mL; ADR) and harvested at indicated time points. Protein levels were analysed by Western blotting. Actin was used to assess equal loading.

2.4 HPV23 E6, HPV148 E6 and Ajuba proteins undergo a complex formation with the p53 protein

The evident involvement of the p53 protein in the Ajuba and HPV E6 complex seen in the siRNA knockdown (Fig. 2.12) and the DNA damage experiments (Fig. 2.13) encouraged the question whether an additional, larger complex would be formed when all three proteins (Ajuba, p53 and HPV E6) come together. Therefore, HA-tagged HPV23 E6 (beta1) or HPV148 E6 (gamma11), YFP-p53 and Flag-Ajuba were expressed in H1299 cells and complex formation was analysed in co-immunoprecipitation assays (see section 5.4). As an input control, 10% or 15% of whole cell lysates were analysed for respective protein levels by Western blotting. As previously shown, (Fig. 2.4B and C) Flag-Ajuba could be efficiently co-precipitated with HPV23 E6-HA and HPV148 E6-HA (Fig. 2.14A

and B). When performing a Flag-IP, no interaction was observed between Flag-Ajuba and p53 (Fig. 2.14A and B). Interestingly, a complex formation was detected between Ajuba, p53 and HPV148 E6-HA (Fig. 2.14B), but no interaction was seen for HPV23 E6-HA (Fig. 2.14A).

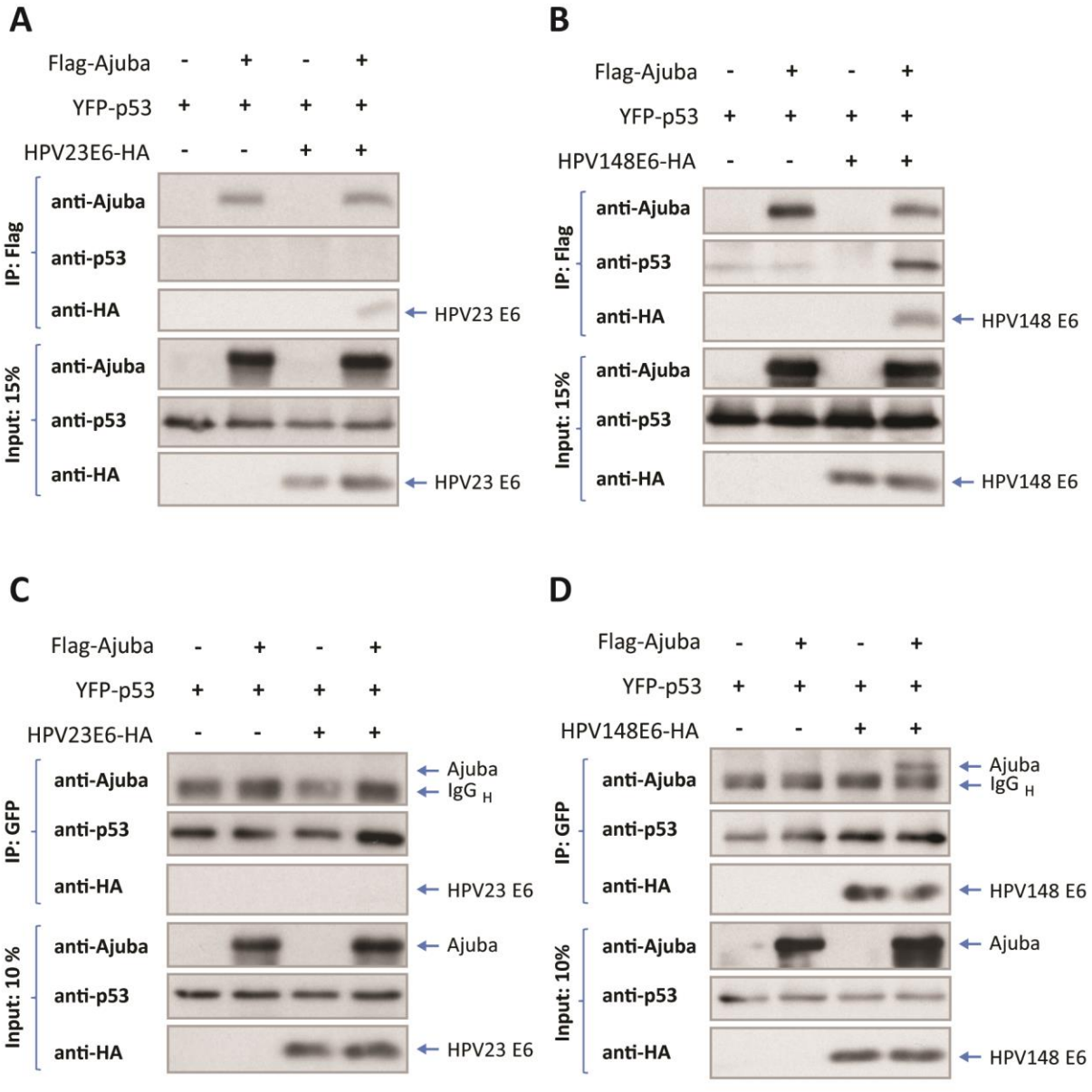

Figure 2.14: p53 forms a complex with Ajuba and HPV148 E6.
H1299 cells were transfected with YFP-p53 and Flag-Ajuba either alone or in combination with HA-tagged HPV23 E6 **(A, C)** or HPV148 E6 **(B, D)** and immunoprecipitated with Flag (IP: Flag) or GFP (IP: GFP) antibodies. Complexes were analysed by Western blotting (upper panels). As input control, 10% or 15% of respective cell lysates were analysed for protein levels (Input, lower panels). The heavy chains of the precipitating antibodies (IgG_H) are indicated.

To address this particular observation from another angle, the same experimental setup was used, but instead of a Flag-IP a GPF-IP was performed. A GFP-IP was chosen, because the GFP antibody can bind to the YFP part of YFP-p53 very efficiently, YFP being a point mutatant of GFP [Wachter *et al.*, 1998]. Moreover, YFP-p53 was transfected in every reaction, whereas Flag-Ajuba was

not. Although the GFP-IP clearly worked, again no complex formation could be observed for HPV23 E6, Ajuba and p53 (Fig. 2.14C). On the other hand, HPV148 E6 showed a clear complex formation with Ajuba and p53. In addition, a novel interaction between p53 and HPV148 E6 could be visualised (Fig. 2.14D). Hence, the results demonstrate a strong complex formation between HPV148 E6-HA, Ajuba and p53 that was highly specific for HPV148 E6 and not for HPV23 E6.

2.4.1 HPV148 E6 interacts with p53 *in vitro* and *in vivo*

The co-immunoprecipitation of the HPV E6 proteins with Ajuba and p53 prompted the question, whether the p53 protein indeed binds to cutaneous HPV E6 proteins *in vitro* and/or *in vivo*. HPV16 E6 as well as HPV18 E6 proteins are known to bind to p53 [Lechner and Laimins, 1994; Werness *et al.*, 1990], whereas cutaneous HPV E6 proteins are reported not to do so. To address whether HPV148 E6 is able to bind p53, first a GST pull-down was performed using full-length *in vitro* transcribed and translated p53 protein (see sections 5.3.1 and 5.3.3). Binding was tested with GST-tagged HPV23 E6 and HPV148 E6. GST-HPV16 E6 was used as a positive control and purified GST protein as a negative control to exclude unspecific binding.

Surprisingly, not only HPV16 E6 was found to bind to the p53 protein *in vitro*, but also cutaneous E6 proteins from both HPV23 and HPV148 (Fig. 2.15A). These newly identified *in vitro* interactions were subsequently also assessed *in vivo*. Therefore separate Co-IP experiments (see section 5.4) were performed using HA-tagged HPV23 as well as HPV148 E6 proteins and the YFP-tagged p53 protein. As already observed in figure 2.14C, HPV23 E6 does not interact with p53 *in vivo* (Fig. 2.15B), even when a 5% input was used, meaning that 95% of the reaction was employed in the immunoprecipitation. On the contrary, HPV148 E6 clearly bound to the p53 protein *in vivo* (Fig. 2.15C). Additionally, it was analysed whether the p53 protein was able to interact with Flag-tagged Ajuba. Also in this case, 5% of the whole reaction mixture was used as input and the residual 95% for the immunoprecipitation reaction. Clearly, Ajuba did not interact with the p53 protein (Fig. 2.15D).

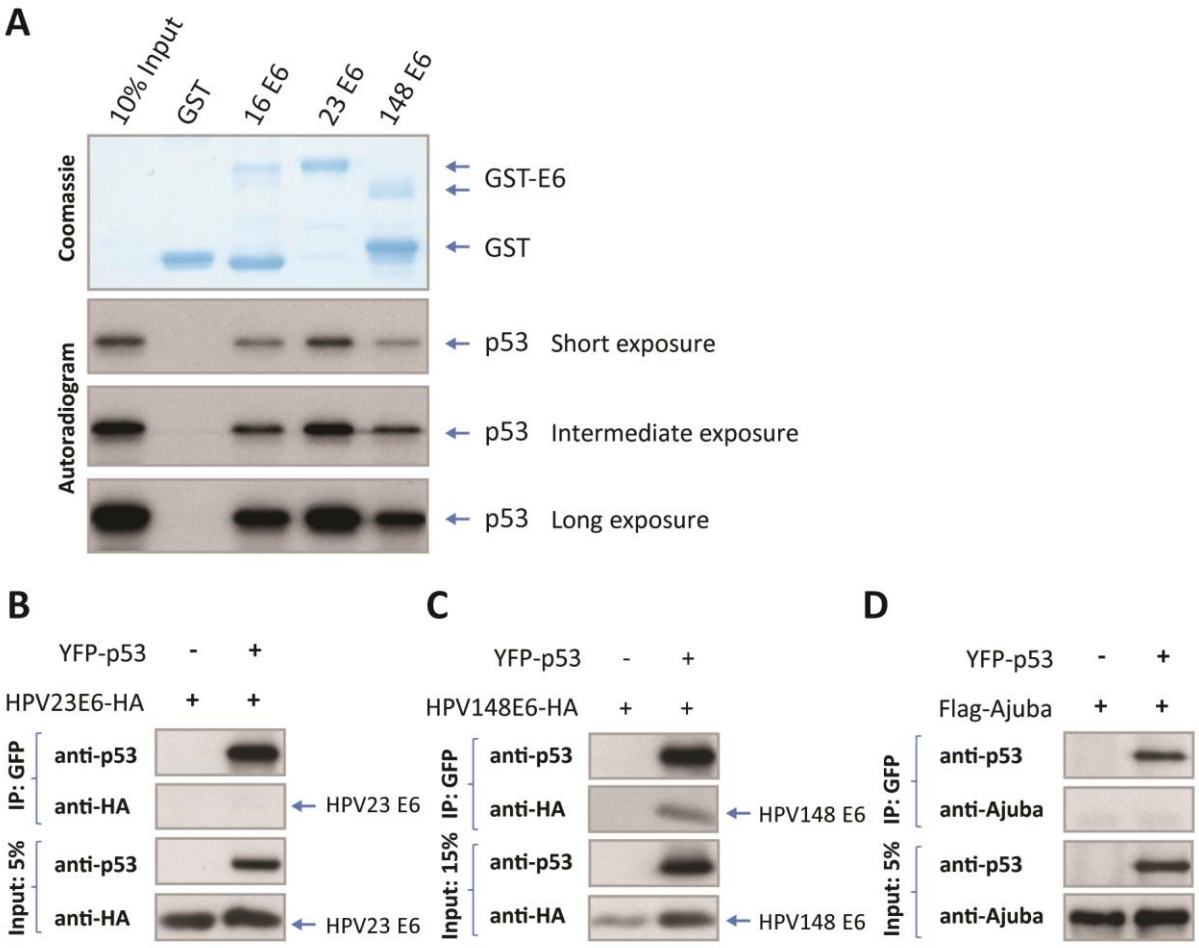

Figure 2.15: HPV148 E6 interacts with p53 *in vitro* and *in vivo*.
(A) GST-tagged E6 fusion proteins of HPV16, -23, and -148 or GST were incubated with *in vitro* translated ^{35}S-radioactively labelled p53. GST and HPV16 were used as negative and positive controls, respectively. GST pull-down experiments were analysed by SDS-PAGE and Coomassie staining (upper panel). The gel was dried and exposed to X-ray films (Autoradiogram, lower panels). 10% of total ^{35}S-radioactively labelled p53 was used as input. **(B, C, D)** H1299 cells were transfected with YFP-p53 and/or HA-tagged HPV23 E6 **(B)**, HPV148 E6 **(C)**, or Flag-Ajuba **(D)** and immunoprecipitated with a GFP antibody (IP: GFP). Immunoprecipitated proteins were analysed by Western blotting (IP, upper panels). As an input control, 5% or 15% of cell lysates were analysed for protein expression (Input, lower panels).

2.4.2 Mapping of the binding site of p53 with HPV148 E6

Based on the finding that HPV148 E6 binds to p53 both *in vitro* and *in vivo*, it was decided to further map the interaction site in p53. Figure 2.16A shows a schematic representation of the p53 protein with its distinct domains, while Figure 2.16B represents the p53 full-length protein and all deletion constructs which were analysed for direct interaction to GST-tagged HPV E6 proteins.

Full-length Flag-p53 showed a distinct binding to HPV16 E6 and a strong binding to HPV148 E6 (Fig. 2.16C, left panel), comparable to figure 2.15A. When only the amino acids 1-70 of p53 were expressed, comprising mainly the Transactivation domain, the binding to HPV148 E6 was completely abrogated, implying that this domain itself was not alone responsible for the interaction

with HPV148 E6. Upon deletion of the C-terminus (Flag-p53 1-298), binding efficiency to HPV148 E6 was increased compared to the full-length p53 protein. When the Transactivation and Proline-rich domains were missing (Flag-p53 80-393), binding of the p53 construct to HPV148 E6 was reduced, but still present. At last, the presence of the C-terminus only, namely the Tetramerization (Tet) and the C-terminal domains (Flag-p53 294-393), resulted in weak binding to HPV148 E6, but background binding was also visible in the GST only negative control (Fig. 2.16C). Hence, the DNA-binding domain together with the Transactivation domain, in particular proved to be highly important for the ability of p53 to interact with the HPV148 E6 protein.

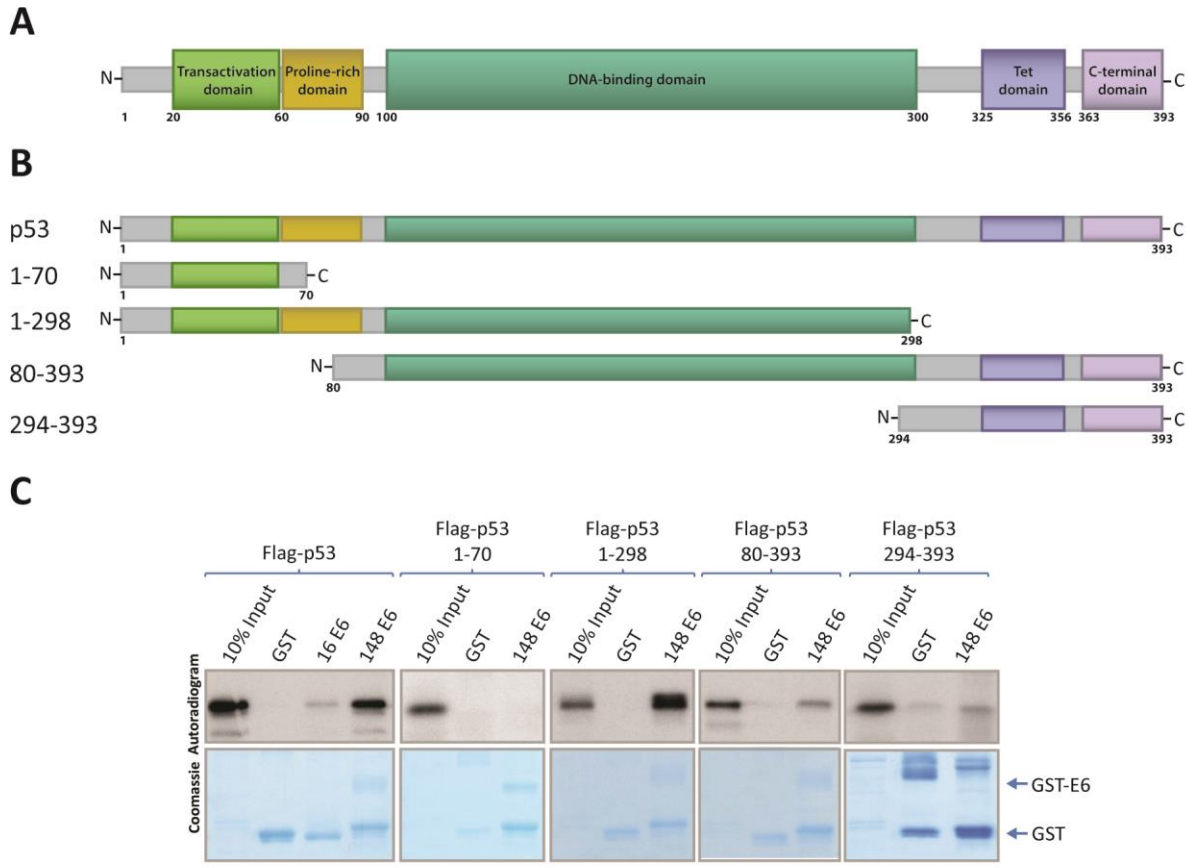

Figure 2.16: HPV148 E6 shows reduced binding capacity to p53 in the absence of the N-terminus and the DNA-binding domain of p53.

(A) Schematic representation of the p53 protein. The p53 protein domains include the Transactivation domain (residues 20-60), the Proline-rich domain (residues 60-90), the sequence-specific core DNA-binding domain (residues 100-300), the Tetramerization domain (Tet domain, residues 325-356), and the lysine-rich C-terminal domain (residues 363-393). Figure adapted from Vousden and Prives [2009]. **(B)** GST-tagged HPV16 E6, HPV148 E6 or GST were incubated with *in vitro* translated ^{35}S-radioactively labelled p53 constructs. GST and HPV16 were used as negative and positive controls, respectively. GST pull-down experiments were analysed by SDS-PAGE and Coomassie staining (lower panels). Gels were dried and exposed to X-ray films (Autoradiograms, upper panels). 10% of total ^{35}S-radioactively labelled p53 was used as input. **(C)** A schematic overview of the *in vitro* transcribed and translated Flag-p53 constructs analysed in GST pull-down experiments.

2.4.3 HPV148 E6 protein co-localises with p53 in different cell lines

The preceding experiments pinpointed the physiological importance of the interaction between p53 and HPV148 E6 proteins. In order to further gain insight into the interaction, the cellular localisation of both proteins was studied. Therefore, immunofluorescence analyses were performed (see section 5.5.7). In these experiments both, U2OS and H1299 cell lines were used, to analyse whether differences in the localisation pattern could be observed. First, the localisation of the p53 protein was analysed using a transiently transfected YFP-p53 expression plasmid or endogenous p53 by immunofluorescence microscopy. Then, the co-localisation of YFP-p53 and the HA-tagged HPV148 E6 was analysed. Immunofluorescence microscopy showed a strong nuclear localisation of YFP-tagged p53 protein, with an overall expression in a diffuse pattern in H1299 and U2OS cells (Fig. 2.17A). Endogenous p53 expression was only analysed in U2OS cells, as H1299 cells are a p53-null cell line. Here, p53 expression was again mainly nuclear, but the protein was also present in the cytoplasm in a diffuse expression pattern (Fig. 2.17B).

In order to examine the cellular localisation of p53 in the presence of HPV148 E6 by means of immunofluorescence analyses, U2OS and H1299 cells were transfected with a combination of YFP-p53 and HA-tagged HPV148 E6 expression plasmids. Upon co-expression of both proteins, the distribution of each protein was not significantly changed in U2OS cells (Fig. 2.18, lower panel). Both proteins mainly co-localised in the nucleus, but they also did so in the cytoplasm. The pattern was diffuse, but co-localisation was also observed in speckles in both nucleus and cytoplasm. When co-expression of HPV148 E6 and YFP-p53 was performed in H1299 cells, the p53 expression pattern changed. Instead of localising mainly in the nucleus it switched to the cytoplasm, still maintaining a diffuse pattern. Hence, co-localisation of p53 and HPV148 E6 was mainly observed in the cytoplasm in H1299 cells (Fig. 2.18, upper panel), which stands in contrast to the U2OS cells.

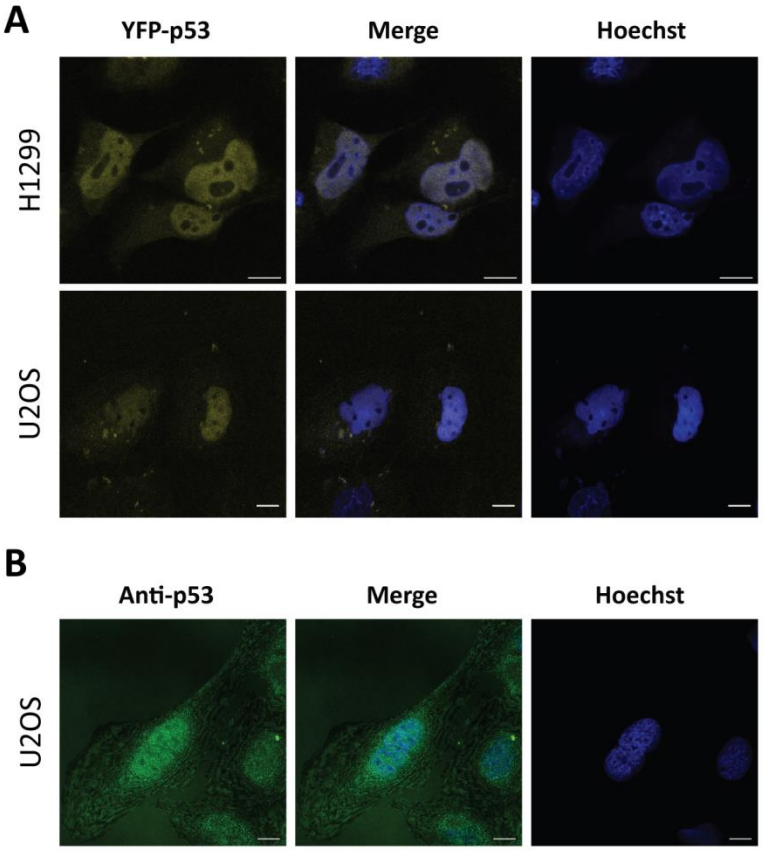

Figure 2.17: p53 localisation in H1299 and U2OS cells.
H1299 and/or U2OS cells were transiently transfected with **(A)** YFP-p53 or **(B)** stained for endogenous p53 and then detected by immunofluorescence microscopy. Nuclear DNA (blue) was stained with Hoechst. The localisation of p53 is presented in yellow **(A)** and green **(B)**. The scale bar represents 10µm.

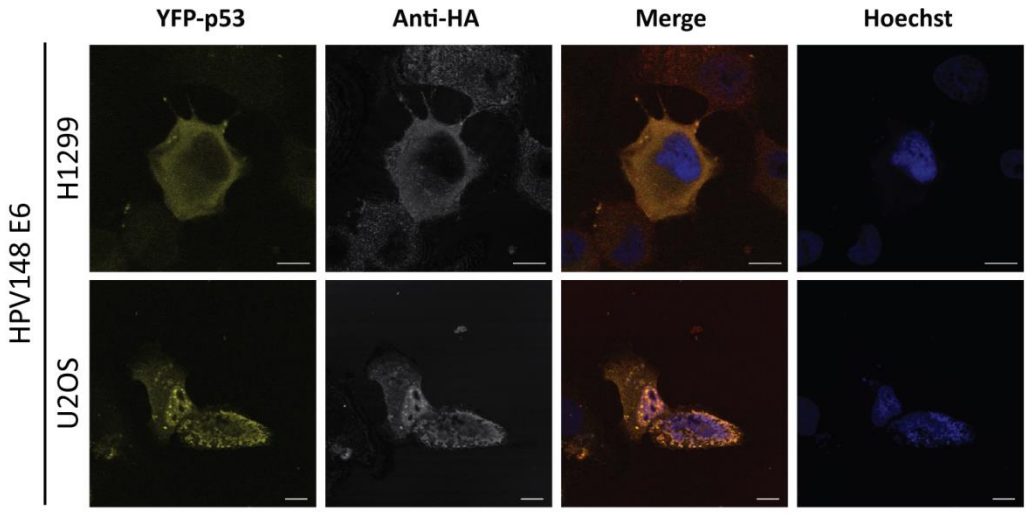

Figure 2.18: p53 co-localises with HPV148 E6 in H1299 and U2OS cells.
H1299 and U2OS cells were transiently transfected with YFP-p53 and HA-tagged HPV148 E6 and then detected by immunofluorescence microscopy. Nuclear DNA (blue) was stained with Hoechst. Co-localisation of HPV148 E6-HA (white) and YFP-p53 (yellow) is presented on merged images (orange). Nuclear DNA (blue) was stained with Hoechst. The scale bar represents 10µm.

2.4.4 The reporter activity of p53 is repressed upon expression of HPV148 E6

The discovery that p53 binds and interacts with HPV148 E6 but not HPV23 E6 has never been reported before, still the question which function lies behind this interaction remains unanswered. To address this issue, luciferase reporter assays were performed using H1299 cells (see section 5.5.8). There, increasing amounts of HA-tagged HPV148 E6 were transfected to determine its impact on p53 activity. In addition, HPV23 E6 was transfected and analysed as a negative control, since it did not interact with p53 *in vivo* in the previous experiments (Fig. 2.15B). The p53 promoter firefly construct was added to every reaction in equal amounts.

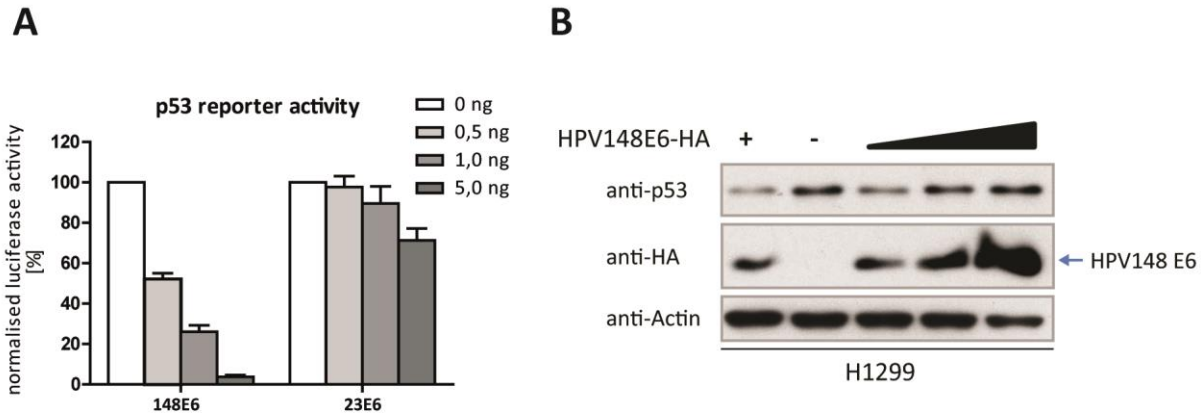

Figure 2.19: HPV148 E6 represses p53 reporter activity.
(A) Luciferase reporter assays in H1299 cells. Cells were transiently transfected with increasing amounts of HA-tagged HPV23 E6 and HPV148 E6 expression plasmids as well as 5ng of firefly p53 promoter construct per reaction. Firefly luciferase activity (relative light units (RLU) normalised against renilla luciferase activity) is expressed as percentage of the signal obtained by transfecting no HPV E6 expression plasmid. Each bar represents the mean values plus standard deviation of four independent experiments. **(B)** H1299 cells were transiently transfected with increasing amounts of HA-tagged HPV148 E6 expression plasmid. Protein levels were analysed by Western blotting. Actin was used to assess equal loading.

Remarkably, upon addition of only 0.5ng HA-tagged HPV148 E6 the activity of p53 was reduced by half to 52%. When increasing the HPV148 E6 dosage to 1ng p53 the activity was again cut in half to 26%. Finally, the highest amount of the E6 protein, namely 5ng resulted in a near complete reduction of p53 activity to 4% (Fig. 2.19A, left panel). On the contrary, only marginal reductions of the reporter activity could be observed for HPV23 E6 when using 0.5 and 1ng of the HA-tagged construct. After using 5ng of HPV23 E6 the activity of the p53 promoter dropped to about 71%, which remained minimal compared to the reduction when using the same amount of HPV148 E6 (Fig. 2.19A, right panel). To rule out the possibility that expression of HA-tagged HPV148 E6 itself influenced p53 protein levels, H1299 cells were transfected with increasing amounts of the HPV148 E6 expression construct. Here, neither an increase nor a reduction of p53 protein expression was observed (Fig. 2.19B). These findings revealed a so far undescribed mechanism of HPV148 E6. It

was shown to not only be able to bind to p53 *in vitro* and *in vivo*, but it also repressed p53 promoter activity.

Section 3

Discussion

Ultraviolet radiation and UVB in particular, is the major risk factor for the development of skin cancer. UVB light, in contrast to UVA, has a much higher phototoxic effect, since DNA directly absorbs incident photons from UVB [Rosenstein and Mitchell, 1987]. An important cellular mechanism to counteract the accumulation of multiple mutations, and in the last instance skin cancer development, is DNA repair [Ichihashi *et al.*, 2003]. The importance of DNA repair mechanisms in the context of UV exposure has been well documented in Xerodema pigmentosum patients, who have a defective nucleotide excision repair mechanism and show hypersensitivity to sunlight combined with an increased incidence of skin cancer [Sijbers *et al.*, 1996].

Furthermore, a role for cutaneous beta HPV E6 proteins in the course of skin carcinogenesis has been predicted in several studies [Bouwes Bavinck *et al.*, 2010; de Koning *et al.*, 2009; Karagas *et al.*, 2006; Struijk *et al.*, 2003]. The E6 proteins of beta-HPV types have been described to activate telomerase and thereby prolong the life span of keratinocytes [Bedard *et al.*, 2008]. Moreover, E6 proteins can inhibit UV-induced apoptosis through the degradation of the pro-apoptotic protein Bak [Jackson *et al.*, 2000] and the lack of p53 phosphorylation at serine 46 via binding of HIPK2 [Muschik *et al.*, 2011]. However, only little is known about the exact role of cutaneous HPVs in skin cancer development, compared to mucosal HPVs and (ano)genital cancers. To gain more insight into virus/host interactions of novel cutaneous HPV E6 proteins with respect to e.g. DNA damage response, the analysis of new interaction partners of novel cutaneous HPV types was performed.

This PhD thesis identifies the LIM protein Ajuba as a novel interaction partner for cutaneous HPV types of the beta2, gamma1 and gamma11 genera. Moreover, the present study describes for the first time that the p53 protein interacts with specific cutaneous HPV types, and is additionally repressed upon expression of the E6 protein from HPV148 (gamma11), suggesting a novel regulatory mechanism of cutaneous E6 proteins.

3.1 Cutaneous HPV E6 proteins from the beta2, gamma1 and gamma11 genera co-localise and interact with Ajuba

The ability of the novel HPV E6 fusion proteins from different HPV genera to directly interact with the *in vitro* translated putative novel interaction partners identified for HPV4 E6 (PDCD6IP, Leupaxin, C9orf102 and Ajuba, see section 2.1.1) was analysed (Fig. 2.2). However, these interaction studies demonstrated that not all of the predicted interaction partners could be verified. The only protein that was confirmed to interact with certain cutaneous HPV E6 proteins both *in vitro* and *in*

vivo was Ajuba. Interestingly, only cutaneous E6 proteins from the beta (HPV23) and gamma genera (HPV4, HPV148) were found to interact with Ajuba, but not genital HPVs from the alpha genus (HPV16, HPV117) (Fig. 2.4 and Fig. 2.5). In order to map the binding region required for the interaction of HPV E6 with Ajuba, the binding of individual E6 proteins to *in vitro* translated Ajuba deletion mutants was analysed (Fig. 2.7). The region required for the binding of the beta and gamma HPV E6 proteins was identified to be the N-terminal part of the Ajuba protein, referred to as the PreLIM region. Whether all three E6 proteins from the beta and gamma genera interact with the same sequence was however not determined in the present thesis. To further map the specific interaction motif of individual HPV types, additional GST pull-down experiments need to be performed.

Notably, the E6 protein of the genital HPV16 also interacted with Ajuba *in vitro*. In contrast to the cutaneous HPV E6 proteins which bound to the PreLIM region, HPV16 E6 interacted with the LIM region of Ajuba. This observation is in concordance with a previous report, where Zyxin, a member of the Ajuba/Zyxin protein family, was identified to interact specifically with the E6 protein of genital HPV6 through its LIM region. The interaction of Zyxin with HPV16 E6 or HPV18 E6 was however not significant [Degenhardt and Silverstein, 2001]. Nonetheless all three E6 proteins represent alpha PVs, indicating that the interaction of E6 proteins of alpha PVs with members of the Ajuba/Zyxin family differs from that of cutaneous HPVs. Furthermore, Ajuba was shown to interact with other proteins like the Aurora-A kinase or the tumour suppressor LATS2 through its LIM region [Abe *et al.*, 2006; Hirota *et al.*, 2003]. On the other hand, Ajuba's PreLIM region was reported to associate with microtubules or the protein Grb2 [Ferrand *et al.*, 2009; Goyal *et al.*, 1999].

In this study, it was further demonstrated that Ajuba preferentially localises in the cytoplasm (Fig. 2.8B), as has been previously reported [Hirota *et al.*, 2003; Hou *et al.*, 2008; Kanungo *et al.*, 2000]. The E6 proteins of HPV23 and HPV148 preferentially localised to the nucleus but were also found in a diffuse distribution throughout the cytoplasm. The E6 proteins of HPV4 and HPV16, on the other hand, were predominantly detected in the cytoplasm (Fig. 2.8). Previous studies also reported that the E6 proteins of low-risk and cutaneous beta HPV types show largely nuclear expression patterns, while high-risk mucosal HPV E6 proteins are expressed much more diffusely throughout the cell [Guccione *et al.*, 2002; Massimi *et al.*, 2008; Sherman and Schlegel, 1996]. In this study, immunofluorescence analyses revealed that the overexpression of Ajuba resulted in the translocation and co-localisation of the HPV23 E6 and HPV148 E6 proteins in the cytoplasm (Fig. 2.9). Interestingly, this effect appeared to be characteristic for E6 of HPV23 and HPV148, since no co-localisation could be observed for HPV16 E6. Accordingly, these findings denote that the co-localisation of E6 proteins and Ajuba is mediated by their direct interaction.

In a previous report it was demonstrated that the co-transfection of HPV6 E6 and Zyxin resulted in the accumulation of both proteins in the nucleus. The study also pointed out that HPV6 E6 was able to mobilise endogenous Zyxin into the nucleus [Degenhardt and Silverstein, 2001]. Although these data stand in contrast to the observed localisation pattern in the present study, the different outcomes can be explained by the already mentioned different functions of the Ajuba and Zyxin proteins. However, a study analysing the co-localisation of HPV E6 and p53 in transformed cell lines, showed that both proteins localise in the cytoplasm [Liang *et al.*, 1993]. The HPV-negative cell line C-33 A displayed a predominantly nuclear localisation of p53. Therefore, co-localisation of an HPV E6 protein with another cellular protein does not necessarily have to take place in the nucleus. However, the presented results demonstrated that HPV E6 proteins from the beta and gamma genera interact and co-localise with Ajuba.

3.2 HPV23 E6 and HPV148 E6 proteins decrease in response to Ajuba knockdown and DNA damage

In order to analyse Ajuba's influence on the E6 proteins of HPV23 and HPV148, further experiments were performed. This study demonstrates that the beta2 HPV23 E6 and the gamma11 HPV148 E6 proteins showed a reduced expression together with Ajuba in response to severe DNA damage, which was induced by either UVB radiation or ADR treatment in U2OS cells. Both treatments lead to the degradation of endogenous Ajuba as well as to the depletion of the respective E6 proteins (Fig. 2.13A and B). Similarly, siRNA-mediated down regulation of Ajuba led to a decrease in the protein levels of HPV23 E6 and HPV148 E6 (Fig. 2.12A and B), suggesting a close interaction between Ajuba and both E6 proteins *in vivo*. Additionally, a reduced protein expression of endogenous p53 was observed upon Ajuba siRNA knockdown in U2OS cells stably transfected with the E6 proteins of HPV23 and HPV148 (Fig. 2.12B) pointing to an additional role of p53 when expressed together with at least Ajuba, since p53 protein levels were also slightly reduced in the vector control lane. Furthermore, Ajuba's ability to accumulate in response to the overexpression of HPV23 E6 and HPV148 E6 further hints at a close functional association of these proteins inside the cell (Fig. 2.11A and B), especially considering that Ajuba did not accumulate upon overexpression of a GFP construct containing the same promoter as the HPV E6 constructs (Fig. 2.11D). Moreover, HPV148 E6 was also able to accumulate upon Ajuba overexpression (Fig. 2.11C), indicating that the observed protein accumulations are mediated by a direct association of Ajuba and the HPV E6 proteins. These observations, in particular the results of induced DNA damage (Fig. 2.13), do however not relate to a previously performed study, where the accumulation of HPV23 E6 after ADR treatment or UVB radiation was reported [Muschik *et al.*, 2011]. This study was performed in H1299 cells which lack endogenous p53, whereas in the presented study U2OS cells harbouring wild type

p53 were used, which might influence the results. Moreover, a similar effect as in the mentioned study was observed when using H1299 cells (data not shown); suggesting that the p53 protein affects the protein levels of Ajuba and HPV23 and HPV148 E6 proteins upon DNA damage.

An additional adaptor protein might also play a role in E6 protein accumulation and the different response to DNA damage. Different studies propose a role for the Aurora-A kinase, an interaction partner of Ajuba, to induce Mdm2-mediated destabilisation and inhibition of p53 after its phosphorylation at Ser315 [Katayama *et al.*, 2004]. Additionally, phosphorylation of p53 at Ser215 by Aurora-A was shown to abrogate its DNA binding and transactivation activity on downstream target genes such as $p21^{Cip/WAF1}$ and *PTEN* [Liu *et al.*, 2004]. Also, upon overexpression of Ajuba an increase in Aurora-A protein levels was observed (data not shown). The putative adaptor protein between p53 and Ajuba could therefore be Aurora-A or any other interaction partner, associating with both proteins.

Noteworthy is also the fact that the novel HPV148 genome was isolated from an actinic keratosis, a precursor of cutaneous SCC, making it additionally interesting to examine [Köhler *et al.*, 2011], as it might turn out to be a potential "high-risk" cutaneous HPV type.

3.3 The effect of p53 on the complex of Ajuba and HPV23 E6/HPV148 E6

p53 has an important function as a key regulator of apoptosis [Vousden, 2000]. In cancers however, its activity is often lost, either due to mutations in p53 itself, because of mutations of regulators upstream of p53 (e.g. CHK2, MDM2) or by disruption of the cell-growth-inhibition pathways that mediate the p53 response (e.g. by loss of components of the apoptotic cascade) [Vousden and Lu, 2002]. Binding of p53 followed by its degradation is a well described property of mucosal HPV E6 oncoproteins to inhibit apoptosis. This mechanism is however missing in their cutaneous counterparts [Doorbar *et al.*, 2012; Elbel *et al.*, 1997]. Nevertheless, cutaneous HPV E6 proteins of the beta genus were shown to inhibit p53-mediated apoptosis after UVB-induced DNA-damage, through e.g. the inhibition of p53 phosphorylation at serine 46 via the interaction with the tumour suppressor HIPK2 [Mantovani and Banks, 2001; Muschik *et al.*, 2011; Struijk *et al.*, 2008]. The previously outlined evident involvement of p53 in the regulation of Ajuba and HPV E6 protein levels was further analysed in this study, revealing that p53 formed a trimeric complex with Ajuba and HPV148 E6, demonstrated by co-precipitation (Fig. 2.14B and D). However, p53 was excluded from the complex formation when using HPV23 E6 and Ajuba (Fig. 2.14A and C), even though a complex between HPV23 E6 and Ajuba was still formed (Fig. 2.14A) as already demonstrated in the initial experiments (Fig. 2.4B). Remarkably, a novel, so far undescribed interaction was observed between HPV148 E6 and p53 (Fig. 2.14D).

As already mentioned, preceding studies showed that cutaneous E6 proteins do not interact with p53 and do not induce ubiquitination or degradation of p53 [Elbel *et al.*, 1997; Harry and Wettstein, 1996; Steger and Pfister, 1992]. However, HPV E6 proteins were demonstrated to bind to two sites within the p53 protein. One site lies within the core structure of p53 and the other one is found at the C-terminus of the protein. Yet, only the core binding is required for E6-mediated degradation of p53 [Li and Coffino, 1996]. Moreover, binding to p53 was suggested to be a prerequisite for the inhibition of p53-mediated transactivation, but does not appear to be sufficient for p53 degradation, a function of the ubiquitin ligase E6AP [Elbel *et al.*, 1997]. To examine whether the observed interaction between HPV148 E6 and p53 was not only the result of a specific experimental setting, p53 binding was further analysed *in vitro* and *in vivo*. Surprisingly, the GST pull-down experiments not only revealed the *in vitro* interaction between HPV16 E6 and p53, but also between the E6 proteins of HPV23 and HPV148 with p53 (Fig. 2.15A). Nevertheless, as depicted in figures 2.14C and D, only HPV148 E6, but not HPV23 E6 was able to interact with p53 *in vivo* (Fig. 2.15B and C). Additional experiments showed that Ajuba did not interact with p53 in the absence of E6 (Fig. 2.15D), pinpointing that the interaction of Ajuba with p53 can only take place in the complex with HPV148 E6. Figure 3.1 summarises all co-immunoprecipitation experiments performed in this study with regard to Ajuba involvement. To find out the exact order of the interaction, more complex co-immunoprecipitation experiments will have to be performed in the future.

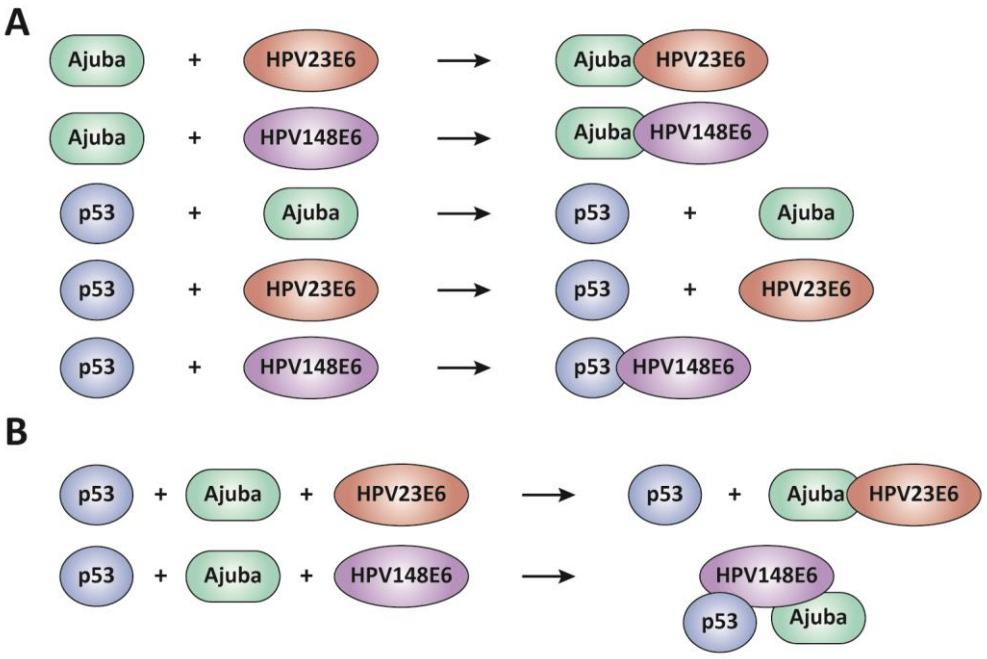

Figure 3.1: Schematic representation of Ajuba interactions with cutaneous HPV E6 proteins and p53.
A model representing all analysed *in vivo* interactions of Ajuba detected by co-immunoprecipitation experiments, using two **(A)** or three **(B)** overexpressed proteins.

The cellular localisation of p53 and HPV148 E6 was analysed by immunofluorescence in U2OS and H1299 cells. Here, endogenous p53 was shown to localise mainly to the nucleus, although a diffuse expression in the cytoplasm could also be observed (Fig. 2.17B). Overexpressed YFP-p53 primarily localised to the nucleus and was diffusely distributed in U2OS and H1299 cells (Fig. 2.17A). p53 is known to shuttle between the cytoplasm and the nucleus in a cell-cycle dependent manner [Hayon and Haupt, 2002]. After cellular stress p53 accumulates in the nucleus, an essential prerequisite for its biological effects to occur. The inhibition of p53 translocation to the nucleus results in the abrogation of many of its biological effects [O'Brate and Giannakakou, 2003]. In the presence of HPV148 E6, a co-localisation with p53 was mainly observed in the nucleus of U2OS cells (Fig. 2.18, lower panel). When co-expression was performed in H1299 cells, the co-localisation took place in the cytoplasm (Fig. 2.18, upper panel).

To gain further insight into the function of the p53/HPV148 E6 interaction it was attempted to map the binding site of HPV148 E6 with p53 (Fig. 2.16). A strong binding of HPV148 E6 to full-length p53 was observed, which was further increased upon deletion of the C-terminus (Flag-p53 1-298). When the N-terminal domains of p53 were deleted (Flag-p53 80-393) the binding of HPV148 E6 was weaker, but still present, indicating that binding was possible in principle, although the interaction site might not be fully accessible due to a different folding of the protein. When only the transactivation domain was present (Flag-p53 1-70), the binding of HPV148 E6 was completely abolished. However, when only the C-terminal part of p53 was present (Flag-p53 294-393), the binding of E6 was very weak and background binding was observed in the GST negative control (Fig. 2.16C). The observed background binding further reduced the objective signal intensity of the HPV148 E6 band. Nevertheless, these results are consistent with the previous reports of two binding sites for HPV E6 proteins within the p53 protein [Li and Coffino, 1996]. In order to map the exact binding site of HPV148 E6 within p53 more deletion constructs containing deletions of the individual domains of p53 can be constructed and analysed in the future, for a clearer readout. Additionally, due to the novel finding of an interaction between p53 and HPV148 E6, experiments regarding the ability of the E6 protein to degrade p53 should also be performed.

To further elucidate the physiological function of the interaction between HPV148 E6 and p53, luciferase reporter assays were performed, identifying the repression of p53 activity upon transfection of increasing amounts of HPV148 E6 (Fig. 2.19A). The reporter activity dropped drastically when even the smallest amounts of HPV148 E6 were introduced, whereas no such dramatic effect was obtained with HPV23 E6. Moreover, expression of the HPV148 E6 protein itself did not influence p53 protein levels (Fig. 2.19B), indicating that HPV148 E6 affected the transactivation activity of p53. This observation is a highly relevant finding in this study since the new interaction of HPV148 E6 with p53 not only takes place, but also strongly affects p53 activity (Fig.

2.19). Therefore, targeting of the transactivation activity of p53 by the cutaneous gamma11 type HPV148 might represent a mechanism whose physiological relevance for the virus is comparable to p53 inactivation by genital HPV types.

3.4 Future perspectives

Up to date, the involvement of cutaneous HPV types in the development of malignancies of the skin is still undefined, a fact that stimulates further investigations [Asgari *et al.*, 2008; Muñoz *et al.*, 2003; Zur Hausen, 2009]. In contrast, the etiologic relationship between cervical cancer development and infections with high-risk mucosal HPVs is well known. Nevertheless, an accumulating body of evidence supports a considerable role for cutaneous HPV types in combination with UV irradiation in the formation of skin cancer [Bouwes Bavinck *et al.*, 2010; Jackson *et al.*, 2000; Jackson and Storey, 2000; Struijk *et al.*, 2008]. Up to now, only HPV5 and HPV8, both belonging to the beta1 genus, are considered to be "oncogenic cutaneous HPV types", (similar to the mucosal high-risk HPVs), due to their association with the development of cutaneous SCC in EV patients [Akgül *et al.*, 2010; Lutzner *et al.*, 1980; Orth, 1986; Ramoz *et al.*, 1999]. Although cutaneous high-risk HPV types have not been defined yet, the study at hand introduces an HPV type from the gamma11 genus, which down regulates the transcriptional activity of p53, an important regulator of apoptosis. This interaction might have a strong impact on cell proliferation and cellular progression into malignancy.

Future studies need to uncover the precise role of the interaction of HPV148 E6 with p53 and moreover to analyse Ajuba's involvement in this process considering that additional binding partners might be involved. Further, to validate the biological significance of the research findings, primary human keratinocytes have to be employed, since the skin represents the natural host for cutaneous HPV infection and here cell lines derived from an osteosarcoma and non-small cell lung carcinoma were used [Doorbar *et al.*, 2012]. Hence, the potential of HPV E6 proteins, of HPV148 E6 in particular, to facilitate the development of cutaneous lesions should be addressed. Thus, primary keratinocytes, infected with distinct HPV types or their respective E6 proteins, can be analysed after UVB radiation or Ajuba depletion under physiological conditions, especially if organotypic skin culture systems are used. Another approach would be the use of transgenic animals expressing preferentially the E6 genes of cutaneous HPV types, or additionally lacking Ajuba. There, the role of UVB radiation and/or chemically induced skin carcinogenesis in the development of skin tumours can be tested, as has been already successfully shown for HPV 38 [Viarisio *et al.*, 2011; Viarisio *et al.*, 2013]. In summary, the present study strengthens the hypothesis that cutaneous HPVs can act as co-factors in the development of skin cancer either in association with UVB radiation or through the interaction with other cellular target proteins. Thus, additional studies should continue focussing on cutaneous HPVs,

which (in case of HPV148) will greatly contribute to the knowledge of the complex cellular network of gamma-PVs.

Section 4

Material

4.1 Chemicals and Reagents

4.1.1 Chemicals, solutions, and reagents

Table 4.1: Chemicals

Chemical	Distributor
2-Mercaptoethanol	Sigma-Aldrich, Steinheim
Acetic acid, p.a. (100 %)	Merck, Darmstadt
Acrylamide/bis Acrylamide (29:1), 30 % solution	SERVA Electrophoresis, Heidelberg
Agarose	Sigma-Aldrich, Steinheim
Albumin bovine (BSA) Fraction V	Biomol Hamburg
Ammonium persulfate (APS)	Sigma-Aldrich, Steinheim
Amplify™ Fluorographic Reagent	GE Healthcare, Munich
Aqua ad iniectabilia	Braun, Melsungen
Beta-Glycerophosphate	AppliChem GmbH, Darmstadt
Bisbenzimide (Hoechst 33258)	Sigma-Aldrich, Steinheim
Bromophenol blue	Sigma-Aldrich, Steinheim
Complete protease inhibitor, EDTA-free	Roche Diagnostics, Mannheim
Coomassie G-250	Sigma-Aldrich, Steinheim
DMSO	Merck, Darmstadt
DNA loading buffer (6x)	Fermentas, St. Leon-Rot
dNTPs set PCR grade	Invitrogen, Karlsruhe
ECL SuperSignal West Dura	Thermo Fischer Scientific, USA
EDTA	Roche Diagnostics, Mannheim
Ethanol, p.a.	Sigma-Aldrich, Steinheim
Ethidium bromide solution, 1%	Sigma-Aldrich, Steinheim
Formaldehyde	Merck, Darmstadt
Glucose	Carl Roth GmbH, Karlsruhe
Glutathione Sepharose™ 4FastFlow beads	GE Healthcare, Munich

Table 4.1: Chemicals (continued)

Chemical	Distributor
Glycerol, p.a. (99.5%)	Carl Roth GmbH, Karlsruhe
Glycine	GERBU Biotechnik GmbH, Heidelberg
HEPES	Eurobio, France
Hydrochloric acid	Merck, Darmstadt
Isopropyl alcohol, p.a.	Merck, Darmstadt
KCl	Merck, Darmstadt
KH_2PO_4	Carl Roth GmbH, Karlsruhe
L-[^{35}S]-methionine, 10mCi/mL	Perkin Elmer, Jügesheim
Magnesium chloride ($MgCl_2$)	Merck, Darmstadt
Magnesium sulphate ($MgSO_4$)	Merck, Darmstadt
Methanol, p.a.	Merck, Darmstadt
MG-132 (Z-Leu-Leu-Leu-al)	Enzo Life Sciences, Lörrach
Mowiol 4-88	Carl Roth GmbH, Karlsruhe
Na_2HPO_4	Carl Roth GmbH, Karlsruhe
NaOH	Carl Roth GmbH, Karlsruhe
Nonidet® P40 (NP40)	AppliChem GmbH, Darmstadt
PMSF	Roche Diagnostics, Mannheim
Powdered milk, blotting grade	Carl Roth GmbH, Karlsruhe
Protein A/G PLUS-Agarose beads	Santa Cruz, Heidelberg
RNase OUT™ Recombinant Ribonuclease Inhibitor	Invitrogen, Karlsruhe
Sodium acetate	Merck, Darmstadt
Sodium chloride, p.a. (NaCl)	Merck, Darmstadt
Sodium dodecyl sulphate (SDS)	Sigma-Aldrich, Steinheim
Sodium fluoride	Merck, Darmstadt
Sodium ortho-vanadate (Na_3VO_4)	Sigma-Aldrich, Steinheim
TEMED	Sigma-Aldrich, Steinheim
Trizma® base	Sigma-Aldrich, Steinheim
Triton® X-100	AppliChem GmbH, Darmstadt
Tween 20	Sigma-Aldrich, Steinheim
Western Lightning Plus-ECL	Perkin Elmer, Jügesheim

4.1.2 Reagents for bacteria cultivation

Table 4.2: Bacteria culture reagents

Reagent	Distributor
Ampicillin	Sigma-Aldrich, Steinheim
Bacto™ Agar	Becton Dickinson, Heidelberg
Bacto™ Trypton	Carl Roth, Karlsruhe
Isopropyl-beta-D-thiogalactopyranoside (IPTG)	AppliChem GmbH, Darmstadt
Chloramphenicol	Sigma-Aldrich, Steinheim
Kanamycin	Sigma-Aldrich, Steinheim
LB-Medium (Lennox)	Carl Roth, Karlsruhe
Sodium chloride, p.a.	Merck, Darmstadt
Terrific-Broth Medium	Carl Roth, Karlsruhe
Yeast extract	GERBU Biotechnik GmbH, Heidelberg

4.1.3 Reagents for cell culture

Table 4.3: Cell culture reagents

Reagent	Distributor
Adriamycin (ADR)	Tebu-Bio, Offenbach
Dulbecco's modified Eagle's medium (DMEM)	Sigma-Aldrich, Steinheim
Dulbecco's Phosphate Buffered Saline (PBS)	Gibco Life Technologies, Karlsruhe
DMSO, sterile	Merck, Darmstadt
Effectene Transfection Reagent	Qiagen, Hilden
Fetal Bovine Serum (FCS)	Linaris GmbH, Wertheim
Geneticin (G418) solution	PAA Laboratories, Austria
Lipofectamine 2000 Transfection Reagent	Invitrogen, Karlsruhe
Opti-MEM serum-free medium	Gibco Life Technologies, Karlsruhe
Trypsin/EDTA (0.25%)	Gibco Life Technologies, Karlsruhe

4.2 Consumables

Table 4.4: Consumables

Item	Distributor
Amersham Hybond™-P (PVDF membrane)	GE Healthcare, Munich
Cell culture flasks (25, 75 cm^2)	Corning Sigma, Munich

Table 4.4: Consumables (continued)

Item	Distributor
Cell culture dishes/plates	TPP, Switzerland
CoolCell® -1 °C/min Cell Freezer	SERVA Electrophoresis, Heidelberg
Cover slides	Thermo Fisher Scientific, Rockslide
Cryo-tubes (2 mL)	Greiner Bio-One, Frickenhausen
Cuvettes	BRAND GMBH + CO KG, Wertheim
Gloves (Blossom Latex Gloves, S)	Mexpo International, USA
Gloves (Dermatril®M)	KCL GmbH, Eichenzell
Microplates 96 well	Greiner Bio-One, Frickenhausen
Object glass slides	Langenbrinck, Emmendingen
Parafilm	Pechinery Inc., USA
Pasteur pipettes	Brand, Wertheim
Petri dishes (for Agar plates)	Greiner Bio-One, Frickenhausen
Pipette tips (10, 100, 1000 µL)	Greiner Bio-One, Frickenhausen
PCR Soft strips	Biozym, Oldendorf
Polypropylene conical tubes (15, 50 mL)	Greiner Bio-One, Frickenhausen
Reaction tubes (0.5, 1.5, 2.0 mL)	Eppendorf, Hamburg
Saran wrap	Cofresco Frischhalteprodukte, Minden
Scalpels, disposable	Feather Safety Razor, Japan
Sterile filters (0.22 µm)	Millipore, Schwalbach
TipOne Filter Tips (10, 200, 1000 µL)	StarLab, Ahrensburg
Whatman 3MM filter paper	Schleicher & Schüll, Dassel
X-ray films, Super RX	Fuji, Japan

4.3 Laboratory equipment

Table 4.5: Instruments and laboratory equipment

Instrument	Distributor
Agarose gel electrophoresis chambers	Renner, Darmstadt
Analytical balance scale 2004 MP	Sartorius, Göttingen
Analytical scale, Acculab VIC-212	Sartorius, Göttingen
Autoradiography cassettes	Kodak, Stuttgart
Bacteria shaker G25	Infors, Switzerland
Balance 1216 MP	Julabo, Seelbach

Table 4.5: Instruments and laboratory equipment (continued)

Instrument	Distributor
Camera, UV light	Renner, Darmstadt
Centrifuge Biofuge fresco 17	Heraeus, Hanau
Centrifuge Biofuge pico	Heraeus, Hanau
Centrifuge Megafuge 1.0R	Heraeus, Hanau
Centrifuge RC5C Sorvall	DuPont, Bad Nauheim
Developing machine CURIX 60	AGFA, Cologne
Duran® glassware	SCHOTT, Croatia
ELISA reader Labsystem Multiscan	Thermo Fisher Scientific, USA
Freezer (-80°C, VIP series)	Sanyo, Munich
Geiger counter LB 1210B	Berthold, Wildbad
Gel dryer model 583	Bio-Rad Laboratories, Munich
Hotplate/stirrer	VWR, Darmstadt
Incubator	Labotec, Göttingen
Magnetic stirrer MR 3001	Heidolph, Rust
Microscope FLUOVIEW FV1000 Confocal Laser	Olympus GmbH, Hamburg
Microwave	AEG, Nürnberg
Minifuge	Heraeus, Hanau
Mini-PROTEAN® II	Bio-Rad Laboratories, Munich
Mini-PROTEAN® Tetra Cell	Bio-Rad Laboratories, Munich
MyCycler Thermal Cycler	Bio-Rad Laboratories, Munich
Neubauer hemocytometer	Bender & Hobein, Bruchsal
Nitrogen tank (ADUR β)	Messer Griesheim, Krefeld
Overhead shaker REAX2	Heidolph, Rust
pH-meter Calimatic 765	Knick, Egelsbach
Pipettes	Eppendorf, Hamburg
Pipetboy acu	Integra Bioscience, Fernwald
Power supply Power Pac HC	Bio-Rad Laboratories, Munich
Rotating wheel	Neolab, Heidelberg
Rotors Sorvall GS-3, SA 600, SS 34	DuPont, Bad Nauheim
Sonifier 250	Branson/Heinemann, Schwäbisch Gemünd
Spectrophotometer NanoDrop® ND-1000	NanoDrop, USA
SterilBioGARD Hood	Baker Company, USA
Thermomixer	Eppendorf, Hamburg

Table 4.5: Instruments and laboratory equipment (continued)

Instrument	Distributor
UV table N90	Benda Konrad, Wiesloch
Variocontrol UV-meter	Waldmann, Villingen
Vortexer	Heidolph, Rust
Waldmann UV181 BL UV-table	Waldmann, Villingen
Water bath	JULABO GmbH, Seelbach
Wet blot Western blotting chamber	Bio-Rad Laboratories, Munich

4.4 Buffers and solutions

Table 4.6: Buffers and stock solutions

Solution/Buffer	Composition
Ammonium persulfate (APS)	10% (w/v), store at -20°C
Ampicillin (1000x)	100 mg/mL, store at -20°C
Blocking buffer for Western blotting	5% (w/v) Milk powder in 1x TBST
BSA solution	1 mg/mL, store at -20°C
Cell culture freezing medium	60% (v/v) DMEM 30% FCS 10% DMSO
Chloramphenicol (1000x)	34 mg/mL in methanol, store at -20°C
Coomassie staining solution for SDS gels	50% methanol 10% acetic acid 40% ddH_2O 0.1% Coomassie G-250
Denaturing lysis buffer	20mM Tris, pH 8.0 1% NP40 0.15M NaCl 5mM EDTA 10% glycerol 1% SDS freshly supplemented with protease and phosphatase inhibitors and MG-132

Table 4.6: Buffers and stock solutions (continued)

Solution/Buffer	Composition
Fixation/destain solution for SDS gels	50% methanol 10% acetic acid 40% ddH_20
In vitro interaction buffer	0.05% NP40 1mM Na_3VO_4 in PBS
Kanamycin (1000x)	50 mg/mL, store at -20°C
Laemmli buffer (10x)	0.25M Tris 1.9M glycine 1% (w/v) SDS
LB-Agar plates	2% Bacto-Agar/1L LB-Medium
LB-Medium (Lennox)	10g NaCl 10g Bacto-Trypton 5g yeast extract ad 1000mL H_2O
Mowiol	2.4g Mowiol 4-88 6g glycerol 12mL 0.2M Tris-HCl, pH 8.5 6 mL ddH_2O
Non-denaturing lysis buffer	20mM HEPES 0.15M NaCl 5mM EDTA 10% glycerol 0.5% Triton X-100 freshly supplemented with protease and phosphatase inhibitors, and MG-132
PBS (10x)	1.24M NaCl 0.22M Na_2HPO4 0.1M KH_2PO_4 adjust to pH 7.8

Table 4.6: Buffers and stock solutions (continued)

Solution/Buffer	Composition
SDS-loading buffer (5x)	10% (w/v) SDS 0.03% (w/v) bromophenol blue 12.5% (v/v) 2-mercaptoethanol 5mM EDTA, pH 8.0 50% (v/v) glycerol 0.3M Tris, pH 6.8 store at -20°C
SOC-Medium	2% (w/v) Bacto-Trypton 0.5% (w/v) yeast extract 10mM NaCl 2.5mM KCl 10mM $MgCl_2$ 10mM $MgSO_4$ 20mM glucose
TAE Buffer (50x)	2M Tris Base 0.25M Sodium acetate 0.05M EDTA, pH 8.0 adjust to pH 7.8 with acetic acid
TBS (10x)	0.1M Tris 1.37M NaCl adjust to pH 7.6
TBST (1x)	1x TBS, pH 7.6 0.1% (v/v) Tween 20
Towbin buffer (10x)	0.25M Tris 1.92M glycine

4.5 Molecular weight markers

Table 4.7: Molecular weight markers

Marker	Distributor
Gene Ruler™ 1kb DNA Ladder	Fermentas, St. Leon-Rot
Page Ruler™ Plus Prestained Protein Ladder	Fermentas, St. Leon-Rot

4.6 Universal enzymes

Table 4.8: Universal enzymes

Enzyme	Distributor
FastAP alkaline phosphatase	Fermentas, St. Leon-Rot
Taq DNA polymerase	Invitrogen, Karlsruhe
PRECISOR High Fidelity DNA polymerase	BioCat, Heidelberg
TNT® T7 polymerase	Promega, Mannheim
T4 DNA Ligase	Fermentas, St. Leon-Rot

4.7 Restriction enzymes

Table 4.9: Restriction enzymes

Enzyme	Distributor
BamHI	New England Biolabs, Schwalbach
EcoRI	New England Biolabs, Schwalbach
NotI	New England Biolabs, Schwalbach
XhoI	New England Biolabs, Schwalbach

4.8 Antibodies

Table 4.10: List of antibodies used for Western blot analyses, immunofluorescence experiments and co-immunoprecipitation experiments

Antibody	Supplier	Catalogue №	Application
Anti-Actin (Clone 4) mouse monoclonal IgG	MP Biomedical	691001	WB 1:10,000 in 5% milk/TBST
Anti-Ajuba	Cell Signaling, USA	4897S	WB 1:1,000 in 5% BSA/TBST
Anti-Flag M2 mouse monoclonal IgG_1	Sigma, USA	F 3165	WB 1:5,000 in 5% milk/TBST Co-IP [3µg]
Anti-GFP (FL) rabbit polyclonal IgG_1	Santa Cruz, Heidelberg	sc-8334	WB 1:1,000 in 5% milk/TBST
Anti-GFP	Roche Diagnostics	11 814 460 001	Co-IP [1µg]

Table 4.10: List of antibodies used for Western blot analyses, immunofluorescence experiments and co-immunoprecipitation experiments (continued)

Antibody	Supplier	Catalogue №	Application
Anti-HA (12CA5) mouse monoclonal IgG_{2b}	Roche Diagnostics	11 583 816 001	IF 1:150 in 1% BSA/PBS Co-IP [5µg]
Anti-HA (3F10) rat monoclonal IgG_1	Roche Diagnostics	11867423001	WB 1:1,000 in 5% milk/TBST
Anti-p53 (DO-1) mouse monoclonal IgG_{2a}	Santa Cruz, Heidelberg	sc-126	WB 1:1,000 in 5% milk/TBST
Anti-PARP-1 (F2)	Santa Cruz, Heidelberg	sc-8007	WB 1:1,000 in 5% milk/TBST
Goat anti-mouse IgG (H+L) HRP	Jackson ImmunoResearch, USA	115-035-062	WB 1:10,000 in 5% milk/TBST
Goat anti-rabbit IgG (H+L) HRP	Jackson ImmunoResearch, USA	111-035-144	WB 1:10,000 in 5% milk/TBST
Goat anti-rat IgG (H+L) HRP	Jackson ImmunoResearch, USA	112-035-143	WB 1:10,000 in 5% milk/TBST
Goat anti-mouse IgG_1 Alexa Fluor® 488	Invitrogen, Karlsruhe	A21121	IF 1:450 in 1% BSA/PBS
Goat anti-mouse IgG_{2a} Alexa Fluor® 488	Invitrogen, Karlsruhe	A21131	IF 1:450 in 1% BSA/PBS
Goat anti-mouse IgG_{2a} Alexa Fluor® 594	Invitrogen, Karlsruhe	A21135	IF 1:450 in 1% BSA/PBS
Goat anti-mouse IgG_{2b} Alexa Fluor® 594	Invitrogen, Karlsruhe	A21145	IF 1:450 in 1% BSA/PBS
Goat anti-rabbit IgG Alexa Fluor® 488	Invitrogen, Karlsruhe	A11008	IF 1:450 in 1% BSA/PBS

4.9 Kits

Table 4.11: Commercial kits

Kit	Distributor
BCA Protein Assay Kit	Thermo Fisher Scientific, USA
Dual-Luciferase® Reporter Assay System	Promega, Mannheim
One Shot® TOP10 chemically competent *E.coli*	Invitrogen, Karlsruhe

Table 4.11: Commercial kits (continued)

Kit	Distributor
PureLINK™ Quick Plasmid Miniprep Kit	Invitrogen, Karlsruhe
QIAEX II Gel Extraction Kit	Qiagen, Hilden
QIAquick Gel Extraction Kit	Qiagen, Hilden
QIAGEN Plasmid Midi Kit	Qiagen, Hilden
QIAprep Spin Miniprep Kit	Qiagen, Hilden
TNT® Coupled Reticulocyte Lysate System	Promega, Mannheim

4.10 Oligonucleotides

4.10.1 PCR primers

Table 4.12: Oligonucleotide primers for the construction of different plasmids
Listed are the primer pairs and separate primers for the construction of the respective plasmids in 4.12. Bold blue regions highlight the sequence of the respective restriction enzymes (Linker). Kozak sequences are marked in green, start codons in magenta and stop codons are shown in red.

Primer name	Sequence	Linker
Ajuba orf FW	5'-GCATCA**CTCGAG**ACCATGGAGCGGTTAGGAGAG-3'	XhoI
Ajuba orf RV	5'-AGTCAC**GCGGCCGC**TCAGATATAGTTGGCAGG-3'	NotI
Ajuba LIM FW	5'-GCATCA**CTCGAG**ACCATGTGTATCAAGTGCAACAAAGGC-3'	XhoI
Ajuba PreLIM RV	5'-AGTCAC**GCGGCCGC**TCAGAAGTAGTCCTCCCT-3'	NotI
LPXN orf FW	5'-GCATCA**GCGGCCGC**ATGGAAGAGTTAGAT -3'	NotI
LPXN orf RV	5'-AGTCAC**GGATCC**CTACAGTGGGAAGAGCTTATT-3'	BamHI
pCMV-Ajuba orf FW	5'-GCATCA**GGATCC**ACCATGGAGCGGTTAGGA-3'	BamHI
pCMV-Ajuba orf RV	5'-AGTCAC**CTCGAG**TCAGATATAGTTGGCAGGGGGTTG-3'	XhoI
pCMV-C9orf102 FW	5'-GCATCA**GGATCC**ACCATGAAATGTTCAAATGAGAAAGTT-3'	BamHI
pCMV-C9orf102 RV	5'-AGTCAC**CTCGAG**TTATGTGGTACTCTGTGTATTGGT-3'	XhoI
pGEX-HPV16 E6 FW	5`-GCATCA**GGATCC**ATGCACCAAAAGAGAACT-3'	BamHI
pGEX-HPV16 E6 RV	5`-AGTCAC**CTCGAG**TTACAGCTGGGTTTCTCT-3'	XhoI
pGEX-HPV117 E6 FW	5`-GATC**GAATTC**GCCATGTCTATGGGTGCACAA-3'	EcoRI
pGEX-HPV117 E6 RV	5`-ATAC**CTCGAG**CTAAGGGATGCGGACCGT-3'	XhoI
pGEX-HPV118 E6 FW	5`-GCATCA**GGATCC**ATGGAGGAGTATCCTATG-3'	BamHI
pGEX-HPV118 E6 RV	5`-AGTCAC**CTCGAG**TTATTTACAAAACTTACAAAGACC-3'	XhoI
pGEX-HPV134 E6 FW	5`-GCATCA**GGATCC**ATGGAACCAGTCTATTCT-3'	BamHI
pGEX-HPV134 E6 RV	5`-AGTCAC**CTCGAG**TTATTTTTTCCTACATAATCTACA-3'	XhoI

Table 4.12: Oligonucleotide primers for the construction of different plasmids (continued)

Primer name	Sequence	Linker
pGEX-HPV148 E6 FW	5`-GCATCA**GGATCC**ATGGAGACCCCAACAGGA -3’	BamHI
pGEX-HPV148 E6 RV	5`-AGTCAC**CTCGAG**TTATTTCTGAGCACAATTTCTGCA-3’	XhoI
pPK-HPV4 E6 FW K	5’-GCATCA**CTCGAG**GCCATGGCAGATGGCAGA-3’	XhoI
pPK-HPV4 E6 RV K	5’-AGTCAC**GGATCC**TTGTTTCCTAATACAATTTCTGCA ATAGCC-3’	BamHI
pPK-HPV117 E6 FW	5’-GATC**GAATTC**GCCATGTCTATGGGTGCACAA-3’	EcoRI
pPK-HPV117 E6 RV	5’-ATAC**GGATCC**AGGGATGCGGACCGT-3’	BamHI
pPK-HPV148 E6 FW K	5’-GCATCA**CTCGAG**GCCATGGAGACCCCAACAGGA-3’	XhoI
pPK-HPV148 E6 RV K	5’-AGTCAC**GGATCC**TTTCTGAGCACAATTTCTGCAATCTCC-3’	BamHI

4.10.2 RNA oligonucleotides for RNA interference (RNAi)

Table 4.13: Oligonucleotides for the siRNA-mediated knock-down experiments

siRNA	Target sequence	Manufacturer	Reference
siAjuba	5’-GGGGCGCCUAAGUGGGUUG-dTdT-3’	Dharmacon, USA	Hirota *et al.* [2003]
siScramble	5’-AACAGUCGCGUUUGCGACUGG-dTdT-3’	Dharmacon, USA	Schneider *et al.* [2006]

4.11 Provided plasmids

Table 4.14: Commercially available and provided expression plasmids

Plasmid name	Backbone/Properties	Reference
JUB Gateway Full ORF clone	Full CDS of human Ajuba	DKFZ, Heidelberg
Flag-p53	pcDNA3.1 (-)	Dr. T. G. Hofmann (DKFZ, Heidelberg)
Flag-p53 1-70	pcDNA3.1 (-)	Dr. T. G. Hofmann (DKFZ, Heidelberg)
Flag-p53 1-298	pcDNA3.1 (-)	Dr. T. G. Hofmann (DKFZ, Heidelberg)
Flag-p53 80-393	pcDNA3.1 (-)	Dr. T. G. Hofmann (DKFZ, Heidelberg)
Flag-p53 294-393	pcDNA3.1 (-)	Dr. T. G. Hofmann (DKFZ, Heidelberg)
LPXN Gateway Full ORF clone	Full CDS of human Leupaxin	DKFZ, Heidelberg
PDCD6 Gateway Full ORF clone	Full CDS of human PDCD6	DKFZ, Heidelberg
pEGFP	-	Clontech
pEYFP-p53	pEYFP	Dr. T. G. Hofmann (DKFZ, Heidelberg)

4.12 Cloned plasmids

Table 4.15: Plasmids used for cloning purposes

For the cloning of the GST-tagged HPV E6 fusion proteins, the vector pGEX-4T1 was used. For C-terminally HA-tagged HPV E6 proteins, the vector pPK-CMV-E3 was used. For the cloning of Flag-tagged expression proteins, the vector pCMV3-Tag-1 was used. The vector pcDNA3.1 (-) was used for the cloning of constructs for the *in vitro* transcription/translation of proteins. The available promoters and tags are represented in *italic*. IPTG: Isopropyl-beta-D-thiogalactopyranosid; GST: glutathione S-transferase; HA: hemagglutinin; CMV: cytomegalovirus

Plasmid name	Description	Reference
pcDNA3.1 (-)	Promoter: CMV promoter	Invitrogen, Karlsruhe
pCMV3-Tag-1	*Promoter:* CMV promoter *Tag:* N-terminal 3x Flag-tag	Agilent Technologies
pGEX-4T1	*Promoter:* IPTG-inducible tac promoter *Tag:* N-terminal GST-tag	GE Healthcare
pPK-CMV-E3	*Promoter:* CMV promoter and enhancer *Tag:* C-terminal HA-tag	PromoKine

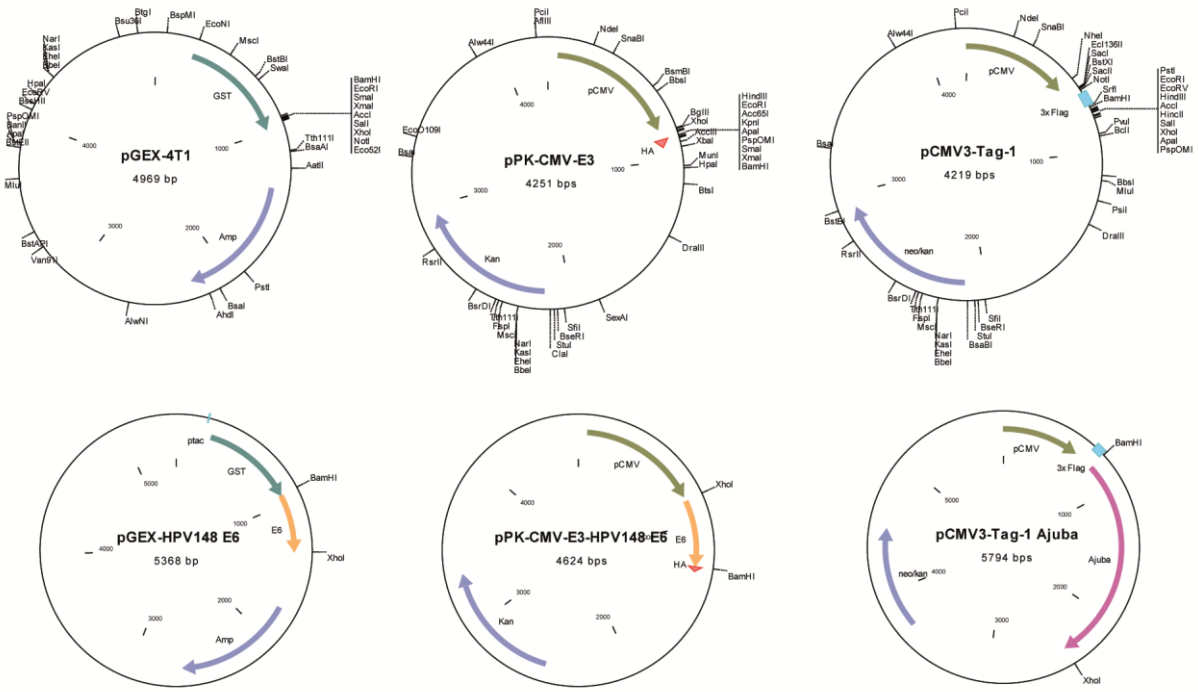

Figure 5.1: Maps of vector backbone and constructed expression plasmid.

Depicted are general features of the empty pGEX-4T1, pPK-CMV-E3 and pCMV3-Tag-1 vectors (upper panel). A representative example for the constructed expression plasmids in this thesis are shown in the lower panel. pCMV: CMV promoter; HA: hemagglutinin tag; 3xFlag: 3x Flag tag; ptac: tac promoter; Neo/Kan/Amp: resistance cassette

4.13 Mammalian cell lines

Table 4.16: List of human cell lines used throughout the presented thesis

Cell line	Characteristics	Reference
C-33 A	*Species:* Homo sapiens (human) *Tissue:* epithelial; cervical carcinoma *Comment:* tumourigenic, HPV-negative, mutant p53, mutant pRb	Crook *et al.* [1991]
CaSki	*Species:* Homo sapiens (human) *Tissue:* epithelial; cervical carcinoma *Comment:* tumourigenic, HPV16-positive (ca. 600 copies per cell)	Pattillo *et al.* [1977]
H1299	*Species:* Homo sapiens (human) *Tissue:* epithelial; non-small cell lung carcinoma *Comment:* homozygous partial deletion of the p53 protein, lack of p53 protein expression	Radhakrishna Pillai *et al.* [2004]
HeLa	*Species:* Homo sapiens (human) *Tissue:* epithelial; cervical adenocarcinoma *Comment:* tumourigenic, HPV18-positive	Jones *et al.* [1971]
HPKn	*Species:* Homo sapiens (human) *Tissue:* primary keratinocytes; neonatal foreskin	Life Technologies Cat#: C001-5C
NIKS	*Species:* Homo sapiens (human) *Tissue:* keratinocytes *Comment:* spontaneously immortal, extra isochromosome of the long arm of chromosome 8	Allen-Hoffmann *et al.* [2000]
SiHa	*Species:* Homo sapiens (human) *Tissue:* epithelial; cervical squamous cell carcinoma *Comment:* tumourigenic, HPV16-positive (1-2 copies per cell)	Friedl *et al.* [1970]
SK-MEL-28	*Species:* Homo sapiens (human) *Tissue:* malignant melanoma	Carey *et al.* [1976]
U2OS	*Species:* Homo sapiens (human) *Tissue:* epithelial; osteosarcoma *Comment:* expression of wt p53 protein	Heldin *et al.* [1986]

4.14 Bacterial strains

Table 4.17: Chemically competent bacteria

The *E. coli* One Shot® TOP10 cells were purchased from Invitrogen and used for cloning purposes. The *E. coli* Rosetta strain was kindly provided by Prof. I. Hoffmann (DKFZ, Heidelberg) and used for the expression of GST-tagged proteins.

Name	Genotype	Reference
E. coli One Shot® TOP10 (DH10B™)	F-*mcrA* Δ(*mrr-hsd*RMS-*mcr*BC) Φ80*lac*Z ΔM15 Δ*lac*X74 recA1 *ara*D139 Δ (*araleu*) 7697 *gal*U *gal*K*rps*L (Str^R) *end*A1 *nup*G	Invitrogen, Karlsruhe
E. coli Rosetta	F$^-$ *ompT hsdS*$_B$(r_B^- m_B^-) *gal dcm* pRARE (Cam^R)	Prof. I. Hoffmann (DKFZ, Heidelberg)

Section 5

Methods

5.1 Preparation, analysis, and cloning of nucleic acids

5.1.1 Generation of PCR products for cloning

The polymerase chain reaction (PCR) is a widely used *in vitro* technique for the selective amplification of specific regions from a DNA template. For cloning purposes, various viral E6 open reading frames (ORFs) as well as ORFs from other proteins were amplified by PCR using the respective templates. Forward and reverse primers were selected to harbour specific recognition sites for restriction enzymes (see section 4.12). The PCR reactions were performed using the proof-reading PRECISOR High-Fidelity DNA polymerase (BioCat). The following reagents were used in a total volume of 50µL in the MyCycler thermal cycler (Bio-Rad):

50-100ng	plasmid DNA containing the respective sequence
10µL	5x HiFi reaction buffer (incl. 2mM $MgCl_2$)
0.5µL	dNTP mix (25mM each)
1µL	primers (20µM each)
1 Unit	PRECISOR DNA polymerase
ad 50µL	water (ddH_2O)

Due to the 3'-5' exonuclease activity of the DNA polymerase, the enzyme was added last to the reaction mixture in order to prevent primer degradation. All PCR reactions were performed using the following PCR program:

Table 5.1: Standard cycling conditions

Cycle Step	Temperature	Time	Cycle(s)
Initial denaturation	98°C	1 min	1
Denaturation	98°C	30 sec	
Annealing	T_{an}°C	30 sec	35
Extension	72°C	30 sec/kb	
Final extension	72°C	10 min	1
Cooling	4°C	∞	

After DNA amplification, the PCR reaction was directly digested using the respective restriction enzymes. It was then run on an agarose gel and subsequently purified (see sections 5.1.2 and 5.1.4).

5.1.2 DNA agarose gel electrophoresis

DNA agarose gel electrophoresis is an extensively used technique for the electrophoretic separation ad analysis of nucleic acids. Thereby, DNA can be characterised according to its size and conformation. Applying an electric field, the negatively charged DNA migrates through the agarose matrix. The concentration of agarose in the agarose gels varied between 0.5 and 2%/TAE (w/v), depending on the expected size of the DNA fragments. The DNA was visualised under UV light (260nm) using the intercalating agent ethidium bromide (1µg/mL), which was added to the liquid agarose solution before polymerisation and electrophoresis.

5.1.3 Restriction enzyme digestion and dephosphorylation of plasmid DNA

Analytical and preparative enzymatic DNA digestions were performed using bacterial type II restriction endonucleases according to the manufacturer's instructions. An analytical digestion contained 1µg of plasmid DNA in a total reaction volume of 20-30µL. For preparative purposes, the DNA was linearised using the respective restriction enzymes. Thereby it obtained sticky ends compatible with the respective linearised cloning vector. PCR products or up to 10µg of plasmid DNA were digested in a total volume of 100µL, dephosphoralyted and purified after agarose gel electrophoresis.

To prevent re-ligation of the digested plasmid DNA, a dephosphorylation reaction was performed. This incubation with an alkaline phosphatase removed the terminal 5'-phosphate group of the linearised plasmid DNA, thereby minimising spontaneous re-ligations of the cloning vector. Therefore the digested plasmid DNA was incubated with the FastAP alkaline phosphatase (Fermentas) according to the manufacturer's instructions. Subsequently, the dephosphorylated plasmid DNA was run on an agarose gel and purified by gel extraction (see section 5.1.4).

5.1.4 Extraction and purification of DNA from agarose gels

For cloning, bands, of the digested and electrophoretically separated PCR products or plasmid DNA, were cut from the agarose gel using sterile scalpels under low energy UV light (366nm). Subsequently, DNA extraction and purification was performed from the gel slices using a Qiagen gel extraction kit according to the manufacturer's instructions. Alternatively, the gel slice could be weight first and then frozen or kept at 4°C for later DNA extractions.

5.1.5 Spectrophotometric quantification of nucleic acids

To determine the concentration of a PCR product or plasmid DNA in a sample, the DNA was analysed using the NanoDrop® ND-1000, a spectrophotometer. The absorption was measured at 260nm (absorption peak of nucleic acids).

5.1.6 Ligation of DNA fragments

For the ligation of DNA fragments, linearised vector DNA and the digested and purified PCR product were connected with their compatible ends, using the T4 DNA ligase (Fermentas) according to the manufacturer's instructions. The ligation reaction was performed using 50-100ng of vector DNA at a molar ratio of 1:3 or 1:5 (vector : insert). The respective DNA concentrations were assessed using the NanoDrop® ND-1000. For the ligation 5 Units of the T4 ligase (1µL in a final volume of 20µL) were added to the reaction mixture which was then incubated over night at 16°C. For inactivation of the T4 DNA ligase, the reaction mix was heated to 65°C for 10 min. The ligated plasmid was subsequently used for the transformation of competent *Escherichia coli*.

5.1.7 Transformation and cultivation of chemically competent *Escherichia coli* (*E. coli*)

The transformation of chemically competent bacteria (see section 4.14) was performed by adding 1µL of plasmid DNA or ligation reaction to 25µL of competent *E. coli*. The bacteria were incubated on ice for 20 min and then heat-shocked for 30-60 sec at 42°C, according to the antibiotic present in the vector backbone. After the heat-shock, the bacteria rested on ice for 15 min, were transferred into 250µL of pre-warmed SOC-medium and then incubated at 37°C and 550rpm for 1h. The transformed bacteria were subsequently plated on LB-agar plates containing the respective antibiotic and then incubated over night at 37°C to allow formation of single colonies. For the isolation and analysis of the clones, 2-5mL of LB-medium containing the respective antibiotic were inoculated with a plastic tip exposed to a single colony. The reaction tube was incubated for 5h or over night at 37°C to allow bacterial growth.

5.1.8 Cryoconservation and reactivation of bacteria

For long-term storage of transformed bacteria, 200µL of 87% glycerol were added to 800µL of bacterial culture and frozen at -80°C. In order to reactivate the bacteria, LB-medium containing the respective antibiotic was inoculated by scratching an adequate amount from the frozen bacteria culture with a plastic tip. This culture was then incubated over night at 37°C on a shaker.

5.1.9 Plasmid DNA preparation and purification

Isolation and purification of plasmid DNA from bacteria culture was performed using the PureLINK™ Quick Plasmid Miniprep Kit (Invitrogen) or the Qiagen Spin Miniprep Kit / Plasmid Midi Kit according to the manufacturer's instructions. For cloning purposes and subsequent DNA sequencing, the plasmid DNA was isolated using the Miniprep kits. Here, 3-5mL of bacterial over night culture were used. The isolated DNA was then analysed by restriction enzyme digestion and verified by DNA

sequencing (GATC Biotech AG). For larger preparations of plasmid DNA, 150-200mL of bacteria culture were purified using the Qiagen Plasmid Midi Kit according to the manufacturer's instructions.

5.1.10 Cloning of HA-tagged and GST-tagged HPV E6 fusion proteins

The pUC19 or pBR322 plasmids containing the complete viral HPV genomes of HPV4, HPV117, HPV118, HPV134 and HPV148 were kindly provided by Prof. Ingo Nindl (Charité, Berlin). The E6 genes were amplified by PCR (see section 5.1.1 and 4.10.1) to introduce the respective restriction sites and were ligated (see section 5.1.6) into the pGEX-4T1 vector for GST pull-down analysis or into the pPK-CMV-E3/pCMV3-Tag-1 vectors for transfection experiments in mammalian cells.

5.2 Preparation and analysis of proteins

5.2.1 Generation of whole cell protein extracts

For Western blot analyses, whole cell protein extracts were prepared using the denaturing lysis buffer (see section 4.4). The buffer was freshly supplemented with protease and phosphatase inhibitors and MG-132. The cells were cultured on 6 or 10cm dishes, then detached from the culture dish and harvested into conical tubes. The cells were washed with 1x PBS by centrifugation (5 min, 4°C, 2000rpm), resuspended in 100-200µL cold denaturing lysis buffer and kept on ice for 30 min. For lysis of the cellular membranes, the cell suspension was sonicated using the Sonifier 250 and subsequently the sample was centrifuged for 1h at 4°C and 13,000rpm. The supernatant containing the whole protein extract was collected in a fresh reaction tube and used to determine the protein concentration (see section 5.2.2). Subsequently, the protein extract was supplemented with 5x loading buffer, incubated at 95°C for 5 min and then stored at -80°C or directly analysed by Western blotting (see section 5.2.5).

5.2.2 Protein quantification

Proteins concentrations from whole cell extracts were measured using the BCA Protein Assay Kit (Thermo Fisher Scientific) according to the manufacturer's instructions [Smith *et al.*, 1985]. The absorbance was measured at 570nm in a 96 well plate using an ELISA plate reader (Thermo Fisher Scientific). The protein concentration was determined on the basis of a standard curve applying 0-2µg of BSA protein. The quantification of the GST-HPV E6 fusion proteins was performed using BSA standards of 0.5-10µg of BSA on a Coomassie-stained SDS-gel (see section 5.2.4).

5.2.3 SDS-polyacrylamide gel electrophoresis (SDS-PAGE)

For Coomassie staining or Western blot analysis, proteins had first to be separated on the basis of the discontinuous SDS-PAGE. This SDS-PAGE is a widely used method to separate proteins according to their electrophoretic mobility. It is based on a stacking gel and a separating gel forming a discontinuous gel system [Laemmli, 1970]. Proteins a separated during migration in the running gel according to their size. The extent of the separation depends on the respective polyacrylamide concentration. In this study, all proteins were separated in gels having a polyacrylamide concentration of either 10% or 12%. The gels were cats and run using the Mini-PROTEAN® system from Bio-Rad.

Table 5.2: Recipe for the preparation of stacking and resolving gels

Resolving gel	Stacking gel
0.25M Tris/HCl pH 8.8	0.25M Tris/HCl pH 6.8
10% or 12% Acrylamide-Bis (29:1)	5% Acrylamide-Bis (29:1)
0.1% SDS	0.1% SDS
0.05% APS	0.05% APS
0.08% TEMED	0.16% TEMED

Depending on the experimental setup, 50-80µg of total protein were loaded onto the gel for ideal signal detection. Before loading, the protein samples were supplemented with 5x protein loading buffer and incubated at 85°C or 95°C for 5 min. For a better readout, a protein size marker (Page Ruler™ Plus Prestained Protein Ladder) was added to the gel. The gels were run at 80V until the proteins reached the resolving gel. Then the voltage was increased to 120V until the desired protein resolution was achieved.

5.2.4 Coomassie staining of polyacrylamide gels

After SDS-PAGE, Coomassie staining was performed to visualise the proteins inside the gel. Therefore, the gel was incubated in fixing solution for 1h to mediate the coupling of the proteins to the gel. Subsequently, the gel was incubated in the Coomassie staining solution for 1h, where the fixed proteins were stained. After destaining for several hours or over night, the gels were dried using a vacuum gel dryer at 80°C for 50 min to facilitate a long-term storage or for subsequent autoradiographic exposures (see section 5.3.3).

5.2.5 Western blotting and protein detection

Whole cell protein extracts or protein complexes were separated by SDS-PAGE and then detected using Western blot analysis. After SDS-PAGE, the proteins were electrophoretically transferred onto a PVDF membrane and probed with antigen-specific antibodies. The electrophoretic transfer was performed using a Wet blot Western chamber (Bio-Rad). First, the PVDF membrane was activated by incubation in methanol for 1 min and then equilibrated in 1x Towbin buffer together with the SDS-PAGE gel and two whatman papers. All components were arranged vertically between the electrodes of the Wet blot chamber according to the manufacturer's instructions. The transfer run was performed for at 4°C for 1h at 390mA under stirring on a magnetic mixer. The proteins immobilised on the PVDF membrane were visualised using antigen-specific primary antibodies and horseradish peroxidase (HRP)-conjugated secondary antibodies (see Tab. 4.10). To reduce unspecific binding of the applied antibodies, the PVDF membrane was incubated in blocking solution (5% milk powder/TBST or 5% BSA/TBST) after the protein transfer for 1h at room temperature or over night at 4°C. Then, it was incubated with the primary antibody diluted in the respective blocking reagent for 1h at room temperature or over night at 4°C, always depending on the manufacturer's recommendations for the respective antibody. Next, the membrane was washed with 1x TBST for 10 min several times and then incubated with the secondary HRP-conjugated antibody for 1h at room temperature, again followed by several washing steps. Finally, the specifically bound antibody complexes were detected using the enhanced chemiluminescence (ECL) reagents (Perkin Elmer and Thermo Fisher Scientific), which employs the HRP-catalysed chemiluminescence reaction for protein visualisation. Therefore, the membrane was incubated with the ECL reagent according to the manufacturer's instructions. The bound antigen-specific antibodies were detected by autoradiography through exposition to X-ray films. The exposition time and the utilised ECL reagent strongly depended on the used antibody.

5.2.6 Membrane stripping

To allow the detection of different proteins of similar size on the same PVDF membrane, bound antigen-specific antibodies had to be removed. Therefore, the membrane was incubated for 10 min in 0.2M NaOH and then washed for 5 min with ddH_2O. The membrane was then incubated in blocking solution (5% milk powder/TBST or 5% BSA/TBST) for 1h and re-incubated with a different antigen-specific antibody as described in section 5.2.5.

5.3 *In vitro* assays

5.3.1 *In vitro* transcription/translation of proteins

For eukaryotic *in vitro* transcription/translation of proteins, the TNT® Coupled Reticulocyte Lysate System (Promega) was employed according to the manufacturer's instructions. First, all needed reagents were thawed on ice. The plasmid DNA templates of Flag-p53 and its deletion mutants as well as the constructs of the putative interaction partners (PDCD6IP, LPXN, C9orf102 and Ajuba) were first diluted to a concentration of 0.5µg/µL. The reaction was performed using the provided TNT® T7 RNA Polymerase together with the following reagents in a 1.5mL reaction tube:

25µL	TNT® Rabbit Reticulocyte Lysate
2µL	TNT® Reaction Buffer
1µL	TNT® T7 RNA Polymerase
1µL	Amino Acid Mixture, Minus Methionine, 1mM
2µL	L-[^{35}S]-methionine
2µL	RNase OUT
2µL	DNA template (0.5µg/µL)
ad 50µL	Nuclease-free water

The reaction mixture was mixed very gently by stirring it using a pipette tip and then incubated for 90 min at 30°C. Before the storage of the *in vitro* translated protein mixture at -80°C, a 3µL aliquot was removed, supplemented with 30µL of 1x protein loading buffer and incubated at 85°C for 5 min for the subsequent analysis of the translation efficiency. Therefore, an SDS-PAGE was performed loading the protein marker and the *in vitro* translated protein onto the gel. After the gel run it was analysed by Coomassie staining. Additionally, the gel was incubated in Amplify Fluorographic Reagent (GE Healthcare) for 15 min at 50°C, which increases the sensitivity of detection for weak beta emitters like ^{35}S. Thereafter, the gel was dried using the vacuum gel dryer for 1h at 80°C, The *in vitro* translated and ^{35}S-radioactively labelled proteins were autoradiographically detected in an autoradiography cassette over night at -80°C.

5.3.2 Expression and purification of recombinant fusion proteins

The GST-tagged recombinant fusion proteins were produced by transformation of the *E. coli* strain Rosetta with the pGEX-4T1 vector containing the PDCD6 or HPV E6 ORFs. The bacteria pre-cultures were grown in 100mL LB-medium supplemented with 100µg/mL ampicillin and 34µg/mL chloramphenicol over night at 37°C. The next day, 400mL of LB-medium supplemented with antibiotics were added to the pre-culture and grown at 37°C until the OD_{600} reached a value of 0.5.

Protein expression was induced by adding 250µM IPTG to the culture and the bacteria were then incubated over night at 24°C on a rotating shaker. After cultivation the bacteria were pelleted at 6,000rpm at 4°C by centrifugation and frozen for 30 min or over night at -80°C. The pellet was then thawed on ice and resuspended in 10mL ice-cold 1x PBS supplemented with 100µM PMSF. The suspension was homogenised twice by sonication using the Sonifier 250. The suspension was incubated on ice for 15 min after the addition of 1.5mL 10% Triton X-100/PBS. The homogenisation step was repeated and the cell debris collected by centrifugation (13,000rpm, 20 min, 4°C). The supernatant was then incubated with 300µL of PBS equilibrated Glutathione Sepharose™ 4FastFlow beads (GE Healthcare) under rotation for 6h at 4°C. The beads were collected by centrifugation at 2,000rpm for 5 min at 4°C, washed twice with 10mL ice-cold 0.1% Triton X-100/PBS and once with cold 1x PBS to remove unspecifically bound proteins. The beads were then resuspended in 200µL 1xPBS and analysed by SDS-PAGE and Coomassie staining in order to estimate the protein concentration of the purified recombinant fusion proteins.

5.3.3 GST pull-down of recombinant GST-tagged HPV E6 fusion proteins

GST pull-down experiments were performed to identify and thereby also confirm supposed direct interactions between two distinct proteins *in vitro*. For the GST pull-down 3µg (in a total volume of 30µL Glutathione Sepharose beads) of purified GST-HPV E6 fusion proteins (see section 5.3.2) were incubated with 6µL of the *in vitro* transcribed and translated ^{35}S-methionine labelled proteins (see section 5.3.1) in 500µL *in vitro* interaction buffer under rotation at 4°C for 90 min. After incubation, the beads were pelleted by centrifugation at 2,000rpm for 2 min and washed up to 10 times with 750µL ice-cold *in vitro* interaction buffer to remove unspecifically bound proteins. The residual beads, containing the bound protein complexes were supplemented with 25µl of 1x protein loading buffer and incubated for 5 min at 85°C. The protein complexes were then separated by SDS-PAGE and the gel was stained with Coomassie. Additionally, the stained gel was incubated in Amplify Fluorographic Reagent (GE Healthcare) at 50°C for 15 min and then dried in a vacuum gel drier for 1h at 80°C, The radioactive signals were detected in an autoradiography cassette after an over night incubation at -80°C.

5.4 *In vivo* co-immunoprecipitation of proteins

Co-immunoprecipitation (Co-IP) analysis is a frequently used method to identify protein-protein interactions occurring in mammalian cells, by using target-specific antibodies. Therefore, cells were transfected in 6cm dishes with the respective plasmids using the Lipofectamine 2000 reagent (Invitrogen) according to the manufacturer's instructions (see section 5.5.3). 24h after transfection, the cells were harvested and washed with 1x PBS by centrifugation (2 min, 2000rpm).

The cell pellets were either frozen at -80°C or directly resuspended in 200µL ice-cold non-denaturing lysis buffer supplemented with protease and phosphatase inhibitors as well as MG-132. The cell suspension was incubated on ice for 1h to allow cell lysis and was subsequently centrifuged at 10,000rpm for 1h at 4°C. The supernatant containing the whole protein extract was transferred into a fresh 1.5mL reaction tube. As input control, 5-30% of the supernatant were supplemented with 5x loading buffer, incubated at 85°C for 5 min and stored at -80°C until the SDS-PAGE. The residual protein suspension was filled to a volume of 500µL with pre-chilled non denaturing lysis buffer. For pre-clearing, the protein suspension was incubated with 30µL of Protein A/G PLUS-Agarose beads (Santa Cruz) for 1h at 4°C under rotation. To remove the beads, the protein suspension was centrifuged for 1 min and 6,000rpm at 4°C. The supernatant containing the cleared, unbound proteins was transferred into a fresh 1.5mL reaction tube. For co-precipitation itself, 1-5µg of a target-specific antibody was incubated with the protein extract for 3h at 4°C under rotation. After incubation, 30µL of Protein A/G PLUS-Agarose beads were added and additionally incubated for 1h at 4°C. The protein suspension was centrifuged (1 min, 6,000rpm, 4°C), the supernatant discarded and the beads harbouring the specifically bound protein complexes were washed several times in cold non-denaturing lysis buffer to remove unspecifically bound proteins. At last, the beads were supplemented with 30µL of 1x protein loading buffer and incubated for 5 min at 85°C. The bound protein complexes as well as the stored input control were analysed by SDS-PAGE and subsequent Western blot analysis (see section 5.2.5).

5.5 Cell culture

5.5.1 Maintenance of mammalian cells

Mammalian cells were grown in Dulbecco's modified Eagle's medium (DMEM) supplemented with 10% fetal calf serum (FCS). The cells were cultivated in cell culture flasks until they reached a confluency of 80-90% and were then passaged or seeded in new dishes for experiments. All cell lines were maintained at 37°C, 5% CO_2 and 95% humidity in an incubator. For passaging, the culture medium was removed and the cells washed once with 1x PBS. In order detach adherent cells from the culture flasks they were incubated with 0.25% trypsin/EDTA solution and incubated at 37°C until they dissociated. The trypsin solution was inactivated by addition of DMEM containing 10% FSC. For cell maintenance, the cells were then transferred into fresh culture flasks at a ratio of 1:10 or 1:20, depending on their growth, and further incubated at 37°C. For experimental set-ups, the cells were first counted in a Neubauer hemocytometer. The required number of cells was transferred into culture flasks or dishes and incubated at 37°C. All cell lines were regularly checked for *Mycoplasma* contaminations.

5.5.2 Cryoconservation and reactivation of mammalian cells

For long-term storage of eukaryotic cells in liquid nitrogen, $1x10^6$ cells or the half of a $75cm^2$ cell culture flask were pelleted by centrifugation at 2,500rpm for 5 min and washed with 1x PBS. The cells were then resuspended in 2mL cold freezing medium and transferred into cryo-tubes. The tubes were cooled down slowly using a cell freezer at -80°C. After several days, the cryo-tubes were transferred the liquid nitrogen tanks. To reactivate the cells, the frozen cryo-tubes were thawed rapidly at 37°C and transferred into 10mL of cultivation medium. The cells were pelleted by centrifugation and washed one with 1x PBS to remove residual DMSO. The cell pellets were then resuspended in fresh culture medium and transferred into cultivation flasks.

5.5.3 Transfection of plasmid DNA into mammalian cells

For transfection of plasmid DNA, $3x10^5$ cells were seeded in 6 cm cell culture dishes one day prior to transfection or grown to a density of 70% confluence. All cell lines were transfected using Lipofectamine 2000 (Invitrogen) according to the manufacturer's instructions. The transfection reagent is lipid-based and encases the DNA thus facilitating the uptake into eukaryotic cells. The cells were transfected with 2-5µg of plasmid DNA and up to 10µL Lipofectamine 2000 reagent. The respective plasmid DNA was diluted in Opti-MEM. Subsequently, the Lipofectamine 2000 was diluted in Opti-MEM and incubated for 5 min at room temperature. The Lipofectamine solution was then added to the DNA suspension and mixed by inverting the reaction tube several times. The mixture was then incubated for 20 min at room temperature and applied evenly to the seeded cells. The cells were incubated for up to 48h prior to protein extraction for Western blot analysis (see section 5.2.5).

5.5.4 Transfection of siRNA into mammalian cells

Upon siRNA transfection, the genes of interest were silenced by the degradation of specific mRNA in mammalian cells. For siRNA-mediated knockdown of proteins, cells were seeded in 6 cm cell culture dishes one day prior to transfection and grown until a confluence of 30%. The cells were transfected with siRNA (Dharmacon) using Lipofectamine 2000 as described in 5.5.3. Here, 100-200 pmoles of specific siRNA or scramble control siRNA were used. The cells were incubated with the respective siRNA for 48h and then repeatedly transfected. 96h after the first transfection, the cells were harvested and analysed by Western blotting (see section 5.2.5).

5.5.5 Generation of stable cell lines

For the generation of stable cell lines, the cells were transfected with 1µg of the respective expression plasmid using the Effectene transfection reagent (Qiagen) according to the manufacturer's instructions. 24h after transfection the cells were transferred from a 6 cm culture

dish into a 75 cm^2 cell culture flask and grown until 70% of confluence were reached. The medium was then supplemented with up to 850µg/mL of the antibiotic Geneticin (G418). In parallel, untransfected control cells were also treated with the same amount of G418. After two weeks of selection pressure, the drug resistant cells were considered "stably" transfected. However, the expression of the respective protein, stably introduced into the cells, was controlled by Western blot analysis.

5.5.6 Adriamycin and UVB treatment

For UVB irradiation, the cells were grown to a minimum of 60% confluence. The growth medium was removed and the cells washed once with 1x PBS, prior to irradiation with UVB using the Waldmann UV181 BL. The UVB dose was set to either 300 J/m^2 or 1,000 J/m^2 with an output range of 280 to 320nm. Additionally, the amount of radiated UVB was measured with an UVB detector (Variocontrol UV-meter). After irradiation, the cells were supplemented with fresh growth medium and harvested after 24h. For Adriamycin treatment (ADR), the cells were grown as for the UVB irradiation. The growth medium was replaced to medium supplemented with ADR (1µg/mL) and the cells were incubated at 37°C and harvested at indicated time points for Western blot analysis.

5.5.7 Immunofluorescence staining of mammalian cells

For monitoring of the localisation of overexpressed or endogenous proteins, immunofluorescence staining was performed. All steps were performed at room temperature. First, the cells were grown on round cover slips in DMEM supplemented with 10% FCS. They were then transfected with the respective plasmids for 48h. After incubation, the cells were washed once in 1x PBS and fixed in 3.7% paraformaldehyde/PBS for 20. After fixation, the cells were washed once with 0.1M glycine and subsequently permeabilised with 0.5% Triton X-100/PBS. The cells were incubated for 1h with 1% BSA/PBS prior to the addition of the primary antibodies for 90 min, which were diluted in 1% BSA/PBS. The cover slips were washed three times for 5 min in 1x PBS and incubated with specific fluorescein-conjugated secondary goat antibodies (Alexa Fluor®, Tab. 4.10) for 45 min. Additionally, all cover slips were incubated with Hoechst staining solution (1:10,000) for 20 min. The stained cells were then washed several times with 1x PBS and water and mounted on glass slides with Mowiol. The slides were dried over night in the dark and analysed by confocal microscopy.

5.5.8 Luciferase reporter assay

One day before transfection H1299 cells were plated in a density of $5x10^4$/well of a 24-well plate. The following day, the cells were transfected with 5ng/well p53-promoter firefly luciferase reporter and 1ng/well of pRL-TATA renilla luciferase plasmid for normalisation. Additionally, the cells

were transfected with increasing amounts (0-5ng) of HA-tagged HPV23 E6 or HPV148 E6. 24h after transfection, the cells were lysed and firefly luciferase activity was analysed and normalised to renilla luciferase activity using the Dual Luciferase Reporter System (Promega) according to the manufacturer's instructions. All experiments were performed four times in triplicates.

References

1. **Abe Y, Ohsugi M, Haraguchi K, Fujimoto J, Yamamoto T** (2006) LATS2-Ajuba complex regulates gamma-tubulin recruitment to centrosomes and spindle organization during mitosis. FEBS Lett 580: 782-8.
2. **Akgül B, Bostanci N, Westphal K, Nindl I, Navsaria H, et al.** (2010) Human papillomavirus 5 and 8 E6 downregulate interleukin-8 secretion in primary human keratinocytes. J Gen Virol 91: 888-92.
3. **Allan LA, Fried M** (1999) p53-dependent apoptosis or growth arrest induced by different forms of radiation in U2OS cells: p21WAF1/CIP1 repression in UV induced apoptosis. Oncogene 18: 5403-12.
4. **Allen-Hoffmann BL, Schlosser SJ, Ivarie CA, Sattler CA, Meisner LF, et al.** (2000) Normal growth and differentiation in a spontaneously immortalized near-diploid human keratinocyte cell line, NIKS. J Invest Dermatol 114: 444-55.
5. **Antman K, Chang Y** (2000) Kaposi's sarcoma. N Engl J Med 342: 1027-38.
6. **Antonsson A, Hansson BG** (2002) Healthy skin of many animal species harbors papillomaviruses which are closely related to their human counterparts. J Virol 76: 12537-42.
7. **Antonsson A, McMillan NA** (2006) Papillomavirus in healthy skin of Australian animals. J Gen Virol 87: 3195-200.
8. **Arends MJ, Benton EC, McLaren KM, Stark LA, Hunter JA, et al.** (1997) Renal allograft recipients with high susceptibility to cutaneous malignancy have an increased prevalence of human papillomavirus DNA in skin tumours and a greater risk of anogenital malignancy. Br J Cancer 75: 722-8.
9. **Asgari MM, Kiviat NB, Critchlow CW, Stern JE, Argenyi ZB, et al.** (2008) Detection of human papillomavirus DNA in cutaneous squamous cell carcinoma among immunocompetent individuals. J Invest Dermatol 128: 1409-17.
10. **Bach I** (2000) The LIM domain: regulation by association. Mech Dev 91: 5-17.
11. **Bedard KM, Underbrink MP, Howie HL, Galloway DA** (2008) The E6 oncoproteins from human betapapillomaviruses differentially activate telomerase through an E6AP-dependent mechanism and prolong the lifespan of primary keratinocytes. J Virol 82: 3894-902.
12. **Bernard HU, Burk RD, Chen Z, van Doorslaer K, Hausen H, et al.** (2010) Classification of papillomaviruses (PVs) based on 189 PV types and proposal of taxonomic amendments. Virology 401: 70-9.
13. **Birkeland SA, Storm HH, Lamm LU, Barlow L, Blohme I, et al.** (1995) Cancer risk after renal transplantation in the Nordic countries, 1964-1986. Int J Cancer 60: 183-9.
14. **Bittner JJ** (1942) The Milk-Influence of Breast Tumors in Mice. Science 95: 462-3.
15. **Bosch FX, Manos MM, Munoz N, Sherman M, Jansen AM, et al.** (1995) Prevalence of human papillomavirus in cervical cancer: a worldwide perspective. International biological study on cervical cancer (IBSCC) Study Group. J Natl Cancer Inst 87: 796-802.
16. **Bosch FX, Lorincz A, Munoz N, Meijer CJ, Shah KV** (2002) The causal relation between human papillomavirus and cervical cancer. J Clin Pathol 55: 244-65.
17. **Boulares AH, Yakovlev AG, Ivanova V, Stoica BA, Wang G, et al.** (1999) Role of poly(ADP-ribose) polymerase (PARP) cleavage in apoptosis. Caspase 3-resistant PARP mutant increases rates of apoptosis in transfected cells. J Biol Chem 274: 22932-40.
18. **Bouwes Bavinck JN, Euvrard S, Naldi L, Nindl I, Proby CM, et al.** (2007) Keratotic skin lesions and other risk factors are associated with skin cancer in organ-transplant recipients: a case-control study in The Netherlands, United Kingdom, Germany, France, and Italy. J Invest Dermatol 127: 1647-56.

19. **Bouwes Bavinck JN, Neale RE, Abeni D, Euvrard S, Green AC, et al.** (2010) Multicenter study of the association between betapapillomavirus infection and cutaneous squamous cell carcinoma. Cancer Res 70: 9777-86.
20. **Brash DE, Ziegler A, Jonason AS, Simon JA, Kunala S, et al.** (1996) Sunlight and sunburn in human skin cancer: p53, apoptosis, and tumor promotion. J Investig Dermatol Symp Proc 1: 136-42.
21. **Bravo IG, Alonso A** (2004) Mucosal human papillomaviruses encode four different E5 proteins whose chemistry and phylogeny correlate with malignant or benign growth. J Virol 78: 13613-26.
22. **Breen JJ, Agulnick AD, Westphal H, Dawid IB** (1998) Interactions between LIM domains and the LIM domain-binding protein Ldb1. J Biol Chem 273: 4712-7.
23. **Caldeira S, Zehbe I, Accardi R, Malanchi I, Dong W, et al.** (2003) The E6 and E7 proteins of the cutaneous human papillomavirus type 38 display transforming properties. J Virol 77: 2195-206.
24. **Campo MS** (1997) Bovine papillomavirus and cancer. Vet J 154: 175-88.
25. **Campo MS** (2002) Animal models of papillomavirus pathogenesis. Virus Res 89: 249-61.
26. **Carey TE, Takahashi T, Resnick LA, Oettgen HF, Old LJ** (1976) Cell surface antigens of human malignant melanoma: mixed hemadsorption assays for humoral immunity to cultured autologous melanoma cells. Proc Natl Acad Sci U S A 73: 3278-82.
27. **Chan SY, Delius H, Halpern AL, Bernard HU** (1995) Analysis of genomic sequences of 95 papillomavirus types: uniting typing, phylogeny, and taxonomy. J Virol 69: 3074-83.
28. **Chang DF, Belaguli NS, Iyer D, Roberts WB, Wu SP, et al.** (2003) Cysteine-rich LIM-only proteins CRP1 and CRP2 are potent smooth muscle differentiation cofactors. Dev Cell 4: 107-18.
29. **Corona R, Dogliotti E, D'Errico M, Sera F, Iavarone I, et al.** (2001) Risk factors for basal cell carcinoma in a Mediterranean population: role of recreational sun exposure early in life. Arch Dermatol 137: 1162-8.
30. **Crawford AW, Beckerle MC** (1991) Purification and characterization of zyxin, an 82,000-dalton component of adherens junctions. J Biol Chem 266: 5847-53.
31. **Crawford AW, Michelsen JW, Beckerle MC** (1992) An interaction between zyxin and alpha-actinin. J Cell Biol 116: 1381-93.
32. **Crook T, Wrede D, Vousden KH** (1991) p53 point mutation in HPV negative human cervical carcinoma cell lines. Oncogene 6: 873-5.
33. **Cullen AP, Reid R, Campion M, Lorincz AT** (1991) Analysis of the physical state of different human papillomavirus DNAs in intraepithelial and invasive cervical neoplasm. J Virol 65: 606-12.
34. **Cyert MS** (2001) Regulation of nuclear localization during signaling. J Biol Chem 276: 20805-8.
35. **Dalton-Griffin L, Kellam P** (2009) Infectious causes of cancer and their detection. J Biol 8: 67.
36. **Damania B** (2004) Modulation of cell signaling pathways by Kaposi's sarcoma-associated herpesvirus (KSHVHHV-8). Cell Biochem Biophys 40: 305-22.
37. **Dawid IB, Breen JJ, Toyama R** (1998) LIM domains: multiple roles as adapters and functional modifiers in protein interactions. Trends Genet 14: 156-62.
38. **de Koning MN, Struijk L, Bavinck JN, Kleter B, ter Schegget J, et al.** (2007) Betapapillomaviruses frequently persist in the skin of healthy individuals. J Gen Virol 88: 1489-95.
39. **de Koning MN, Weissenborn SJ, Abeni D, Bouwes Bavinck JN, Euvrard S, et al.** (2009) Prevalence and associated factors of betapapillomavirus infections in individuals without cutaneous squamous cell carcinoma. J Gen Virol 90: 1611-21.
40. **de Martel C, Ferlay J, Franceschi S, Vignat J, Bray F, et al.** (2012) Global burden of cancers attributable to infections in 2008: a review and synthetic analysis. Lancet Oncol 13: 607-15.
41. **de Villiers EM, Fauquet C, Broker TR, Bernard HU, zur Hausen H** (2004) Classification of papillomaviruses. Virology 324: 17-27.
42. **Deane JE, Ryan DP, Sunde M, Maher MJ, Guss JM, et al.** (2004) Tandem LIM domains provide synergistic binding in the LMO4:Ldb1 complex. EMBO J 23: 3589-98.

43. **Degenhardt YY, Silverstein S** (2001) Interaction of zyxin, a focal adhesion protein, with the e6 protein from human papillomavirus type 6 results in its nuclear translocation. J Virol 75: 11791-802.
44. **Doorbar J, Ely S, Sterling J, McLean C, Crawford L** (1991) Specific interaction between HPV-16 E1-E4 and cytokeratins results in collapse of the epithelial cell intermediate filament network. Nature 352: 824-7.
45. **Doorbar J** (2005) The papillomavirus life cycle. J Clin Virol 32 Suppl 1: S7-15.
46. **Doorbar J** (2006) Molecular biology of human papillomavirus infection and cervical cancer. Clin Sci (Lond) 110: 525-41.
47. **Doorbar J, Quint W, Banks L, Bravo IG, Stoler M, et al.** (2012) The biology and life-cycle of human papillomaviruses. Vaccine 30 Suppl 5: F55-70.
48. **Drees BE, Andrews KM, Beckerle MC** (1999) Molecular dissection of zyxin function reveals its involvement in cell motility. J Cell Biol 147: 1549-60.
49. **Dubina M, Goldenberg G** (2009) Viral-associated nonmelanoma skin cancers: a review. Am J Dermatopathol 31: 561-73.
50. **Elbel M, Carl S, Spaderna S, Iftner T** (1997) A comparative analysis of the interactions of the E6 proteins from cutaneous and genital papillomaviruses with p53 and E6AP in correlation to their transforming potential. Virology 239: 132-49.
51. **Ellerman V, Bang O** (1908) Experimentelle Leukämie bei Hühnern. Zentralbl: Bakteriol Parasitenkd Infectionskr Hyg Abt I 46: 595-609.
52. **Epstein MA, Achong BG, Barr YM** (1964) Virus Particles in Cultured Lymphoblasts from Burkitt's Lymphoma. Lancet 1: 702-3.
53. **Epstein MA** (1971) The possible role of viruses in human cancer. Lancet 1: 1344-7.
54. **Euvrard S, Kanitakis J, Claudy A** (2003) Skin cancers after organ transplantation. N Engl J Med 348: 1681-91.
55. **Favre M, Ramoz N, Orth G** (1997) Human papillomaviruses: general features. Clin Dermatol 15: 181-98.
56. **Fehrmann F, Laimins LA** (2003) Human papillomaviruses: targeting differentiating epithelial cells for malignant transformation. Oncogene 22: 5201-7.
57. **Feltkamp MC, Broer R, di Summa FM, Struijk L, van der Meijden E, et al.** (2003) Seroreactivity to epidermodysplasia verruciformis-related human papillomavirus types is associated with nonmelanoma skin cancer. Cancer Res 63: 2695-700.
58. **Feng Y, Longmore GD** (2005) The LIM protein Ajuba influences interleukin-1-induced NF-kappaB activation by affecting the assembly and activity of the protein kinase Czeta/p62/TRAF6 signaling complex. Mol Cell Biol 25: 4010-22.
59. **Ferlay J, Shin HR, Bray F, Forman D, Mathers C, et al.** (2010) Estimates of worldwide burden of cancer in 2008: GLOBOCAN 2008. Int J Cancer 127: 2893-917.
60. **Ferrand A, Chevrier V, Chauvin JP, Birnbaum D** (2009) Ajuba: a new microtubule-associated protein that interacts with BUBR1 and Aurora B at kinetochores in metaphase. Biol Cell 101: 221-35.
61. **Florin L, Sapp C, Streeck RE, Sapp M** (2002) Assembly and translocation of papillomavirus capsid proteins. J Virol 76: 10009-14.
62. **Freyd G, Kim SK, Horvitz HR** (1990) Novel cysteine-rich motif and homeodomain in the product of the Caenorhabditis elegans cell lineage gene lin-11. Nature 344: 876-9.
63. **Friedl F, Kimura I, Osato T, Ito Y** (1970) Studies on a new human cell line (SiHa) derived from carcinoma of uterus. I. Its establishment and morphology. Proc Soc Exp Biol Med 135: 543-5.
64. **Gillison ML, Alemany L, Snijders PJ, Chaturvedi A, Steinberg BM, et al.** (2012) Human papillomavirus and diseases of the upper airway: head and neck cancer and respiratory papillomatosis. Vaccine 30 Suppl 5: F34-54.
65. **Goodwin EC, DiMaio D** (2000) Repression of human papillomavirus oncogenes in HeLa cervical carcinoma cells causes the orderly reactivation of dormant tumor suppressor pathways. Proc Natl Acad Sci U S A 97: 12513-8.

66. **Gottschling M, Wibbelt G, Wittstatt U, Stockfleth E, Nindl I** (2008) Novel papillomavirus isolates from Erinaceus europaeus (Erinaceidae, Insectivora) and the Cervidae (Artiodactyla), Cervus timorensis and Pudu puda, and phylogenetic analysis of partial sequence data. Virus Genes 36: 281-7.
67. **Gottschling M, Goker M, Stamatakis A, Bininda-Emonds OR, Nindl I, et al.** (2011) Quantifying the phylodynamic forces driving papillomavirus evolution. Mol Biol Evol 28: 2101-13.
68. **Goyal RK, Lin P, Kanungo J, Payne AS, Muslin AJ, et al.** (1999) Ajuba, a novel LIM protein, interacts with Grb2, augments mitogen-activated protein kinase activity in fibroblasts, and promotes meiotic maturation of Xenopus oocytes in a Grb2- and Ras-dependent manner. Mol Cell Biol 19: 4379-89.
69. **Gross L** (1951) "Spontaneous" leukemia developing in C3H mice following inoculation in infancy, with AK-leukemic extracts, or AK-embrvos. Proc Soc Exp Biol Med 76: 27-32.
70. **Guccione E, Massimi P, Bernat A, Banks L** (2002) Comparative analysis of the intracellular location of the high- and low-risk human papillomavirus oncoproteins. Virology 293: 20-5.
71. **Hanahan D, Weinberg RA** (2011) Hallmarks of cancer: the next generation. Cell 144: 646-74.
72. **Harry JB, Wettstein FO** (1996) Transforming properties of the cottontail rabbit papillomavirus oncoproteins Le6 and SE6 and of the E8 protein. J Virol 70: 3355-62.
73. **Hartevelt MM, Bavinck JN, Kootte AM, Vermeer BJ, Vandenbroucke JP** (1990) Incidence of skin cancer after renal transplantation in The Netherlands. Transplantation 49: 506-9.
74. **Harwood CA, Surentheran T, McGregor JM, Spink PJ, Leigh IM, et al.** (2000) Human papillomavirus infection and non-melanoma skin cancer in immunosuppressed and immunocompetent individuals. J Med Virol 61: 289-97.
75. **Harwood CA, Proby CM** (2002) Human papillomaviruses and non-melanoma skin cancer. Curr Opin Infect Dis 15: 101-14.
76. **Harwood CA, Surentheran T, Sasieni P, Proby CM, Bordea C, et al.** (2004) Increased risk of skin cancer associated with the presence of epidermodysplasia verruciformis human papillomavirus types in normal skin. Br J Dermatol 150: 949-57.
77. **Hayon IL, Haupt Y** (2002) p53: an internal investigation. Cell Cycle 1: 111-6.
78. **Heilman CA, Law MF, Israel MA, Howley PM** (1980) Cloning of human papilloma virus genomic DNAs and analysis of homologous polynucleotide sequences. J Virol 36: 395-407.
79. **Heldin CH, Johnsson A, Wennergren S, Wernstedt C, Betsholtz C, et al.** (1986) A human osteosarcoma cell line secretes a growth factor structurally related to a homodimer of PDGF A-chains. Nature 319: 511-4.
80. **Hirota T, Kunitoku N, Sasayama T, Marumoto T, Zhang D, et al.** (2003) Aurora-A and an interacting activator, the LIM protein Ajuba, are required for mitotic commitment in human cells. Cell 114: 585-98.
81. **Hobert O, Schilling JW, Beckerle MC, Ullrich A, Jallal B** (1996) SH3 domain-dependent interaction of the proto-oncogene product Vav with the focal contact protein zyxin. Oncogene 12: 1577-81.
82. **Hou Z, Peng H, Ayyanathan K, Yan KP, Langer EM, et al.** (2008) The LIM protein AJUBA recruits protein arginine methyltransferase 5 to mediate SNAIL-dependent transcriptional repression. Mol Cell Biol 28: 3198-207.
83. **Ichihashi M, Ueda M, Budiyanto A, Bito T, Oka M, et al.** (2003) UV-induced skin damage. Toxicology 189: 21-39.
84. **Jablonska S, Dabrowski J, Jakubowicz K** (1972) Epidermodysplasia verruciformis as a model in studies on the role of papovaviruses in oncogenesis. Cancer Res 32: 583-9.
85. **Jackson S, Harwood C, Thomas M, Banks L, Storey A** (2000) Role of Bak in UV-induced apoptosis in skin cancer and abrogation by HPV E6 proteins. Genes Dev 14: 3065-73.
86. **Jackson S, Storey A** (2000) E6 proteins from diverse cutaneous HPV types inhibit apoptosis in response to UV damage. Oncogene 19: 592-8.
87. **Jones HW, Jr., McKusick VA, Harper PS, Wuu KD** (1971) George Otto Gey. (1899-1970). The HeLa cell and a reappraisal of its origin. Obstet Gynecol 38: 945-9.

88. **Kadrmas JL, Beckerle MC** (2004) The LIM domain: from the cytoskeleton to the nucleus. Nat Rev Mol Cell Biol 5: 920-31.
89. **Kalan S, Matveyenko A, Loayza D** (2013) LIM Protein Ajuba Participates in the Repression of the ATR-Mediated DNA Damage Response. Front Genet 4: 95.
90. **Kanungo J, Pratt SJ, Marie H, Longmore GD** (2000) Ajuba, a cytosolic LIM protein, shuttles into the nucleus and affects embryonal cell proliferation and fate decisions. Mol Biol Cell 11: 3299-313.
91. **Karagas MR, Nelson HH, Sehr P, Waterboer T, Stukel TA, et al.** (2006) Human papillomavirus infection and incidence of squamous cell and basal cell carcinomas of the skin. J Natl Cancer Inst 98: 389-95.
92. **Karlsson O, Thor S, Norberg T, Ohlsson H, Edlund T** (1990) Insulin gene enhancer binding protein Isl-1 is a member of a novel class of proteins containing both a homeo- and a Cys-His domain. Nature 344: 879-82.
93. **Katayama H, Sasai K, Kawai H, Yuan ZM, Bondaruk J, et al.** (2004) Phosphorylation by aurora kinase A induces Mdm2-mediated destabilization and inhibition of p53. Nat Genet 36: 55-62.
94. **Kiss H, Kedra D, Yang Y, Kost-Alimova M, Kiss C, et al.** (1999) A novel gene containing LIM domains (LIMD1) is located within the common eliminated region 1 (C3CER1) in 3p21.3. Hum Genet 105: 552-9.
95. **Ko CB, Walton S, Keczkes K, Bury HP, Nicholson C** (1994) The emerging epidemic of skin cancer. Br J Dermatol 130: 269-72.
96. **Köhler A, Gottschling M, Forster J, Rowert-Huber J, Stockfleth E, et al.** (2010) Genomic characterization of a novel human papillomavirus (HPV-117) with a high viral load in a persisting wart. Virology 399: 129-33.
97. **Köhler A, Gottschling M, Manning K, Lehmann MD, Schulz E, et al.** (2011) Genomic characterization of ten novel cutaneous human papillomaviruses from keratotic lesions of immunosuppressed patients. J Gen Virol 92: 1585-94.
98. **Kosa JL, Michelsen JW, Louis HA, Olsen JI, Davis DR, et al.** (1994) Common metal ion coordination in LIM domain proteins. Biochemistry 33: 468-77.
99. **Kripke ML, Cox PA, Alas LG, Yarosh DB** (1992) Pyrimidine dimers in DNA initiate systemic immunosuppression in UV-irradiated mice. Proc Natl Acad Sci U S A 89: 7516-20.
100. **Laemmli UK** (1970) Cleavage of structural proteins during the assembly of the head of bacteriophage T4. Nature 227: 680-5.
101. **Langer EM, Feng Y, Zhaoyuan H, Rauscher FJ, 3rd, Kroll KL, et al.** (2008) Ajuba LIM proteins are snail/slug corepressors required for neural crest development in Xenopus. Dev Cell 14: 424-36.
102. **Lax AJ, Thomas W** (2002) How bacteria could cause cancer: one step at a time. Trends Microbiol 10: 293-9.
103. **Lazarczyk M, Pons C, Mendoza JA, Cassonnet P, Jacob Y, et al.** (2008) Regulation of cellular zinc balance as a potential mechanism of EVER-mediated protection against pathogenesis by cutaneous oncogenic human papillomaviruses. J Exp Med 205: 35-42.
104. **Lazarczyk M, Cassonnet P, Pons C, Jacob Y, Favre M** (2009) The EVER proteins as a natural barrier against papillomaviruses: a new insight into the pathogenesis of human papillomavirus infections. Microbiol Mol Biol Rev 73: 348-70.
105. **Lechner MS, Laimins LA** (1994) Inhibition of p53 DNA binding by human papillomavirus E6 proteins. J Virol 68: 4262-73.
106. **Lecoq H** (2001) [Discovery of the first virus, the tobacco mosaic virus: 1892 or 1898?]. C R Acad Sci III 324: 929-33.
107. **Leptak C, Ramon y Cajal S, Kulke R, Horwitz BH, Riese DJ, 2nd, et al.** (1991) Tumorigenic transformation of murine keratinocytes by the E5 genes of bovine papillomavirus type 1 and human papillomavirus type 16. J Virol 65: 7078-83.

108. **Li PM, Reichert J, Freyd G, Horvitz HR, Walsh CT** (1991) The LIM region of a presumptive Caenorhabditis elegans transcription factor is an iron-sulfur- and zinc-containing metallodomain. Proc Natl Acad Sci U S A 88: 9210-3.
109. **Li X, Coffino P** (1996) High-risk human papillomavirus E6 protein has two distinct binding sites within p53, of which only one determines degradation. J Virol 70: 4509-16.
110. **Liang XH, Volkmann M, Klein R, Herman B, Lockett SJ** (1993) Co-localization of the tumor-suppressor protein p53 and human papillomavirus E6 protein in human cervical carcinoma cell lines. Oncogene 8: 2645-52.
111. **Lindelof B, Sigurgeirsson B, Gabel H, Stern RS** (2000) Incidence of skin cancer in 5356 patients following organ transplantation. Br J Dermatol 143: 513-9.
112. **Liu Q, Kaneko S, Yang L, Feldman RI, Nicosia SV, et al.** (2004) Aurora-A abrogation of p53 DNA binding and transactivation activity by phosphorylation of serine 215. J Biol Chem 279: 52175-82.
113. **Lutzner M, Croissant O, Ducasse MF, Kreis H, Crosnier J, et al.** (1980) A potentially oncogenic human papillomavirus (HPV-5) found in two renal allograft recipients. J Invest Dermatol 75: 353-6.
114. **Lutzner MA** (1978) Epidermodysplasia verruciformis. An autosomal recessive disease characterized by viral warts and skin cancer. A model for viral oncogenesis. Bull Cancer 65: 169-82.
115. **Majewski S, Jablonska S** (2006) Current views on the role of human papillomaviruses in cutaneous oncogenesis. Int J Dermatol 45: 192-6.
116. **Mantovani F, Banks L** (2001) The human papillomavirus E6 protein and its contribution to malignant progression. Oncogene 20: 7874-87.
117. **Marie H, Pratt SJ, Betson M, Epple H, Kittler JT, et al.** (2003) The LIM protein Ajuba is recruited to cadherin-dependent cell junctions through an association with alpha-catenin. J Biol Chem 278: 1220-8.
118. **Martin D, Gutkind JS** (2008) Human tumor-associated viruses and new insights into the molecular mechanisms of cancer. Oncogene 27 Suppl 2: S31-42.
119. **Massimi P, Thomas M, Bouvard V, Ruberto I, Campo MS, et al.** (2008) Comparative transforming potential of different human papillomaviruses associated with non-melanoma skin cancer. Virology 371: 374-9.
120. **Matsuoka M, Jeang KT** (2007) Human T-cell leukaemia virus type 1 (HTLV-1) infectivity and cellular transformation. Nat Rev Cancer 7: 270-80.
121. **Michelsen JW, Schmeichel KL, Beckerle MC, Winge DR** (1993) The LIM motif defines a specific zinc-binding protein domain. Proc Natl Acad Sci U S A 90: 4404-8.
122. **Michelsen JW, Sewell AK, Louis HA, Olsen JI, Davis DR, et al.** (1994) Mutational analysis of the metal sites in an LIM domain. J Biol Chem 269: 11108-13.
123. **Momparler RL, Karon M, Siegel SE, Avila F** (1976) Effect of adriamycin on DNA, RNA, and protein synthesis in cell-free systems and intact cells. Cancer Res 36: 2891-5.
124. **Moreno-Lopez J, Ahola H, Eriksson A, Bergman P, Pettersson U** (1987) Reindeer papillomavirus transforming properties correlate with a highly conserved E5 region. J Virol 61: 3394-400.
125. **Muller JM, Metzger E, Greschik H, Bosserhoff AK, Mercep L, et al.** (2002) The transcriptional coactivator FHL2 transmits Rho signals from the cell membrane into the nucleus. EMBO J 21: 736-48.
126. **Munger K, Baldwin A, Edwards KM, Hayakawa H, Nguyen CL, et al.** (2004) Mechanisms of human papillomavirus-induced oncogenesis. J Virol 78: 11451-60.
127. **Muñoz N, Bosch FX, de Sanjose S, Herrero R, Castellsague X, et al.** (2003) Epidemiologic classification of human papillomavirus types associated with cervical cancer. N Engl J Med 348: 518-27.
128. **Muñoz N, Castellsague X, de Gonzalez AB, Gissmann L** (2006) Chapter 1: HPV in the etiology of human cancer. Vaccine 24 Suppl 3: S3/1-10.

129. **Murphy GM** (2009) Ultraviolet radiation and immunosuppression. Br J Dermatol 161 Suppl 3: 90-5.
130. **Muschik D, Braspenning-Wesch I, Stockfleth E, Rosl F, Hofmann TG, et al.** (2011) Cutaneous HPV23 E6 prevents p53 phosphorylation through interaction with HIPK2. PLoS One 6: e27655.
131. **Nakazawa H, English D, Randell PL, Nakazawa K, Martel N, et al.** (1994) UV and skin cancer: specific p53 gene mutation in normal skin as a biologically relevant exposure measurement. Proc Natl Acad Sci U S A 91: 360-4.
132. **Nindl I, Gottschling M, Stockfleth E** (2007) Human papillomaviruses and non-melanoma skin cancer: basic virology and clinical manifestations. Dis Markers 23: 247-59.
133. **Nindl I, Rösl F** (2008) Molecular concepts of virus infections causing skin cancer in organ transplant recipients. Am J Transplant 8: 2199-204.
134. **Nix DA, Beckerle MC** (1997) Nuclear-cytoplasmic shuttling of the focal contact protein, zyxin: a potential mechanism for communication between sites of cell adhesion and the nucleus. J Cell Biol 138: 1139-47.
135. **O'Banion MK, Reichmann ME, Sundberg JP** (1986) Cloning and characterization of an equine cutaneous papillomavirus. Virology 152: 100-9.
136. **O'Brate A, Giannakakou P** (2003) The importance of p53 location: nuclear or cytoplasmic zip code? Drug Resist Updat 6: 313-22.
137. **Orth G, Jablonska S, Favre M, Croissant O, Jarzabek-Chorzelska M, et al.** (1978) Characterization of two types of human papillomaviruses in lesions of epidermodysplasia verruciformis. Proc Natl Acad Sci U S A 75: 1537-41.
138. **Orth G** (1986) Epidermodysplasia verruciformis: a model for understanding the oncogenicity of human papillomaviruses. Ciba Found Symp 120: 157-74.
139. **Orth G** (2006) Genetics of epidermodysplasia verruciformis: Insights into host defense against papillomaviruses. Semin Immunol 18: 362-74.
140. **Pagano JS, Blaser M, Buendia MA, Damania B, Khalili K, et al.** (2004) Infectious agents and cancer: criteria for a causal relation. Semin Cancer Biol 14: 453-71.
141. **Parkin DM** (2006) The global health burden of infection-associated cancers in the year 2002. Int J Cancer 118: 3030-44.
142. **Parkin DM, Bray F** (2006) Chapter 2: The burden of HPV-related cancers. Vaccine 24 Suppl 3: S3/11-25.
143. **Pattillo RA, Hussa RO, Story MT, Ruckert AC, Shalaby MR, et al.** (1977) Tumor antigen and human chorionic gonadotropin in CaSki cells: a new epidermoid cervical cancer cell line. Science 196: 1456-8.
144. **Perez-Alvarado GC, Miles C, Michelsen JW, Louis HA, Winge DR, et al.** (1994) Structure of the carboxy-terminal LIM domain from the cysteine rich protein CRP. Nat Struct Biol 1: 388-98.
145. **Perz JF, Armstrong GL, Farrington LA, Hutin YJ, Bell BP** (2006) The contributions of hepatitis B virus and hepatitis C virus infections to cirrhosis and primary liver cancer worldwide. J Hepatol 45: 529-38.
146. **Petit MM, Mols R, Schoenmakers EF, Mandahl N, Van de Ven WJ** (1996) LPP, the preferred fusion partner gene of HMGIC in lipomas, is a novel member of the LIM protein gene family. Genomics 36: 118-29.
147. **Petit MM, Fradelizi J, Golsteyn RM, Ayoubi TA, Menichi B, et al.** (2000) LPP, an actin cytoskeleton protein related to zyxin, harbors a nuclear export signal and transcriptional activation capacity. Mol Biol Cell 11: 117-29.
148. **Pfister H** (2003) Chapter 8: Human papillomavirus and skin cancer. J Natl Cancer Inst Monogr: 52-6.
149. **Poiesz BJ, Ruscetti FW, Gazdar AF, Bunn PA, Minna JD, et al.** (1980) Detection and isolation of type C retrovirus particles from fresh and cultured lymphocytes of a patient with cutaneous T-cell lymphoma. Proc Natl Acad Sci U S A 77: 7415-9.

150. **Pufall MA, Graves BJ** (2002) Autoinhibitory domains: modular effectors of cellular regulation. Annu Rev Cell Dev Biol 18: 421-62.
151. **Purdie KJ, Pennington J, Proby CM, Khalaf S, de Villiers EM, et al.** (1999) The promoter of a novel human papillomavirus (HPV77) associated with skin cancer displays UV responsiveness, which is mediated through a consensus p53 binding sequence. EMBO J 18: 5359-69.
152. **Raab-Traub N** (1992) Epstein-Barr virus and nasopharyngeal carcinoma. Semin Cancer Biol 3: 297-307.
153. **Raab-Traub N** (2012) Novel mechanisms of EBV-induced oncogenesis. Curr Opin Virol 2: 453-8.
154. **Radhakrishna Pillai G, Srivastava AS, Hassanein TI, Chauhan DP, Carrier E** (2004) Induction of apoptosis in human lung cancer cells by curcumin. Cancer Lett 208: 163-70.
155. **Ramoz N, Rueda LA, Bouadjar B, Favre M, Orth G** (1999) A susceptibility locus for epidermodysplasia verruciformis, an abnormal predisposition to infection with the oncogenic human papillomavirus type 5, maps to chromosome 17qter in a region containing a psoriasis locus. J Invest Dermatol 112: 259-63.
156. **Ramoz N, Rueda LA, Bouadjar B, Montoya LS, Orth G, et al.** (2002) Mutations in two adjacent novel genes are associated with epidermodysplasia verruciformis. Nat Genet 32: 579-81.
157. **Rastogi RP, Richa, Kumar A, Tyagi MB, Sinha RP** (2010) Molecular mechanisms of ultraviolet radiation-induced DNA damage and repair. J Nucleic Acids 2010: 592980.
158. **Reinhard M, Zumbrunn J, Jaquemar D, Kuhn M, Walter U, et al.** (1999) An alpha-actinin binding site of zyxin is essential for subcellular zyxin localization and alpha-actinin recruitment. J Biol Chem 274: 13410-8.
159. **Renfranz PJ, Siegrist SE, Stronach BE, Macalma T, Beckerle MC** (2003) Molecular and phylogenetic characterization of Zyx102, a Drosophila orthologue of the zyxin family that interacts with Drosophila Enabled. Gene 305: 13-26.
160. **Rosenstein BS, Mitchell DL** (1987) Action spectra for the induction of pyrimidine(6-4)pyrimidone photoproducts and cyclobutane pyrimidine dimers in normal human skin fibroblasts. Photochem Photobiol 45: 775-80.
161. **Rous P** (1911) A Sarcoma of the Fowl Transmissible by an Agent Separable from the Tumor Cells. J Exp Med 13: 397-411.
162. **Ruhland A, de Villiers EM** (2001) Opposite regulation of the HPV 20-URR and HPV 27-URR promoters by ultraviolet irradiation and cytokines. Int J Cancer 91: 828-34.
163. **Schiffman M, Castle PE, Jeronimo J, Rodriguez AC, Wacholder S** (2007) Human papillomavirus and cervical cancer. Lancet 370: 890-907.
164. **Schmeichel KL, Beckerle MC** (1994) The LIM domain is a modular protein-binding interface. Cell 79: 211-9.
165. **Schmeichel KL, Beckerle MC** (1997) Molecular dissection of a LIM domain. Mol Biol Cell 8: 219-30.
166. **Schneider G, Saur D, Siveke JT, Fritsch R, Greten FR, et al.** (2006) IKKalpha controls p52/RelB at the skp2 gene promoter to regulate G1- to S-phase progression. EMBO J 25: 3801-12.
167. **Schulz E, Gottschling M, Wibbelt G, Stockfleth E, Nindl I** (2009) Isolation and genomic characterization of the first Norway rat (Rattus norvegicus) papillomavirus and its phylogenetic position within Pipapillomavirus, primarily infecting rodents. J Gen Virol 90: 2609-14.
168. **Schulz E, Gottschling M, Ulrich RG, Richter D, Stockfleth E, et al.** (2012) Isolation of three novel rat and mouse papillomaviruses and their genomic characterization. PLoS One 7: e47164.
169. **Schwarz E, Freese UK, Gissmann L, Mayer W, Roggenbuck B, et al.** (1985) Structure and transcription of human papillomavirus sequences in cervical carcinoma cells. Nature 314: 111-4.
170. **Schwarz T** (2002) Photoimmunosuppression. Photodermatol Photoimmunol Photomed 18: 141-5.
171. **Schwarz T** (2005) [Ultraviolet radiation--immune response]. J Dtsch Dermatol Ges 3 Suppl 2: S11-8.

172. **Sheppard SA, Savinova T, Loayza D** (2011) TRIP6 and LPP, but not Zyxin, are present at a subset of telomeres in human cells. Cell Cycle 10: 1726-30.
173. **Sherman L, Schlegel R** (1996) Serum- and calcium-induced differentiation of human keratinocytes is inhibited by the E6 oncoprotein of human papillomavirus type 16. J Virol 70: 3269-79.
174. **Shope RE, Hurst EW** (1933) Infectious Papillomatosis of Rabbits : With a Note on the Histopathology. J Exp Med 58: 607-24.
175. **Sijbers AM, de Laat WL, Ariza RR, Biggerstaff M, Wei YF, et al.** (1996) Xeroderma pigmentosum group F caused by a defect in a structure-specific DNA repair endonuclease. Cell 86: 811-22.
176. **Simmonds M, Storey A** (2008) Identification of the regions of the HPV 5 E6 protein involved in Bak degradation and inhibition of apoptosis. Int J Cancer 123: 2260-6.
177. **Smith PK, Krohn RI, Hermanson GT, Mallia AK, Gartner FH, et al.** (1985) Measurement of protein using bicinchoninic acid. Anal Biochem 150: 76-85.
178. **Stanley MA** (2012) Epithelial cell responses to infection with human papillomavirus. Clin Microbiol Rev 25: 215-22.
179. **Steger G, Pfister H** (1992) In vitro expressed HPV 8 E6 protein does not bind p53. Arch Virol 125: 355-60.
180. **Stockfleth E, Ulrich C, Meyer T, Arndt R, Christophers E** (2001) Skin diseases following organ transplantation--risk factors and new therapeutic approaches. Transplant Proc 33: 1848-53.
181. **Stockfleth E, Nindl I, Sterry W, Ulrich C, Schmook T, et al.** (2004) Human papillomaviruses in transplant-associated skin cancers. Dermatol Surg 30: 604-9.
182. **Struijk L, Bouwes Bavinck JN, Wanningen P, van der Meijden E, Westendorp RG, et al.** (2003) Presence of human papillomavirus DNA in plucked eyebrow hairs is associated with a history of cutaneous squamous cell carcinoma. J Invest Dermatol 121: 1531-5.
183. **Struijk L, van der Meijden E, Kazem S, ter Schegget J, de Gruijl FR, et al.** (2008) Specific betapapillomaviruses associated with squamous cell carcinoma of the skin inhibit UVB-induced apoptosis of primary human keratinocytes. J Gen Virol 89: 2303-14.
184. **Sum EY, Peng B, Yu X, Chen J, Byrne J, et al.** (2002) The LIM domain protein LMO4 interacts with the cofactor CtIP and the tumor suppressor BRCA1 and inhibits BRCA1 activity. J Biol Chem 277: 7849-56.
185. **Sundberg JP, Van Ranst M, Montali R, Homer BL, Miller WH, et al.** (2000) Feline papillomas and papillomaviruses. Vet Pathol 37: 1-10.
186. **Sweet BH, Hilleman MR** (1960) The vacuolating virus, S.V. 40. Proc Soc Exp Biol Med 105: 420-7.
187. **Ulrich C, Kanitakis J, Stockfleth E, Euvrard S** (2008) Skin cancer in organ transplant recipients--where do we stand today? Am J Transplant 8: 2192-8.
188. **Underbrink MP, Howie HL, Bedard KM, Koop JI, Galloway DA** (2008) E6 proteins from multiple human betapapillomavirus types degrade Bak and protect keratinocytes from apoptosis after UVB irradiation. J Virol 82: 10408-17.
189. **van Duin M, Snijders PJ, Schrijnemakers HF, Voorhorst FJ, Rozendaal L, et al.** (2002) Human papillomavirus 16 load in normal and abnormal cervical scrapes: an indicator of CIN II/III and viral clearance. Int J Cancer 98: 590-5.
190. **Vasioukhin V, Bauer C, Yin M, Fuchs E** (2000) Directed actin polymerization is the driving force for epithelial cell-cell adhesion. Cell 100: 209-19.
191. **Viarisio D, Mueller-Decker K, Kloz U, Aengeneyndt B, Kopp-Schneider A, et al.** (2011) E6 and E7 from beta HPV38 cooperate with ultraviolet light in the development of actinic keratosis-like lesions and squamous cell carcinoma in mice. PLoS Pathog 7: e1002125.
192. **Viarisio D, Decker KM, Aengeneyndt B, Flechtenmacher C, Gissmann L, et al.** (2013) Human papillomavirus type 38 E6 and E7 act as tumour promoters during chemically induced skin carcinogenesis. J Gen Virol 94: 749-52.
193. **Vogelstein B, Kinzler KW** (1993) The multistep nature of cancer. Trends Genet 9: 138-41.
194. **Vousden KH** (2000) p53: death star. Cell 103: 691-4.
195. **Vousden KH, Lu X** (2002) Live or let die: the cell's response to p53. Nat Rev Cancer 2: 594-604.

196. **Vousden KH, Lane DP** (2007) p53 in health and disease. Nat Rev Mol Cell Biol 8: 275-83.
197. **Vousden KH, Prives C** (2009) Blinded by the Light: The Growing Complexity of p53. Cell 137: 413-31.
198. **Wachter RM, Elsliger MA, Kallio K, Hanson GT, Remington SJ** (1998) Structural basis of spectral shifts in the yellow-emission variants of green fluorescent protein. Structure 6: 1267-77.
199. **Walboomers JM, Jacobs MV, Manos MM, Bosch FX, Kummer JA, et al.** (1999) Human papillomavirus is a necessary cause of invasive cervical cancer worldwide. J Pathol 189: 12-9.
200. **Wang Y, Gilmore TD** (2003) Zyxin and paxillin proteins: focal adhesion plaque LIM domain proteins go nuclear. Biochim Biophys Acta 1593: 115-20.
201. **Way JC, Chalfie M** (1988) mec-3, a homeobox-containing gene that specifies differentiation of the touch receptor neurons in C. elegans. Cell 54: 5-16.
202. **Werness BA, Levine AJ, Howley PM** (1990) Association of human papillomavirus types 16 and 18 E6 proteins with p53. Science 248: 76-9.
203. **Wilczynski SP, Oft M, Cook N, Liao SY, Iftner T** (1993) Human papillomavirus type 6 in squamous cell carcinoma of the bladder and cervix. Hum Pathol 24: 96-102.
204. **Wilson VG, West M, Woytek K, Rangasamy D** (2002) Papillomavirus E1 proteins: form, function, and features. Virus Genes 24: 275-90.
205. **World Health Organization (WHO) fsN** (2013) Cancer.
206. **Yi J, Beckerle MC** (1998) The human TRIP6 gene encodes a LIM domain protein and maps to chromosome 7q22, a region associated with tumorigenesis. Genomics 49: 314-6.
207. **Yi J, Kloeker S, Jensen CC, Bockholt S, Honda H, et al.** (2002) Members of the Zyxin family of LIM proteins interact with members of the p130Cas family of signal transducers. J Biol Chem 277: 9580-9.
208. **Zhang B, Spandau DF, Roman A** (2002) E5 protein of human papillomavirus type 16 protects human foreskin keratinocytes from UV B-irradiation-induced apoptosis. J Virol 76: 220-31.
209. **Zheng Q, Zhao Y** (2007) The diverse biofunctions of LIM domain proteins: determined by subcellular localization and protein-protein interaction. Biol Cell 99: 489-502.
210. **Zheng ZM, Baker CC** (2006) Papillomavirus genome structure, expression, and post-transcriptional regulation. Front Biosci 11: 2286-302.
211. **Ziegler A, Jonason AS, Leffell DJ, Simon JA, Sharma HW, et al.** (1994) Sunburn and p53 in the onset of skin cancer. Nature 372: 773-6.
212. **Zuckerman V, Wolyniec K, Sionov RV, Haupt S, Haupt Y** (2009) Tumour suppression by p53: the importance of apoptosis and cellular senescence. J Pathol 219: 3-15.
213. **zur Hausen H** (2002) Papillomaviruses and cancer: from basic studies to clinical application. Nat Rev Cancer 2: 342-50.
214. **Zur Hausen H** (2009) The search for infectious causes of human cancers: where and why. Virology 392: 1-10.

Section 7

Appendix

7.1 Abbreviations

A

ActA	ActA repeat region
ADR	Adriamycin
AK	Actinic keratosis
ALV	Avian leukemia virus
aPKC	Atypical protein kinase C
APS	Ammonium persulfate
ATL	Adult T-cell leukemia
ATR	Ataxia telangiectasia and Rad3-related protein

B

BCA	Bicinchoninic acid
BCC	Basal cell carcinoma
BSA	Bovine serum albumin

C

CDS	Coding DNA sequence
CH	Calponin homology
CHK2	Checkpoint kinase 2
CIN	Cervical intraepithelial neoplasia
CMV	Cytomegalovirus
CO_2	Carbon dioxide
Co-IP	Co-immunoprecipitation
CRP	Cysteine-rich protein
CRPV	Cottontail rabbit papilloma virus
C9orf102	Chromosome 9 Open Reading Frame 102

D

ddH_2O	Double distilled water
DKFZ	German Cancer Research Centre
DMEM	Dulbecco's modified Eagle's medium
DMSO	Dimethyl sulfoxide
DNA	Deoxyribonucleic acid
dNTPs	Deoxy nucleotide triphosphates

E

EBV	Epstein-Barr virus
ECL	Enhanced Chemiluminescence Substrate
E.coli	*Escherichia coli*

EDTA	Ethylenediaminetetraacetate
e.g.	Exempli gratia
ELISA	Enzyme-linked immunosorbent assay
Ena/VASP	Enabled/Vasodilator-stimulated phosphoprotein
et al.	Et alii
EV	*Epidermodysplasia verruciformis*
E6AP	E6-associated protein

F

FCS	Fetal Calf Serum
FHL	Four-and-a-half LIM
Fig.	Figure

G

G418	Geneticin
GFP	Green fluorescent protein
Grb2	Growth factor receptor-bound protein 2
GST	Glutathione S-transferase

H

h	hour
HA	Haemagglutinin
HBV	Hepatitis B virus
HCV	Hepatitis C virus
HD	Homeodomain
HEPES	4-(2-Hydroxyethyl)-1-piperazineethanesulfonic acid
HEK	Human Embryonic Kidney
HHV	Human herpesvirus
HIPK2	Homeodomain-interacting protein kinase 2
HPKn	Neonatal human primary keratinocytes
HPV	Human papillomavirus
HRP	Horseradish peroxidase
HTLV-1	Human T-cell lymphotropic virus

I

IF	Immunofluorescence
IgG (H+L)	Immunoglobulin G (heavy and light chain)
IP	Immunoprecipitation
IPTG	Isopropyl β-D-1-thiogalactopyranoside

J

J	Joule

K

KSHV	Kaposi's sarcoma-associated herpesvirus

L

LATS	Large tumour suppressor
LB	Lysogeny broth
LCR	Long control region
LD	Leucine-aspartate domain
LHX	LIM-homeodomain protein
LIM	Lin11, Isl-1, Mec-3
LIMD1	LIM domain-containing protein 1
LIMK	LIM kinase
LMO	LIM only protein
LPP	Lipoma preferred partner
LPXN	Leupaxin

M

MAP	Mitogen-activated protein
mg	Milligram
Mdm2	Mouse double minute 2 homolog
MICAL	Molecule interacting with CASL protein-1
mL	Millilitre
µg	Microgram
µm	Micrometre
mRNA	Messenger RNA

N

NES	Nuclear export signal
NIKS	Normal immortal keratinocytes
NMSC	Non-melanoma skin cancer

O

OD	optical density
ORF	open reading frame
OTR	Organ transplant recipient

P

p.a.	pro analysi
PAE	Early polyadenylation site
PAL	Late polyadenylation site
PARP	Poly ADP ribose polymerase
PBS	Phosphate buffered saline
pCMV	Cytomegalovirus promoter
PCR	Polymerase chain reaction
PDCD6	Programmed Cell Death 6
PDCD6IP	Programmed Cell Death 6 Interacting Protein
PDZ	Postsynaptic density-95, Discs large, Zona occludens-1
PET	Prickle, espinas, testin
PINCH	Particularly interesting new cysteine and histidine-rich protein

PMSF	Phenylmethylsulfonyl fluoride
pRb	Retinoblastoma protein
PRMT5	Protein arginine methyltransferase 5
PTEN	Phosphatase and tensin homolog
PV	Papillomavirus
PVDF	Polyvinylidene fluoride

R

RNA	Ribonucleic acid
RNAi	RNA interference
rpm	Revolutions per minute
RSV	Rous sarcoma virus

S

SCC	Squamous cell carcinoma
SDS	Sodium dodecyl sulfate
SDS-PAGE	SDS-Polyacrylamide gel electrophoresis
SH3	Src-homology-3
siRNA	Small interfering RNA
SOC	Super optimal broth with glucose

T

Tab.	Table
TAE	Tris base, acetic acid and EDTA
TBS	Tris-buffered saline
TBST	Tris-buffered saline/Tween20
TEMED	Tetramethylethylenediamine
TMC	Transmembrane channel-like
TMV	Tobacco mosaic virus
TRAF6	Tumour necrosis factor receptor-associated factor 6
Trip6	Thyroid hormone interacting protein 6

U

URR	Upstream regulatory region
UV	Ultraviolet

V

V	Volt
v/v	Volume percent

W

WHO	World Health Organization
WTIP	Wilms tumour 1 interacting protein
w/v	Weight percent

XYZ…

Y2H	Yeast Two-Hybrid
YFP	Yellow fluorescent protein

7.2 Publications and presentations

Niebler M, Qian X, Höfler D, **Kogosov V**, Kaewprag J, Kaufmann AM, Ly R, Böhmer G, Zawatzky R, Rösl F, Rincon-Orozco B (2013) Post-Translational Control of IL-1β via the Human Papillomavirus Type 16 E6 Oncoprotein: A Novel Mechanism of Innate Immune Escape Mediated by the E3-Ubiquitin Ligase E6-AP and p53. PLoS Pathog. Aug;9(8) e1003536.

Schneider I, Lehmann MD, **Kogosov V**, Stockfleth E, Nindl I (2013) Eyebrow hairs from actinic keratosis patients harbor the highest number of cutaneous human papillomaviruses. BMC Infect Dis. Apr24;13:186

Kogosov V, New Interaction Partners with E6 of Novel Cutaneous HPV Types. Oral presentation and poster. 6th International Conference: HPV, Polyomavirus & UV in Skin Cancer, Oct. 18th 2012, Berlin, Germany

Danksagung

Ich danke Prof. Dr. Ingo Nindl für die Möglichkeit, meine Dissertation in seiner Arbeitsgruppe anfertigen zu können, für die herausfordernde und sehr interessante Themenstellung, die wissenschaftliche Betreuung und das entgegengebrachte Vertrauen sowie die Freiheit, auch den eigenen Ideen nachzugehen.
Prof. Dr. Frank Rösl möchte ich danken für die Möglichkeit, unter wundervollen Bedingungen in seinen Laboren forschen zu können, für das stete Interesse an meinem Projekt, die Übernahme des Zweitgutachtens meiner Arbeit sowie die immerwährende Förderung sowohl während meines langjährigen Schaffens am DKFZ, als auch außerhalb. Nie vergessen bleiben die unterhaltsamen Mittagessen, sowie das rechtzeitige Aufbrechen zu diesen.
Ich danke Prof. Dr. Rainer Zawatzky für die Übernahme des Erstgutachtens, das Teilen der Zellkultur, die wissenschaftlichen Ratschläge während und außerhalb der Seminare, sowie die vielen anregenden und amüsanten Unterhaltungen und Erzählungen aus seiner Zeit als junger und junggebliebener Forscher.
PD Dr. Thomas G. Hofmann möchte ich für die zahlreichen guten Ratschläge zu meinen Versuchen und die Bereitstellung von Plasmiden und Antikörpern danken. Darüber hinaus verdienen alle Mitarbeiter der Arbeitsgruppe „Zelluläre Seneszenz“ ein riesengroßes Dankeschön für die durchgehende Bereitschaft, sich mit mir und meinen Fragen und Wünschen auseinanderzusetzen, besonders hervorheben möchte ich Vera, Christoph, Tilman, Carolina und Nadja.
Für die allgemeine Unterstützung und die sehr gute Arbeitsatmosphäre möchte ich Nicolas, Regina, Heribert, Elke, Johanna, Prajakta, Melanie, Daniel, Simone und Kai danken.
Der 10.30 Uhr Kaffeerunde, auch „Elisabethaner“ genannt, danke ich für die herzliche Aufnahme in die Kaffeetrinkerei und Kuchennascherei, die ich als Ilonas Anhängsel genießen durfte. Ilona Braspenning-Wesch danke ich ganz besonders für ihre unermüdliche Hilfsbereitschaft im Labor und allen sonstigen Lebenslagen, für die Naschereien aus dem Nachbarland und dafür, dass sie Ihre Rolle als Labormutti wirklich sehr gut ausgeführt hat! „Danke Dir für die dreieinhalb Jahre an deiner Seite und die stetige Aufmunterung, wenn es mal nicht so rund lief!“
Zu einem riesigen Dankeschön bin ich meiner „Leidensgenossin“ Martina Sabine Niebler verpflichtet, die die gesamte Doktorandenzeit über, zwar auf der anderen Stockwerksseite, ganz woanders, und doch praktisch an meiner Seite gearbeitet hat. „Nur“ Kollegen sind wir schon lange nicht mehr! „Vielen, vielen Dank für Deine Versuche mir die Welt der Säugetiere nahezubringen, Deine Fütterungsversuche mit gelatinehaltigen Lebensmitteln, nur damit ich dir Deine Süßigkeiten nicht wegesse und vor allem für Deine vergeblichen Versuche, Dich freitagabends ins Wochenende zu verabschieden, die so manch interessante Unterhaltung ergeben haben!“
Sabrina Eugenia Vinzon möchte ich für Ihre „Einwanderung“ ins Labor 1.221 danken, ihre immer ausführlichen Erklärung zu allen Fragen unabhängig davon wie beschäftigt sie gerade war und für ihre Einführung in die argentinische Esskultur. „To cite Alejandro: Hhhhm, Lomo!“
Nicht vergessen kann ich meine „externe“ und doch gruppeninterne Kollegin Mandy, die obwohl ganz selten in Person, aber geistig ganz nah dabei war und immer einen witzigen Spruch auf Lager hatte. „Nach einem Gespräch mit Dir ist man einfach immer motiviert weiterzumachen! “
Allen weiteren Kollegen vom 1.OG Ost danke ich für den Austausch von Süßigkeiten, Materialien und wissenswertem rund ums Labor, vor allem Michael Behr für die gegenseitigen Wochenendgefälligkeiten und Zufütterungen.

Ganz besonders möchte ich mich bei meinen Eltern bedanken, die mich immer unterstützt haben und die alle wichtigen Lebensereignisse in den letzten drei Jahren mitgetragen haben, ohne an meinen Entscheidungen zu zweifeln.
Der wohl größte Dank gilt meinem Mann Michael, der mich mit aller ihm möglichen Kraft in diesen letzten Zügen der Doktorarbeit unterstützt hat. „Vielen Dank für Deine Geduld mit mir, Deine stets großartige Verpflegung und Deine (oft vergeblichen) Versuche dir Abends mit mir eine DVD anzusehen. Du bist der große, zottelige Kuschelbär und die heimliche Stütze hinter mir. Looove you!“